Signal Peptide and Chaperone Engineering for Secretion and Excretion in *Escherichia coli*

Weiran Zhang

A dissertation

submitted in partial fulfillment of the

requirements for the degree of

Doctor of Philosophy

University of Washington

2015

Reading Committee:

François Baneyx, Chairman

Jim Pfaendtner

Beth Traxler

Qiuming Yu

Program Authorized to Offer Degree:

Department of Chemical Engineering

University of Washington

Abstract

Signal Peptide and Chaperone Engineering for Secretion and Excretion in *Escherichia coli*

Weiran Zhang

Chair of the Supervisory Committee:

Department Chair and Charles W.H. Matthaei Professor of Chemical Engineering

François Baneyx, Ph.D.

Department of Chemical Engineering

Secretory proteins play critical role in cell survival and pathogenicity and make up approximately 30% of all polypeptides synthesized by gram-negative bacteria. They may be found in a soluble form in the periplasm (the interstitial space between inner and outer membranes), integrated within the outer membrane or excreted outside of the cell in a vesicular or globular form. In all cases, they must first translocate across the inner membrane. A substantial fraction of secretory proteins do so by making use of a cleavable N-terminal extension called signal sequence (or peptide) that is recognized by a dedicated translocation system known as the Sec pathway. Typical Sec-dependent signal sequences have a tripartite structure with a central hydrophobic core and are about 20 residues in length. However, certain secretory proteins implicated in virulence employ Sec-dependent signal peptides that are over 40 residues long. To determine if repetition of canonical, Sec-dependent signal peptides would benefit secretory protein production, we fused the signal sequences of *E. carotovora* PelB and *E. coli* OmpA to one another to produce synthetic PelB-OmpA and OmpA-PelB leader peptides. Using periplasmic maltose binding protein (MBP) and outer membrane protein A (OmpA) as model systems, we found that dual signal peptides support Sec-dependent protein translocation and are preferentially cleaved at the signal peptidase I site vicinal to the mature protein. In the case of native OmpA, dual signal peptides increased the requirement for the molecular chaperone Trigger Factor but reduced the accumulation of misfolded precursor and mature species and delayed the acquisition of P_{BAD} promoter mutations that restore cell growth by shutting down recombinant protein synthesis. On the other hand, dual signal sequences did not improve the incorporation of an $OmpA_{1-183}$-mCherry fusion protein within extracellular outer membrane vesicles (OMVs), as highest yields were obtained with the PelB signal peptide. However, co-expression of periplasmic chaperones (primarily SurA) and components of the outer membrane protein assembly machinery (primarily BamA) improve OMV production by nearly twofold. Overall, our results highlight the potential and limitations of signal sequence and chaperone engineering strategies for the production of secretory proteins and OMVs in *E. coli.*

TABLE OF CONTENTS

LIST OF FIGURES

LIST OF TABLES

ACKNOWLEDGEMENTS

I'm extremely grateful for everything I've experienced and everyone I've met along the way over the past 5.5 years here in the graduate school. To my research advisor, Dr. François Baneyx, for your unlimited support and patience. Your tremendous help has guided me into the world of scientific research and molded me into a much better scientist/engineer than I've ever thought I'd be. All those transferable skills, especially thinking in logic and attention to details will benefit the rest of my career. To all my lab mates, both past and present, Dr. Weibin Zhou, Dr. Brent Nannenga, Dr. Sathana Kitayaporn, Dr. Carolynn Grosh, Dr. Bandon Coyle, Dr. David Chiu, Dr. James Matthaei, Brian Swift, Jessica Soto-Rodriguez and Cristina Nelson, without your generous help, I wouldn't have accomplished what I have today. To my fellow students and friends Yingxin Deng, Wei Sun and Erik Josberger at Dr. Marco Rolandi's group, whom I've had so much fun working with on a collaborative project. Also to my committee members, Dr. Jim Pfaendtner, Dr. Qiuming Yu and Dr. Beth Traxler, and many other faculties who provide countless advice and guidance along the way.

My thanks also go to the wonderful human beings I've friended with volunteering at Purrfect Pals for the past 2 years. Jill Yercovich, who has been such an amazing lead for our group at North Seattle Petsmart adoption branch. Julie Morgan and Brook Mckinnon, whom I always had a blast with hanging out, and many others fellow volunteers whom I've learned so much from. Together as a team, we've been through a lot of joy and sorrow, all these experiences makes me appreciate life even more, and also strengthens my belief in that, no matter how trial the effort seems, everyone can make a difference in making a better world.

Last but not least, my heart goes to my parents and family, also to a lot of friends both in the US and at home abroad. I miss you all and thanks for being so wonderful and understanding to have me in all your lives. Everyone has something special that I can learn from, and I've become a better person because of you all.

DEDICATION

To Handsome and Mighty,
for your unconditional love

Chapter 1 Introduction

1.1 SECRETORY PROTEINS AND SECRETION PROCESS IN GRAM-NEGATIVE BACTERIA

Secretory proteins make up approximately 30% of all polypeptides synthesized in Gram-negative bacteria (1, 2), and play important roles in various biochemical processes within the cell envelope. They also contribute to pathogenesis when targeted to the outer membrane or further excreted into the growth medium. These essential functions can only be carried out outside the cytoplasm, either in the periplasm - the interstitial space in between the inner and outer membrane (OM) - in the OM, or outside of the cell. Thus, targeting proteins for secretion is a major concern to most bacterial species (3). In fact, Gram-negative bacteria have evolved at least 9 types of secretion systems (T1SS – T9SS) to meet this need (4).

β-barrel outer membrane proteins (OMPs) and periplasmic proteins are translocated across the first barrier – the phospholipid inner membrane – via the Sec-dependent, SRP-dependent and Twin-Arginine (Tat)-pathway. Proteins residing in the periplasm are released and fold in this subcellular compartment while OMPs and extracellular proteins are bound by periplasmic chaperones that escort them to the β-barrel assembly machinery (Bam) which is responsible for the final translocation step (5-9). A description of these pathways and of the key players involved in secretion process is provided in the following sections.

1.2 SECRETION PATHWAYS

1.2.1 *Sec-dependent protein export*

The majority of proteins destined for export are translocated across the cytoplasmic membrane in an unfolded or partially folded state via the Sec-dependent secretory pathway (Figure 1.1). Sec-dependent preproteins are outfitted with an N-terminal signal sequence that marks them for secretion (see section 4). After about 100 residues have been synthesized by the ribosome (10), nascent chains are bound by the cytoplasmic chaperone Trigger Factor (TF), which shields them from proteolytic degradation and premature folding in the cytoplasm. Newly translated preproteins may also be captured and maintained in a partially folded form by SecB, a tetrameric molecular chaperone dedicated to protein export (11). TF- or SecB-bound preproteins are then transferred to SecA, a key component of the Sec-dependent export pathway that functions as an ATP-fueled molecular motor (see section 1.3.4). SecA threads the preprotein cargo into the central pore of SecYEG translocon, a protein complex residing in the inner membrane. Interactions with SecDFYajC facilitate late steps in the translocation process, the signal sequence is cleaved by the membrane-associated signal peptidase I (SPase I), and secretory proteins are eventually released the substrate into the periplasmic space (12, 13).

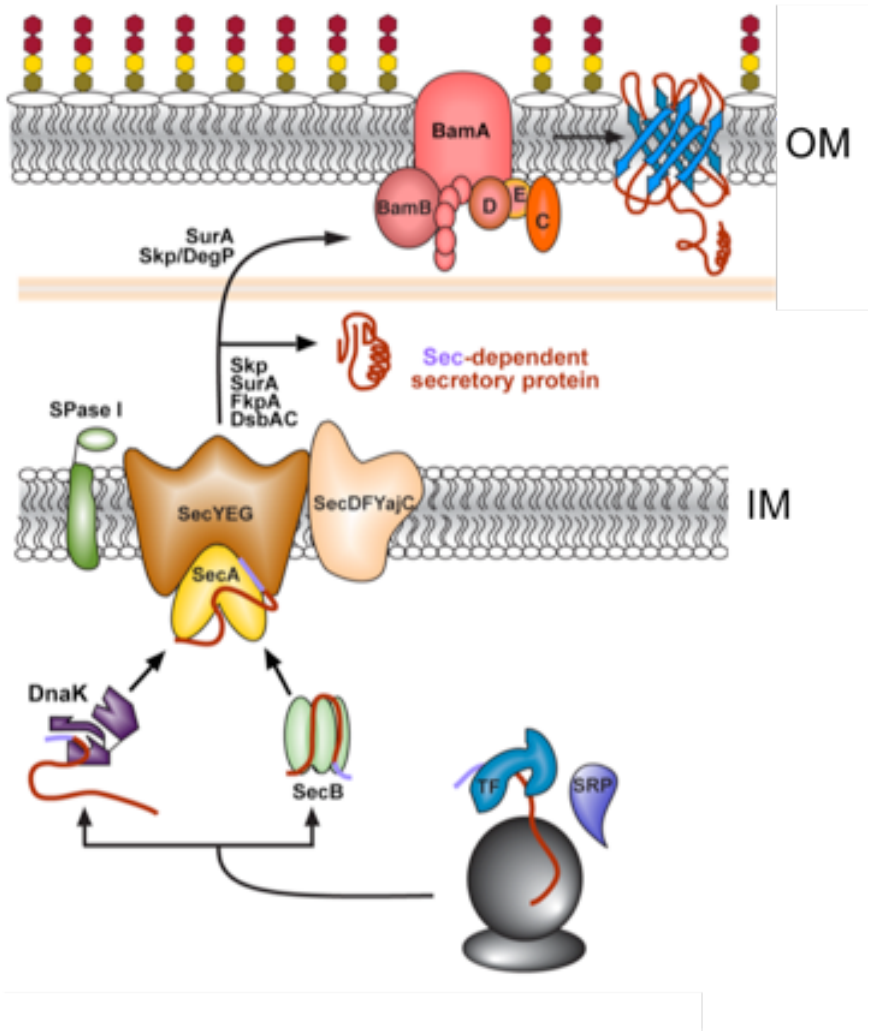

Figure 1.1 Sec-dependent secretory pathway

Nascent periplasmic proteins or OMPs emerging from the ribosome and are engaged by Trigger factor (TF) (14, 15), which shields them from premature folding or degradation. Newly synthesized proteins are then passed on to other cytoplasmic chaperones (primarily SecB, but in some instances DnaK) and further transferred to the SecA molecular motor which uses energy from ATP-hydrolysis to thread the preproteins through the inner membrane (IM) embedded SecYEG translocon. Sec-dependent translocation is finalized after signal peptidase I (SPase I) cleaves the signal peptide.

1.2.2 *SRP-dependent protein export*

The Signal Recognition Particle (SRP) secretory pathway is mainly responsible for inner membrane protein (IMP) biogenesis, but it also supports the translocation of a small number of secretory proteins equipped with highly hydrophobic signal sequences (e.g. that of the periplasmic disulfide oxidoreductase DsbA)(16, 17). Unlike the Sec system, SRP functions co-translationally (18) (19): it selectively recognizes and binds the transmembrane segments of IMPs or highly nonpolar signal peptides as they emerge from the ribosome exit tunnel. It then delivers the ribosome-nascent protein complex to its inner membrane-bound receptor FtsY. Using energy provided by GTP hydrolysis, SRP and FtsY transfer their substrates to SecYEG and lateral transfer to the lipid bilayer (in the case of IMPs) or translocation to the periplasm (in the case of secretory proteins) (19, 20).

1.2.3 *Twin-arginine (Tat)-dependent protein export*

The twin-arginine translocation (Tat) pathway is mainly responsible for the export of folded proteins across the inner membrane and engages ~ 6% of all proteins secreted by *E. coli* (21, 22). The Tat-pathway is named after a highly conserved twin-arginine motif S**RR**XFLK (where X is usually, but not always a polar residue) present in the signal peptide of Tat-dependent substrates. These include cofactor-containing redox proteins (e.g. hydrogenases, nitrate reductases, and dimethyl sulfoxide (DMSO) reductases) (21), multimeric proteins that must assemble into a complex prior to export (e.g., hydrogenase components HyaA-HyaB and HybO-HybC) (23, 24), and proteins whose folding is too rapid for the Sec-dependent export. Tat-dependent transport relies on the TatA, TatB and TatC proteins. TatC, the largest and most

highly conserved component is composed of 6 transmembrane helices, while TatA and TatB both contain an N-terminal transmembrane helix followed by a short hinge region. Together, TatABC form an active transport system that is energized by the proton motive force (PMF) (25).

1.3 CYTOPLASMIC CHAPERONES AND THE SEC TRANSLOCON

From the brief description of the major secretion pathways above, it is evident that a number of proteins participate in the translocation of secretory proteins across the inner membrane, and that they work in concert to ensure that the process is efficient. This section will discuss the key players in greater detail. Since this dissertation focuses on periplasmic and outer membrane proteins that are translocated in a partially folded state, we will limit the discussion to the Sec- and SRP-dependent pathways.

1.3.1 *Trigger Factor*

Trigger Factor (TF) is a 48-kDa cytoplasmic chaperone composed of three distinct domains that adopts a "crouching dragon" structure (14). The N-terminal domain (the dragon "tail") is mainly responsible for docking onto the L23 ribosomal protein, which is located in the vicinity of the ribosome exit tunnel. The central peptidyl-prolyl *cis-trans* isomerase (PPIase) domain forms the dragon's "head" and is the most distant from the ribosome binding site. It is connected to the "tail" by a long linker region (14) (26) that is dispensable for chaperone activity *in vivo*, but that been shown to serve as an auxiliary substrate-binding site *in vitro* (27).

The C-terminal domain of TF forms the main body of the dragon. Two protruding helical "arms" constitutes almost 50% of its residues and are key to the chaperone function by binding

to partially folded substrates. Mechanistically, TF binds to the ribosome via its N-terminal tail, and projects over the exit tunnel to create a protective space where newly synthesized polypeptide chains are shielded from degradation by cytoplasmic proteases. Ribosome profiling analysis of TF-ribosome-nascent chain complexes indicates that *in vivo*, TF may pre-bound to ribosomes, but that TF-nascent chain interaction do not occur until after ~100 amino acids have been translated (10). For secretory proteins, the TF-bound newly synthesized chain is passed on to SecA (SecB may or may not interact with the complex prior to SecA) for the next step in translocation. Besides its function as 'holdase', TF has recently been shown to acts as an 'unfoldase' capable of rescuing misfolded or aggregated substrates by proactively unfolding the pre-existing folded structure (15, 28).

1.3.2 *Signal Recognition Particle*

The signal recognition particle (SRP)-dependent pathway and its components were elucidated in eukaryotic systems in the 1980s. A decade later, genes coding for their bacterial homologs were discovered (20) (29). Nowadays, it is widely acknowledged that SRP and its receptor are universally conserved in all species (19) and that ~25% of exported proteins may contain signal sequences that are recognized by SRP (30). In *E. coli*, SRP consists of a 54kDa homolog of the eukaryotic SRP protein named Ffh encoded by *ffh* gene, and a 4.5S RNA encoded by *ffs*. Ffh has two distinct domains: a M-domain enriched in methionine residues that recognizes SRP-dependent signal sequence and IMP transmembrane segments and binds to the 4.5S RNA, and a GTPase domain that interacts with a homologous GTPase domain of FtsY, the SRP-receptor protein. FtsY, also contains an N-terminal A-domain that enables its peripheral association with the inner membrane.

1.3.3 *SecB*

SecB is a 17-kDa cytoplasmic chaperone that usually functions as a homo tetramer (31). It is largely involved in shielding and delivering preproteins to the SecA molecular motor (32) in an unfolded and translocation-competent state. SecB does not bind directly to ribosome-nascent protein chain complex like TF does, but the two chaperones have overlapping pools of exported substrate including the precursors of OmpA, OmpC, OmpF, LamB, PhoE, TolC, DegP, FkpA and MBP (33) (11).

1.3.4 *SecA*

SecA is an essential ATPase with a size around 100-kDa and an intracellular concentration of 6 to 8 μM (34). This motor protein is composed of 4 major domains (35): a nucleotide binding domain (NBD), an intramolecular regulator of ATP hydrolysis domain (IRA2), a preprotein binding domain (PBD), and a C-domain. NBD and IRA2 sandwich ATP molecules which provide energy for the translocation event, while the C-domain is mainly in charge of controlling preprotein docking to the SecYEG translocase but also interacts with SecB for preprotein transfer (32) (36). Huber *et al*. (37) found that SecA can directly dock on the L23 ribosomal protein, suggesting that trafficking to the Sec translocon may not always rely on SecB or TF. Upon binding of a SecA-preprotein complex to the SecYEG translocase and subsequent capture of ATP, translocation is initiated through the inner membrane using energy from ATP hydrolysis, SecA remains bound to the translocase during the process and cycles off when export is complete (29) (38).

1.3.5 *The Sec translocase*

The Sec translocase lies in the *E. coli* inner membrane and consists of two heterotrimeric complexes: SecYEG and SecDFYajC. SecY is the central subunit and forms the protein-conducting channel. It contains ten α-helical transmembrane segments (TMS) organized into two pseudo-symmetrically aligned groups (TMS 1-5 and 6-10) that resemble a bivalve shell structure in the inner membrane, TMS 6/7 and 8/9 also form extensive contacts with the ribosome and SecA (39) (40) (41). SecE is another essential inner membrane protein made up of 3 TMS. It wraps around the SecY channel in a V-shaped manner, and helps stabilize the ten-TMS pore by clamping the two shells together (38). The other component of the SecYEG translocon is the bi-TMS SecG protein, it is not essential for cell viability, but translocation efficiency appears to be enhanced in its presence.

SecDFYajC is an accessory protein complex that is mainly associated with SecY (31), although SecG was also found to contact SecDF. SecD and SecF are each composed of 6 TMS and have large periplasmic loops, suggesting that the complex acts in the later stages of protein translocation and presumably pulls translocating proteins from the channel to the periplasmic side of the inner membrane (38). On the other hand, although the *yajC* gene was discovered in the *secDF* operon and although YajC co-purifies with SecDF (29), its role in the translocation process remains unclear.

1.4 SIGNAL PEPTIDES: STRUCTURE AND FUNCTION

1.4.1 *Sec-dependent Signal Peptides*

Secretory proteins are generally synthesized as preproteins that contain short N-terminal extensions (~20 amino acids in length) in front of their mature regions. These short peptides or signal sequences serve as a zip code that mark secretory proteins for extracytoplasmic translocation and direct them to specific secretion pathways. In addition to performing this targeting function, signal peptides also play a role in preventing the premature folding of preproteins in the cytoplasm and in facilitating transport across the inner membrane by coordinating interactions with components of the secretory apparatus (42-48).

Typical Sec-dependent signal peptides have a tripartite structure (Figure 1.2 A). The N-region consists of 1-3 amino acids and carries a net positive charge. The central H-region is hydrophobic, 10-15 residues in length and has a tendency to adopt an α-helical structure within the inner membrane, Finally, the C-region provides a helix breaking signal (most commonly via a turn-forming amino acids such as Proline, Glycine and Serine (49)). It also specifies the Ala-X-Ala (where X stands for any amino acid) recognition sequence of signal peptidase I (SPase I), the membrane-embedded protease that is responsible for cleaving off the signal sequence of preproteins, so that mature proteins can be released into periplamic space.

Miller *et al.* (42) and Lecker *et al.* (50) have demonstrated that signal sequences interact with the cytoplasmic molecular chaperone SecB and the SecA molecular motor, respectively. In addition, by interacting with the mature region of preproteins, signal peptides maintain preproteins in an unfolded conformation that is suitable for engagement by the Sec system (49). Increasing the average hydrophobicity of the H-region will reroute a preprotein from Sec-

dependent secretory pathway to SRP-dependent export, indicating that the chemical characteristics of the signal peptides can have a strong influence on preprotein recognition and routing. Mutagenesis experiments have also shown that replacing the positively charged amino acids of the N-region of Sec-dependent signal sequences by negative or neutral residues significantly reduces translocation efficiency (51). This implies that electrostatic interactions between the signal peptide N-region and the negatively charged inner leaflet of the inner membrane play an important role in the initiation of Sec-dependent translocation.

Upon delivery to the SecYEG translocon, signal peptides insert and orient themselves into the inner membrane by adopting an α-helical structure which serves as a transient membrane anchor. The C-terminal Ala-X-Ala recognition sequences docks into the catalytic site of the SPase I binding pocket, and the mature region is threaded through the membrane by SecA and exposed to the periplasm. When at least 80% of a preprotein has translocated in this fashion (2), SPase I cleaves the signal peptide from the mature region by utilizing a Lysine-Serine catalytic dyad processing mechanism (Figure 1.2 B). Mature proteins are released into the periplasm, and signal peptides are further degraded by signal peptide peptidase (SPP) (52, 53), which also resides in the inner membrane.

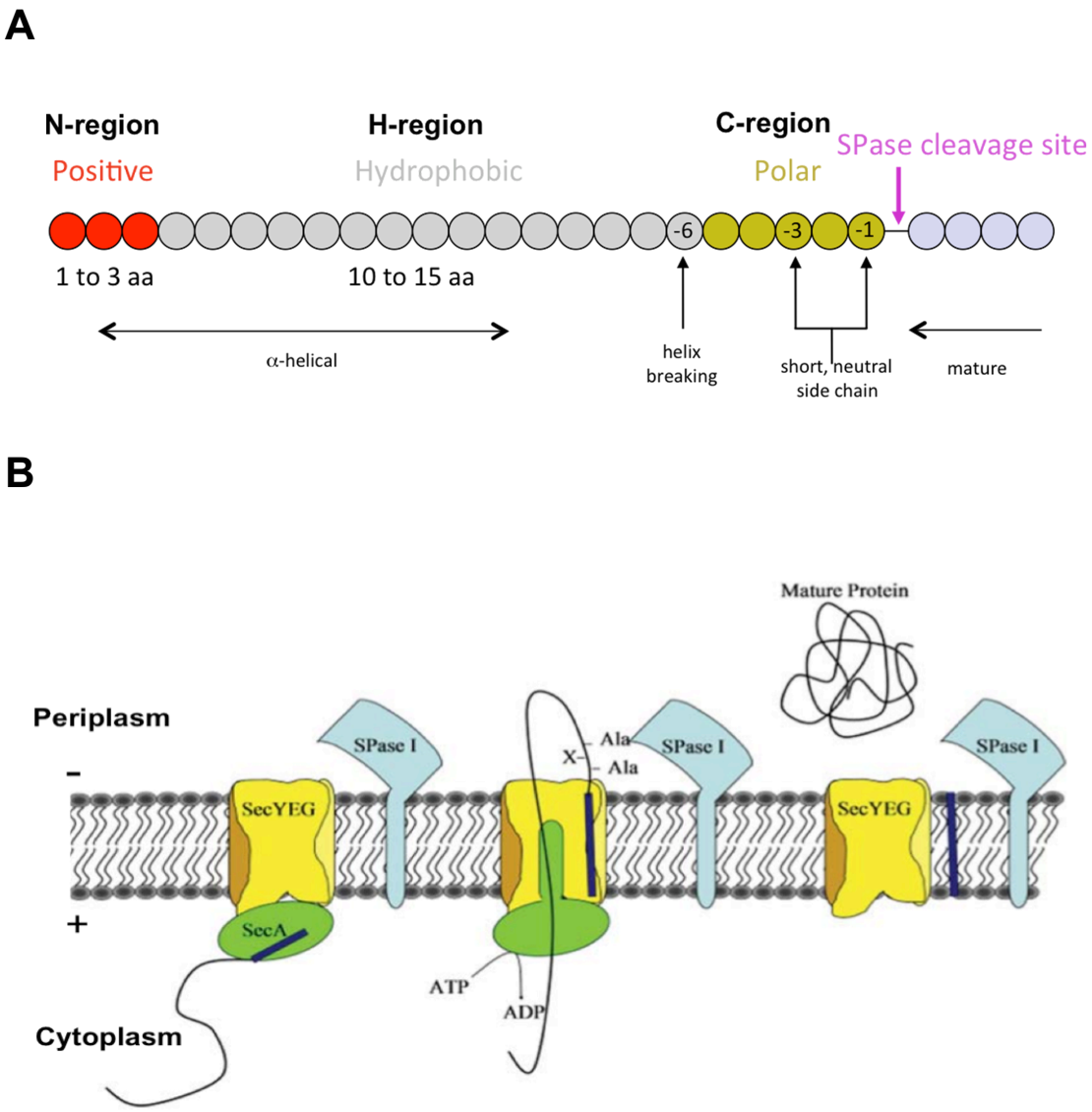

Figure 1.2 Structure of Sec-dependent signal peptides and an illustration of the process through which Sec-dependent preproteins are translocated across the inner membrane

A. The three-domain structure of a typical Sec-dependent signal peptide. See text for details.

B. The signal peptide inserts itself into the inner membrane by adopting an α-helical structure (dark blue rectangle) while the mature region is threaded through the SecYEG translocon by SecA. SPase I cleaves the signal peptide at the Ala-X-Ala recognition sequence to release a mature protein into the periplasm (Panel adapted from reference (2)).

1.4.2 *Autotransporter signal peptides and the Extended Signal Peptide Region (ESPR)*

Although signal sequences utilized in different pathways vary in overall hydrophobicity (SRP-dependent signal peptides usually are more hydrophobic than others), amino acid composition (Tat-dependent signal peptides contain signature RR tandem repeats), and have degenerate composition, the canonical signal peptide structure depicted in Figure 1.2 is ubiquitous in all cases.

However, some unusually long (>40 aa) signal peptides have also been identified in both prokaryotic and eukaryotic preproteins (54-57). In gram-negative bacteria, these long signal sequences are predominantly found in the Serine Protease Autotransporter of *E. coli* and *Shigella* (SPATE) protein family (58). Autrotransporters are a class of secreted proteins commonly involved in pathogenesis that consist of a N-terminal passenger domain (α-domain) and a C-terminal β-barrel domain. Virulence functions are typically associated with the α-helical passenger domains (Figure 1.3 A). The C-terminal region forms an OMP-like β-barrel pore in the outer membrane that is used to translocate the passenger domain and release it into extracellular environment (1, 59, 60).

Autotransporters are secreted across the inner membrane via Sec-dependent export (61, 62) and it is therefore not surprising that their C-terminal signal peptides contain the signature N, H and C regions of canonical Sec-dependent signal peptides. However, their N-terminal domain (called the Extended Signal Peptide Regions or ESPRs) that contributes most to overall length, are unique (Figure 1.3 B) (3, 60).

ESPR sequences are highly conserved across species, and therefore likely to play a functional role. Indeed, several recent studies (57, 58, 61) have reported that these regions

regulate the rate at which SPATEs are translocated to the periplasm. For instance, Desvaux *et al*. have shown that the ESPR region is proved to be transcribed and translated as a real functional portion of the signal peptide *in vivo* by using Pet – one of the SPATEs members as a model protein (3), thus dispute the hypothesis that the DNA encoding these ESPRs are only present as a region involved in regulating transcription or translation. In addition, SPATEs lacking an N-terminal ESPR or for which the entire signal peptide has been replaced by a canonical, Sec-dependent signal sequences localize to the outer membrane, albeit with much lower yields (58) (63). Finally, Szabady *et al.* (58) have proposed that ESPRs play an additional role after completion of translocation across the inner membrane, based on the observation that modifications of the ESPR of *E. coli* EspP prevent its delivery to the outer membrane due to periplasmic misfolding.

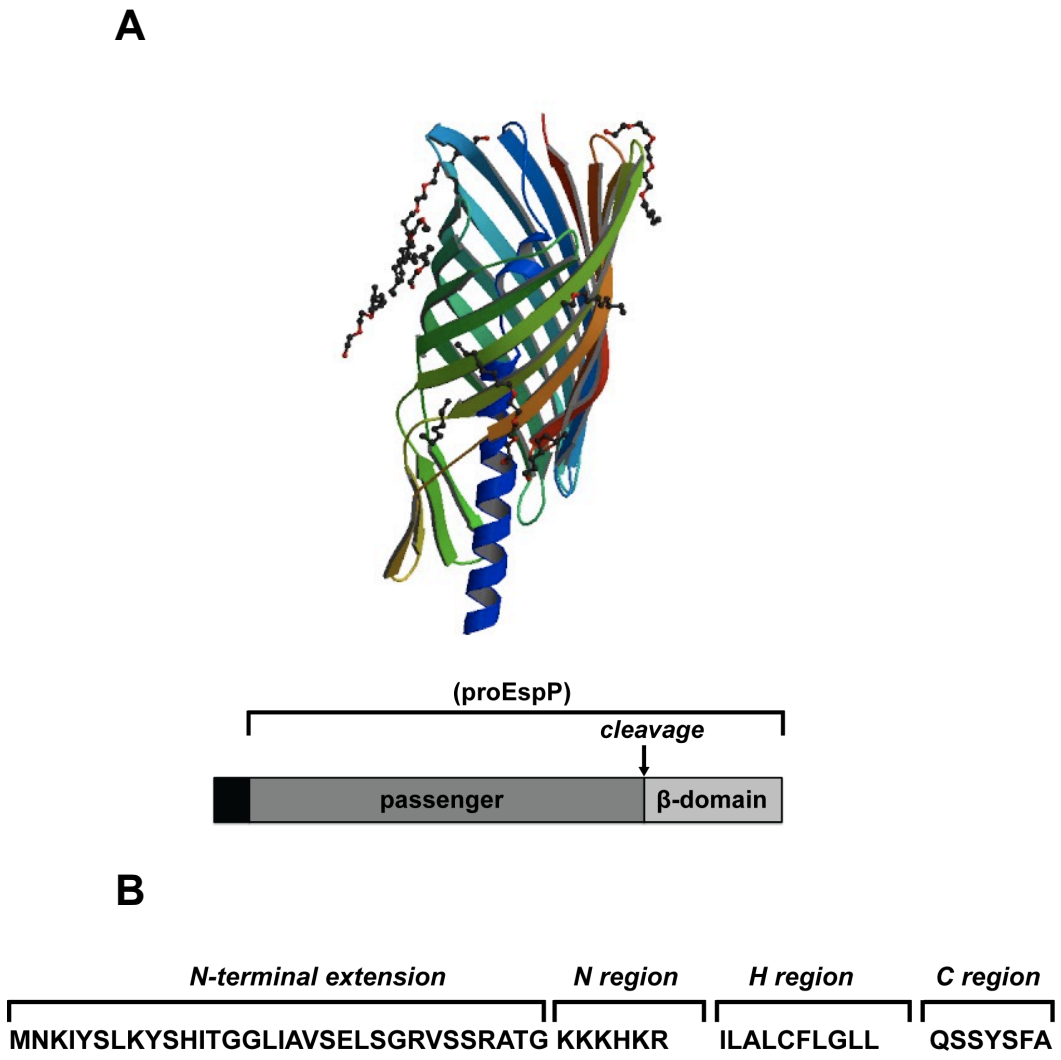

Figure 1.3 Ribbon structure of the *E. coli* EspP autotransporter and structure of SPATE's signal peptides

A. An example of E. coli SPATE: EspP. The structure of the autotransporter is shown before the passenger domain (internal α-helix) is cleaved and released from the β-barrel domain that has allowed for its translocation across the outer membrane (PDB 3SLJ). The schematic structure of the protein is shown below with the black box corresponding to the signal peptide (61).

B. Amino acid sequence of the EspP signal peptide: the N-terminal extended signal peptide region (ESPR) and the C-terminal region which resembles a canonical Sec-dependent signal peptides are depicted.

1.5 PERIPLASMIC CHAPERONES AND THE BAM INSERTASE

Following signal sequence processing and release into the periplasm, OMPs and other extracellular proteins face the challenge of trafficking across the viscous periplasmic space to reach the outer membrane (OM). Several periplasmic chaperones and a multi-component machinery dedicated to the insertion of OMPs into the outer membrane assist in the process. A brief summary of the structural, biochemical and genetic characteristics of each of these players is provided below.

1.5.1 *Skp*

Skp (Seventeen kilodalton protein) was identified as a periplasmic chaperone in 1996 (64) based on its ability to bind to a variety of affinity-immobilized OMPs. The crystal structure (65) shows that the functional Skp is a jellyfish-like homotrimer in which each monomer contributes a tentacular α-helical domain to a large hydrophobic cavity that accommodates partially folded OMPs.

A number of *in vitro* and *in vivo* studies (66-70) have confirmed that Skp is capable of selectively interacting with OMP substrates. For instance, Walton *et al* (70) have shown that Skp protects the β-barrel domain of OmpA from aggregating while allowing its C-terminal domain to independently fold in the periplasm. Skp can be cross-linked to the SecYEG in vivo (71), suggesting that it binds OMPs as they emerge from the translocon. However, it has also been argued that Skp acts late in OMP biogenesis since it contains a putative lipopolysaccharide (LPS)-binding site (one of the main components of the OM) and because LPS and Skp synergistically improve the efficiency of OmpA insertion into lipid bilayers *in vitro* (65, 67).

1.5.2 *SurA*

SurA was initially identified in 1990 as essential for the survival of bacteria stationary phase (72). It consists of 4 structural domains (Figure 1.4 B), two of which (P1 and P2) are implicated in its petidyl-prolyl *cis-trans* isomerase (PPIase) activity. SurA also functions as a molecular chaperone by using its N and C-terminal domains along with its P1 domain to form a globular core with a crevice capable of shielding extended peptides from the solvent (73).

A series of biochemical studies (74, 75) have shown that SurA preferentially binds to unfolded OMPs and to peptides enriched in aromatic residues arranged in a Ar-X-Ar pattern, where Ar represents an aromatic residue and X is any amino acid. This signature pattern occurs frequently within (and in particular at the C-terminus) of OMPs compared to soluble or inner membrane proteins. Indeed, strains lacking *surA* contain lower levels of major OMPs in their outer membrane (76-79). Although some studies have reported that only a subset of OMPs depend on SurA for insertion into the OM (80) (81), it is widely accepted that SurA plays a key role in OMP biogenesis.

1.5.3 *DegP and other periplasmic chaperones*

Aside from Skp and SurA, a number of periplasmic proteins function as chaperones. One of these is DegP, a housekeeping serine protease belonging to the HtrA family. DegP actively hydrolyzes misfolded proteins to relieve cellular stress (82, 83). However, it can also function as a periplasmic chaperone at lower temperature by switching to a different oligomeric state (66, 84-86). Other likely chaperone molecules include FkpA, PpiA and PpiD (87-89). For instance, although FkpA was identified as a heat shock periplasmic PPIase, it has been shown to suppress

the misfolding of a maltose-binding protein variant (88) and although PpiD overexpression can not compensate for the absence of SurA in the maturation of OMPs, it rescue the viability of *surA skp* double mutants (90). A more recent study (91) has shown that PpiD transiently interacts with the SecY translocon *in vitro* and *in vivo*, suggesting that it facilitates early steps in periplasmic translocation.

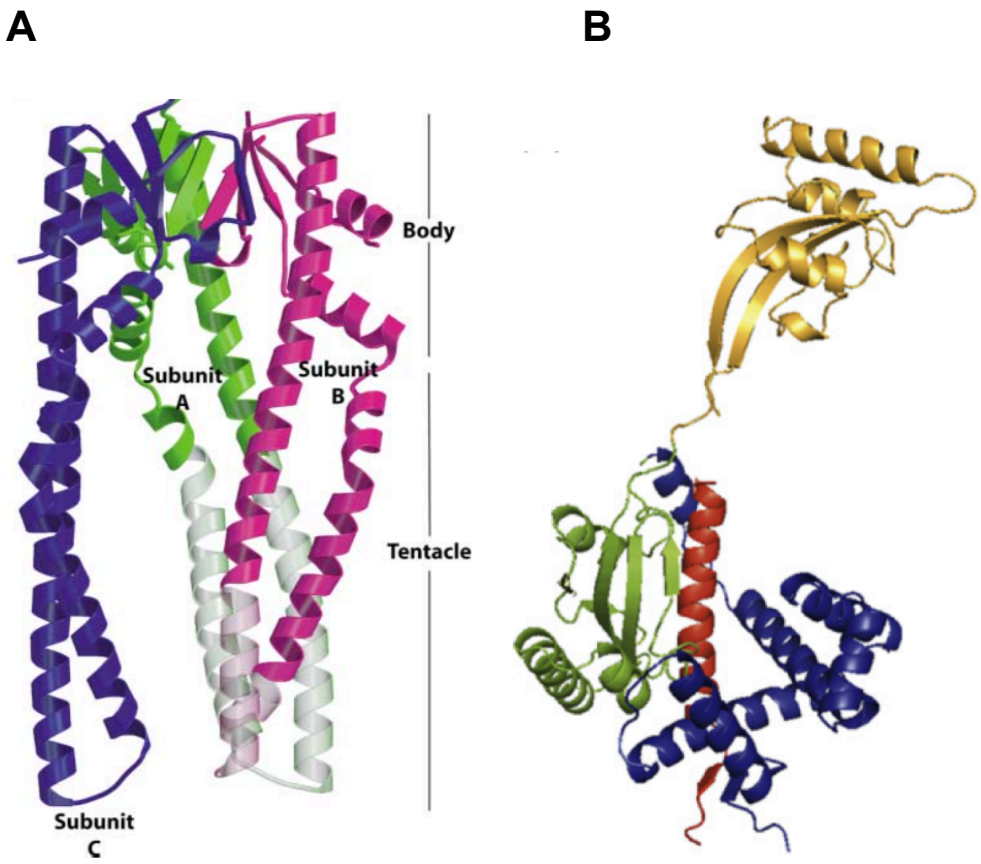

Figure 1.4 Structure of the periplasmic chaperones Skp and SurA

A. Ribbon structure of the Skp trimer. The three tentacular subunits are labeled. The light grey domain is not resolved in the crystal structure. Based on PDB 1U2M and adapted from reference (65).

B. Ribbon structure of SurA. The N- and C-terminal domains involved in chaperone function are colored in red and blue, respectively. The PPIase domains are colored in gold and green. Based on PDB 1M5Y and adapted from reference (73)

1.5.4 *The Bam (beta-barrel assembly machinery) translocation system*

The Bam translocon resides in the outer membrane. It is a multi-component system composed of a central pore, BamA (formerly known as YaeT) associated with four lipoproteins: BamB (formerly YfgL), BamC (NlpB), BamD (YfiO) and BamE (SmpA). BamA, which is highly conserved across bacterial species, is organized as a 16-stranded β-barrel (92) with a C-terminus spanning the outer memrbrane, and an N-terminal region residing in the periplasm. The N-domain consists of 5 POTRA (polypeptide translocation associated) modules, which is one the most distinguishing features of the Bam machinery. Several structural studies (81, 93-96) have revealed how the components of the Bam system associate with one another via POTRA-mediated interactions. BamA interacts directly with BamB and BamD, while the remaining two lipoproteins BamC and BamE, associate with the translocon by interacting with BamD (93). Aside from 'gluing' the various components together, there is evidence that the POTRA domains are also involved in OMP binding (97, 98), potentially by recognizing their C-terminal Ar-X-Ar signature sequences (99). The conserved *bamA* and *bamD* genes are essential for *E. coli* viability and inactivation of BamB leads to impairments in OMP assembly (92). On the other hand, loss of BamC or BamE only causes minor defects in OMP biogenesis (93).

Using LamB as a model system, Ureta *et al.* (100) have concluded that BamB is involved in early steps of OMP biogenesis. However, a study investigating the biogenesis of the autotransporter protein EspP suggests that BamB and BamD are involved at a late step of EspP assembly, based on the fact that their interactions with this substrate are longer than those of BamA (101). At present, how the Bam system (and especially its lipoprotein components) binds to and facilitates folding and insertion into the outer membrane remains unclear.

1.5.5 *Interplay between periplasmic chaperones and components of the Bam system*

It has been argued that SurA is the primary chaperone in charge of escorting OMPs across the periplasm, and that although Skp-DegP are also capable of performing this function, they primarily capture substrates that have escaped the SurA pathway. This conclusion is primarily based on the observation that, whereas combinations of *surA-skp* and *surA-degP* deletions are lethal to *E. coli* under normal growth conditions, *skp-degP* double mutants are viable (76). Nevertheless FRET experiments have revealed that DegP interacts with both Skp and SurA (102), and there is evidence that Skp can be cross-linked to the Sec translocon *in vivo* (71, 103), Thus, Skp may be the first chaperone involved in the capture OMPs. A hand-over to SurA would occur at a later stage of the process since SurA associates with the OM (75) and directly contacts the P1 POTRA domain of BamA (76) (104). Clearly, further investigations will be needed to elucidate the role of SurA, DegP and Skp in the OMP trafficking across the periplasm.

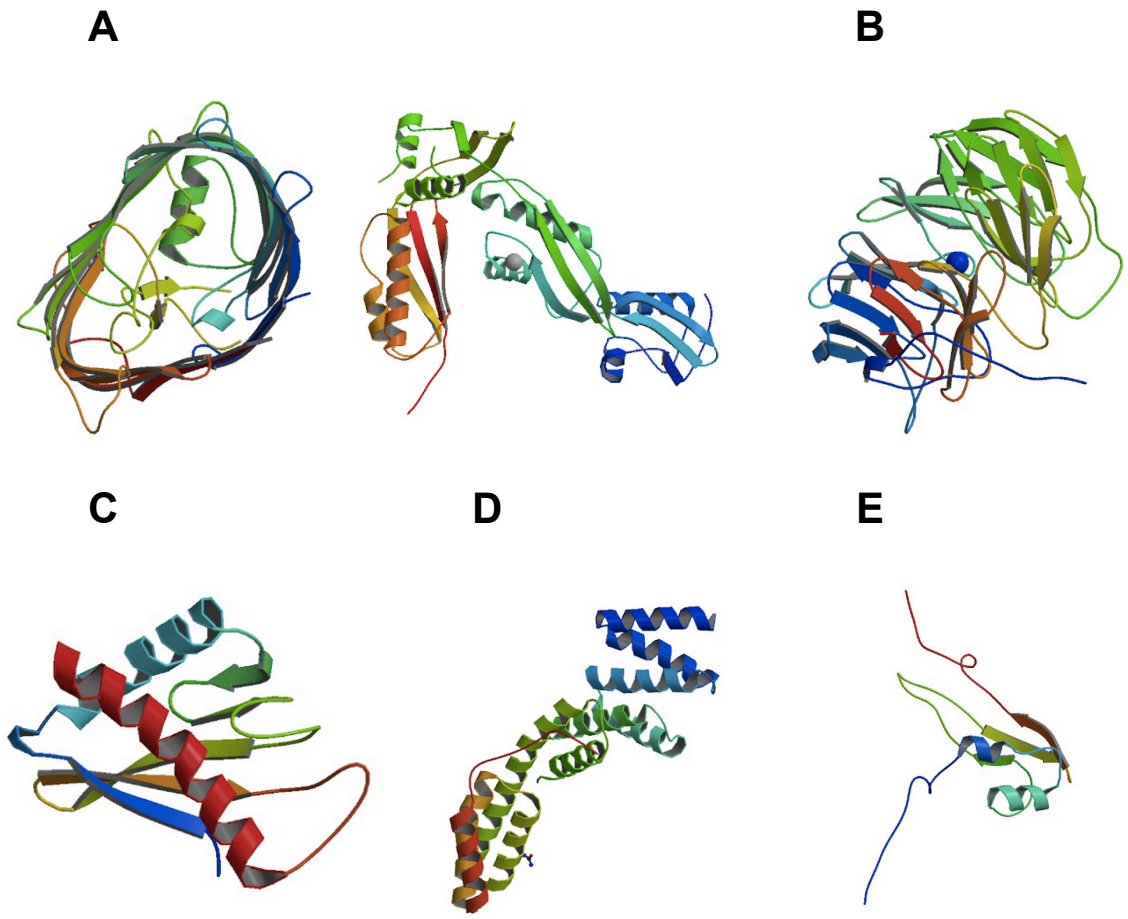

Figure 1.5 Components of the Bam translocation system

A. Ribbon structure of BamA: The C-terminal β-barrel domain (left) (PDB 4N75) (92) and N-terminal POTRA domain (right) (PDB 2QDF) (94) are shown. Figure 1.6 also provided an illustration of how BamA is assembled and interact with other Bam components.

(B-E) The ribbon structures of (B) BamB (PDB 3P1L) (105), (C) BamC (PDB 2LAE) (106) (D) BamD (PDB 2YHC) (107), and (E) BamE (PDB 2KM7) (108) are also shown.

1.6 OUTER MEMBRANE VESICLES AND EXCRETION

Outer membrane vesicles (OMVs) were first discovered in the 1960s while examining the ultrastructure of exotoxin-producing *Vibrio cholera* cells under the electron microscope (109). Today, vesiculation is recognized as a ubiquitous secretion mechanism in a variety of species including *E. coli*. OMVs are produced when a portion of the outer membrane starts bulging and pinching off from the membranous surface, releasing small vesicles with diameters ranging from 20 to 250 nm. As a result, OMVs can incorporate OMPs in a native orientation and entrap periplasmic fluid and proteins within their lumen (110-115).

Although the detailed biophysical mechanism responsible for OMV formation remains unclear, several hypothesis have been advanced. One attributes the main cause of vesiculation to the loss of OM-peptidylglycan linking components such as Lpp (113, 116). Alternative theories invoke the existence of regulatory curvature-inducing molecules (111), or that vesiculation may be triggered by stress in the cell envelope (e.g., the accumulation of misfolded periplasmic proteins and OMPs) (117, 118). Recent evidence correlating OMV formation to the level of misfolded proteins in the outer membrane (118) favor the latter scenario and it has been proposed that the role of OMVs is to alleviate cell envelope stress by selectively packing and eliminating unwanted materials. In addition, the genotypes of hyper-vesiculating mutants have been directly linked to genes governing the σ^E-dependent extracytoplasmic stress response in an elegant genetic study (119).

Because OMVs incorporate proteins and biomolecules from the donor bacterium (120, 121), they also perform a variety of biological functions (111, 113, 122-124). These include the delivery of virulence factors such as toxins, proteases and pro-inflammatory molecules, and, surprisingly that of DNA (125, 126). All of these molecules may help OMV-producing cells to

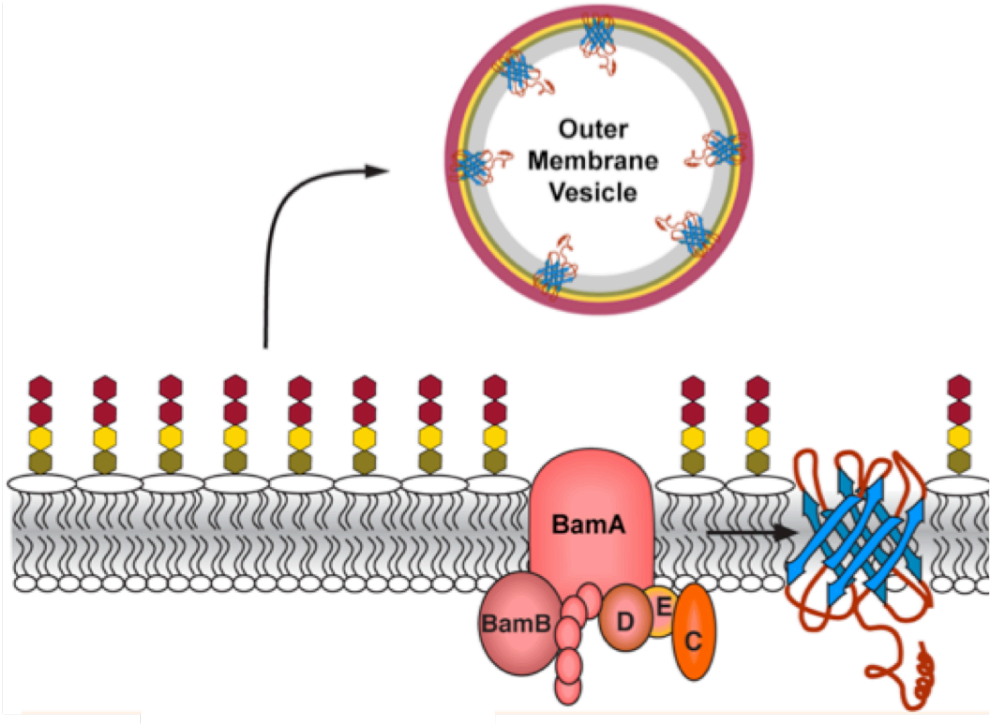

Figure 1.6 OMV biogenesis as an excretion mechanism

overcome competitors for nutrients or infect eukaryotic hosts (113, 124, 127-134). In addition, OMVs have been implicated in certain 'defense' mechanisms, such as alleviating stress in the cell envelope (117, 118, 135) and contributing to cell survival by adsorbing antimicrobials and bacteriophages (136, 137). Several studies have also demonstrated that OMVs play an important role in biofilm formation and maintenance by promoting communications and nutrient transport among cells and/or by enhancing the rigidity of the matrix (122) (138-141). Interestingly, OMVs from a community of eight bacterial strains that co-inhabit sedimentary rocks were found to participate in biomineralization (142).

Being equipped with self-adjuvant properties, OMVs are very effective at inducing immune responses and their potential for vaccination has been extensively explored (122, 129, 143-145). In fact, *Neisseria meningitis* OMVs are currently licensed and used for vaccination against serogroup B which causes meningococcal diseases (146-150). Kesty and Kuehn (151) first demonstrated that Ail, a heterologous outer membrane adhesin/invasin, could be selectively incorporated into *E. coli* OMVs and two subsequent studies showed that the immunogenicity of cytotoxin (ClyA) was greatly enhanced upon insertion into *E. coli* OMVs (152, 153). Gao *et al* (154) recently found that 30 nm gold nanoparticle coated with OMV membranes through a simple extrusion process induce strong and durable immune responses relative to OMVs alone.

The potential of OMVs is also being explored beyond vaccines. For example, Park *et al* (155) recently showed that a cascade of three enzymes displayed on the surface of OMVs was functional in the conversion of cellulose to glucose. Although these studies remain scarce, better tools for producing OMVs and for targeting engineered proteins to their membrane should increase their usefulness in the bionanotechnology arena.

1.7 SUMMARY

Secretory proteins make up approximately 30% of all polypeptides synthesized by gram-negative bacteria and they play critical role in cell survival and pathogenicity. They may be found in a soluble form in the periplasm (the interstitial space between inner and outer membranes), integrated within the outer membrane or excreted outside of the cell in a vesicular or globular form. In all cases, they must first translocate across the inner membrane. A substantial fraction of secretory proteins do so by making use of a cleavable N-terminal extension called signal sequence (or peptide) that is recognized by a dedicated translocation system known as the Sec pathway. Typical Sec-dependent signal sequences have a tripartite structure with a central hydrophobic core and are about 20 residues in length. However, certain secretory proteins implicated in virulence employ Sec-dependent signal peptides that are over 40 residues long.

Inspired by this phenomenon from nature, we first set out to test the possibility that extending signal sequence length might improve the yields of certain secretory proteins. To this end, we fused two Sec-dependent signal peptides to one another and compared their ability to support the translocation of secretory proteins across the inner membrane, especially for periplasmic and outer membrane proteins. In addition, these novel synthetic dual signal peptides were further investigated for their feasibility in the process of extracellular secretion, particularly in the form of outer membrane vesicles. The potential of an alternative strategy using periplasmic chaperones and Beta-assembly machinery components co-expression was also analyzed for the purpose of enhancing OMV production.

Chapter 2 Influence of synthetic dual Signal Peptides on the secretion of Periplasmic Proteins: Maltose Binding Protein (MBP) as a Case Study

2.1 INTRODUCTION

To determine if an extended leader sequence consisting of two consecutive Sec-dependent signal peptides would support protein translocation across the *E.coli* inner membrane, we selected the well-characterized signal sequences of *Escherichia coli* outer membrane protein A (OmpAss), and *Erwinia carotovora* pectate lyase B (PelBss). We fused these two peptides to one another to create synthetic dual signal sequences abbreviated POss (for PelB-OmpAss in which PelBss is followed by OmpAss) and OPss (for OmpA-PelBss in which OmpAss is followed by PelBss)

As an initial test of function, we constructed a series of plasmids encoding single and dual signal sequences followed by a mature version of maltose binding protein (MBP) under transcriptional control of the P_{BAD} promoter, and examined the performance of these synthetic signal sequences in supporting the secretion of this model protein. MBP, which is encoded by the *malE* gene, is normally translocated across the inner membrane via a typical Sec-dependent signal sequence (MalEss) and localizes to the periplasm where it binds to freely diffusing maltose (Figure 2.1 A). In concert with the maltose transport complex ($MalFGK_2$) which resides in the inner membrane (156) (157) (158), MBP facilitates maltose transport to the cytoplasm and therefore performs an essential role in metabolism. Here, we replaced native MalEss with POss and OPss and single signal sequence counterparts (Figure 2.1 B) to determine how the various leaders would impact MBP secretion.

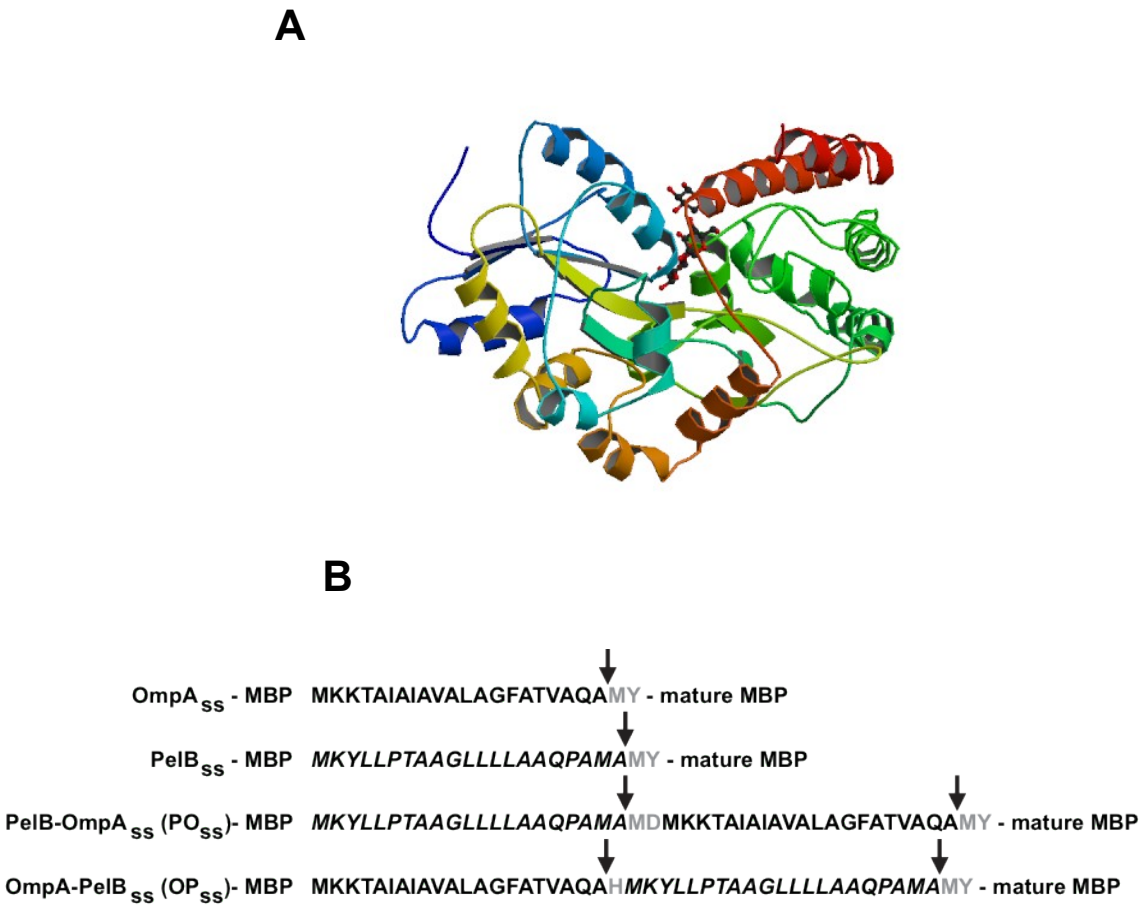

Figure 2.1 Structure of Maltose Binding Protein (MBP) and of single and dual signal sequences

A. Ribbon structure of maltose-bound MBP from Protein Data Bank (PDB1ANF).

B. Structure of the various signal sequences fused to the N-terminus of MBP. Arrows show the location of the SPase I cleavage site. Extra amino acids inserted to preserve the reading frame are identified in grey.

2.2 MATERIALS AND METHODS

2.2.1 *Plasmid constructions*

Skp (Seventeen kilodalton protein) was identified as a periplasmic chaperone in 1996 (64) based on its ability to bind to a variety of affinity-immobilized OMPs. The crystal structure (65) shows that the functional Skp is a jellyfish-like homotrimer in which each monomer contributes a tentacular α-helical domain to a large hydrophobic cavity that accommodates partially folded OMPs.

To build an MBP expression plasmid, pBAD33MutHpa (159) was digested with *Xba*I and *Hpa*I and the fragment specifying the *araC* gene and the P_{BAD} promoter was ligated in the same sites of pET-27b(+) to replace the T7 promoter. The resulting plasmid was named pWZ100. A DNA cassette encoding mature MBP was PCR amplified from pMAL-c2 (New England Biolabs) using primers 5'- GACGAGCGCATATGAAAATCGAAGAAGGTAAA-CTG-3' and 5'-ATCCGA-TCTCGAGTTACCTTCCCTCGATCCC- 3' which introduce *Nde*I and *Xho*I site at 5' and 3' ends of the amplified fragment, respectively. The PCR product was digested with the corresponding restriction enzymes and ligated into the same sites of pWZ100 to create pMBP, which serves as a signal-sequence-less control. To build OmpAss-MBP, primers 5'-GCGGACACATGTATATGAAA-ATCGAAGAAGGTAAACTGG- 3' and 5'-ATCCGATCTCGAGTTACCTTC-CCTCGATCCC- 3' were employed to amplify mature MBP with flanking *Afl*III and *Xho*I sites. The digested fragment was inserted into *Nco*I-*Xho*I digested pOmpAss-OmpA (see section 3.2.1). The same fragment was also ligated into *Nco*I-*Xho*I digested pWZ100, pPOss and pOPss-OmpA (see section 3.2.1) to yield pPelBss-MBP, pPOss-

MBP and pOPss-MBP, respectively. All MBP constructs were introduced in strain HS2019 for subsequent experiments. Strains and plasmids used in this chapter are listed in Table 2.1.

Table 2.1 Strains and plasmids used in Chapter 2

Name	Description	Source or reference
Strain		
Top10	F' *endA1 recA1 hsdR17* (r_K^-,m_K^+) λ^- *supE44 thi1 gyrA96 relA1* ϕ*80*Δ*lac*Δ*M15*Δ(*lacZYA-argF*)U169 *deoR*	Invitrogen
MC4100	F^- *araD* Δ(*argF-lac*)*U169 rpsL150 relA1 deoC1 ptsF25 flbB5301 rbsR*	(157)
HS2019	MC4100F^- *araD139* Δ*lac* U169 *rpsL thi* Δ*malE444*	(160)
Plasmid		
pET-27(b)+	pBR322-derived T7 expression vector (Kan^R)	Novagen
pWZ100	pET-27(b)+ derivative in which the T7 promoter has been replaced with the P_{BAD} promoter and the *araC* gene.	This study
pMAL-c2	Plasmid encoding a signal sequence-less version of MBP under transcriptional control of the P_{lac} promoter. Produces a cytoplasmic version of MBP.	NEB
pMBP	pWZ100 derivative encoding a signal sequence-less version of MBP under P_{BAD} promoter control	This study
pOmpAss-MBP	pWZ100 derivative encoding a version of MBP fitted with the OmpA signal sequence under P_{BAD} promoter control	This study
pPelBss-MBP	pWZ100 derivative encoding a version of MBP fitted with the PelB signal sequence under P_{BAD} promoter control	This study
pPOss-MBP	pWZ100 derivative encoding a version of MBP fitted with the synthetic PelB-OmpA signal sequence under P_{BAD} promoter control	This study
pOPss-MBP	pWZ100 derivative encoding a version of MBP fitted with the synthetic OmpA-PelB signal sequence under P_{BAD} promoter control	This study

2.2.2 *Cell growth and protein expression*

Shake flasks (125mL) containing 25mL of LB media supplemented with 50 μg/mL kanamycin were inoculated to an OD_{600} of ~0.05 and grown at 37°C to mid-exponential phase. At $OD_{600} \approx 0.5$, protein synthesis was induced by addition of 0.2% L-arabinose to the growth medium. Optical density was measured every 30 min to obtain growth curves. At 1.5h post-induction, 1mL of cells were collected and sedimented by centrifugation at 10,000*g* for 2 min. Pellets were washed with 20 mM Tris-HCl buffer (pH 7.5), resuspended in sample buffer and fractionated by SDS-PAGE. In all cases, the volume of sample buffer added was normalized to the optical density at the time of harvest, so that each sample corresponded to same amount of cells. Duplicate aliquots were loaded on duplicate 12.5% SDS gels, one of which was used for immunoblotting and the other stained with Coomassie blue. For Western blots, gels were incubated in transfer solution (25 mM Tris-HCl, pH 8.3, 0.2 M glycine, 3 mM SDS, 20% vol/vol methanol) and proteins were transferred to a nitrocellulose membrane overnight at 15 V and 4°C. Membranes were probed with rabbit anti-MBP antibody (NEB) at 1:5000 dilution, incubated with goat-anti-rabbit IgG Alkaline Phosphatase (Biorad) at 1:3000 dilution, and detected by colorimetry with 5-bromo-4-chloro-3-indolyl phosphate and nitrotetrazodium blue. Protein production was quantified using the ImageJ software (NIH).

2.2.3 *Microscopy imaging technique*

Approximately 10 μL of cells from each flask (volume normalized to OD_{600}) were deposited onto microscope slides, covered with a cover slip and allowed to settle for ~10 min at room temperature. Cells were imaged by phase-contrast on a Nikon Eclipse TE2000-U equipped

with a CCD camera (Photometrics Coolsnap ES). All images were taken at the same exposure level and magnification (90X).

2.2.4 *Viability Testing*

Samples were harvested at the indicated time points and volumes used for spotting were normalized to OD_{600} using the formula OD x μL = 5. As a result, each undiluted spot contains approximately the same amount of cells. Serial 10x dilutions were conducted with LB medium. All samples (XX μL) were spotted onto LB-agar plates supplemented with 50 μg/mL kanamycin. Plates were incubated overnight at 37°C and photographed.

2.2.5 *MBP activity assay*

Maltose-MacConkey agar was used to probe MBP function. Cell samples collected 1.5h post-induction were streaked on MacConkey base agar (Difco) supplemented with 1% (wt/vol) maltose and 50 μg/mL kanamycin. Plates were incubated at 37°C for ~16h and photographed.

2.3 RESULTS AND DISCUSSION

2.3.1 *Dual signal peptides are functional for MBP secretion*

A series of plasmids encoding mature MBP preceeded by the OmpA, PelB, PO or OP signal peptides and under transcriptional control of the arabinose-inducible P_{BAD} promoter were constructed as described in Materials and Methods. HS 2019 (Δ*malE*) cells harboring the corresponding plasmids were grown in LB medium at 37°C, induced in mid-exponential phase and cell growth was monitored for 3h post-induction. Figure 2.2 shows that expression of MBP from the dual signal sequence variants (open circles and squares) was more deleterious to cell growth compared to single sequence constructs (closed circles and squares) or a control lacking a secretion signal (inverted triangle). Although cultures producing MBP from the OmpAss exhibited healthiest growth, phase contrast microscopy conducted on cells harvested 1.5h post-induction revealed irregular morphology instead of the expected rod shape of healthy *E.coli* (Figure 2.3). Viability spot testing conducted on the same samples confirmed that these cells were at least 100 times less viable than those synthesizing MBP outfitted with $PelB_{SS}$ or one of the two synthetic signal sequences.

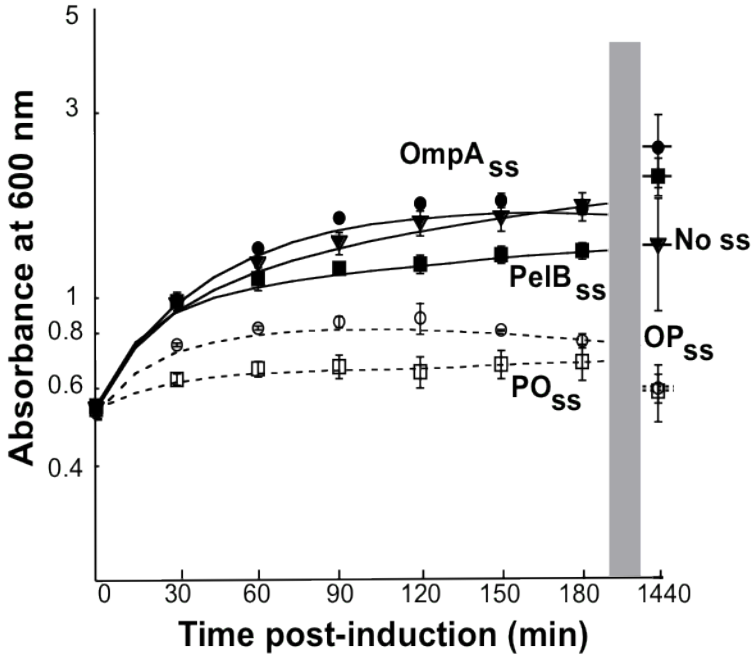

Figure 2.2 Influence of signal peptides on the growth of cells overexpressing MBP.

.

Growths of HS2019 Cells harboring MBPs fused with different signal peptides at 37°C were monitored by optical density till 3h (180min) post induction. OD600 at 24h post-induction were also shown in the figure. Symbol representations are as follows:

Inverted triangles: NO ss; Closed circles: OmpAss; Closed square: PelBss;

Open square: POss; Open circles: OPss.

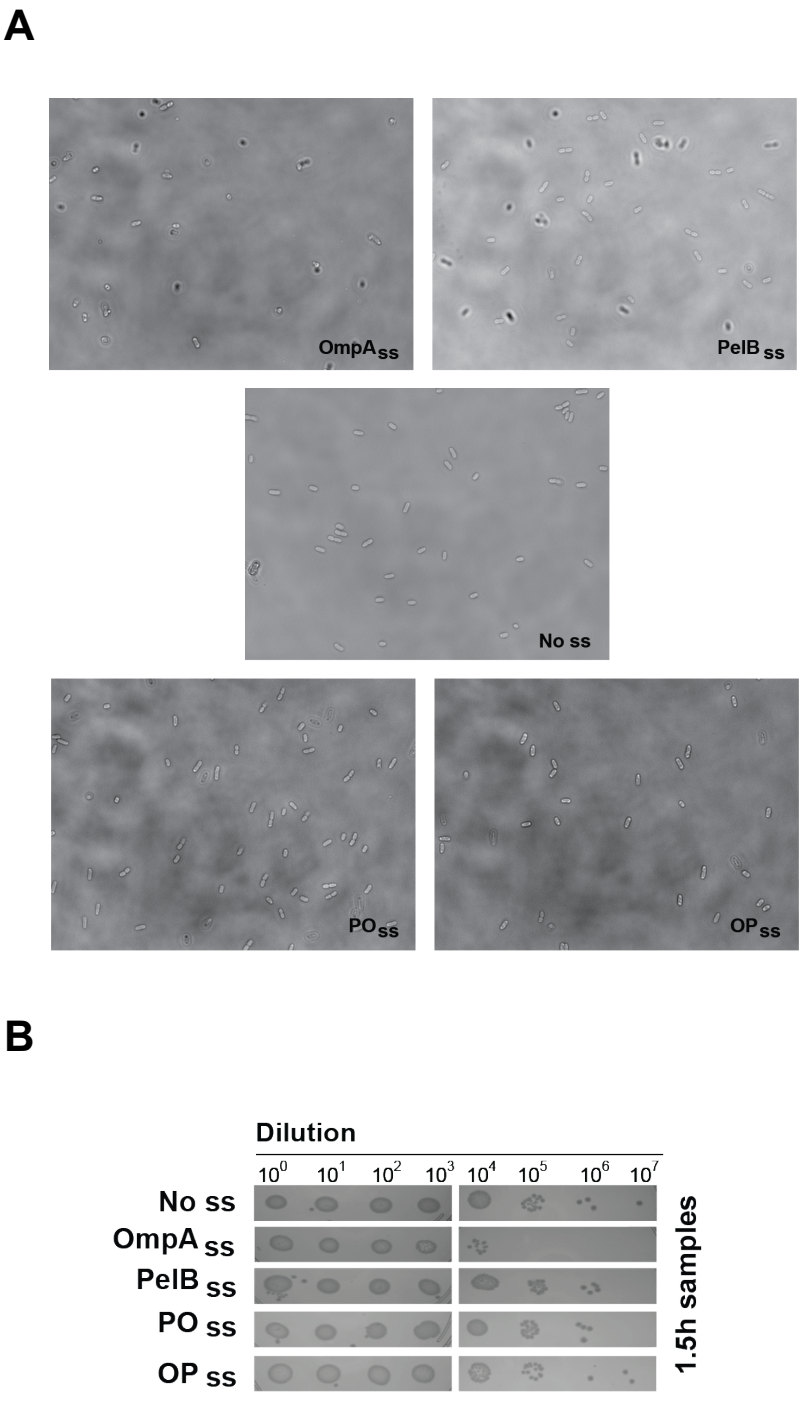

Figure 2.3 Influence of different signal peptides on the viability of cells overexpressing MBP

Cells overexpressing MBPs were collected at 1.5h post-induction from each signal peptide fusion. Their morphology were imaged by phase-contrast microscopy as in panel A, a duplicate cell sample from each construct was also subject to viability testing as in panel B.

To correlate growth and viability results with protein expression levels and signal peptide processing efficiency, samples harvested 1.5h post-induction were fractionated by SDS-PAGE and subjected to immunoblotting with anti-MBP antiserum. Figure 2.4 shows that mature MBP (*m*) could be detected in all samples, indicating that both single and dual signal sequences remain capable of supporting secretion.

To quantitatively compare secretion efficiencies, the levels of precursor and mature MBP were quantified by normalized videodensitometric analysis of gels and blots. Figure 2.4 A shows that although the use of OmpAss led to the highest levels of mature MBP accumulation (arrow m), over 90% of the protein produced was aggregated precursor (p1). The use of PelBss led to a ~ 3.5 fold reduction in total MBP accumulation. However, because 30% of this material was correctly processed by SPase I, comparable levels of mature MBP were obtained whether OmpAss- or PelBss-directed secretion. From a secretion standpoint, the dual signal sequence variants recapitulated the behavior of their initiator signal sequence. Total MBP accumulation was 2.5-fold higher in cultures synthesizing OPss-MBP relative to POss-MBP, but more efficient processing of the PO signal peptide led to similar level of mature product in each cell. Overall, however, there was a > 60% reduction in the total levels of MBP accumulation (precursor and mature) when POss was used in place of OPss.

To confirm that the secreted MBP was functional, samples collected 1.5h post-induction were streaked on maltose-MacConkey agar, an indicator medium, that changes color in proportion to the amount of maltose fermented (157, 158), and where redder colonies reflect the presence of larger amounts of active MBP in the periplasm. As expected, HS2019 (Δ*malE*) cells harboring the signal sequence-less control plasmid pMBP formed white colonies. Surprisingly, cells expressing MBP from the PelBss and POss were only slightly pink, while cells producing

MBP from the OPss were of a darker shade of red (Figure 2.5). Additionally, although cells producing MBP from the OmpAss were redder on maltose-McConkey agar, few colonies were viable after 16h incubation on selective medium and in good agreement with the spot test results of Figure 2.3.

Taken together, the above results suggest that each signal peptide has merit and disadvantages depending on whether one prioritize signal peptide processing, levels of precursor or mature protein accumulation, or production of properly folded protein. Among our dual signal sequence constructs, OPss combines the benefits of OmpAss (high yield of functional protein) with those of PelBss (higher viability and lower precursor accumulation).

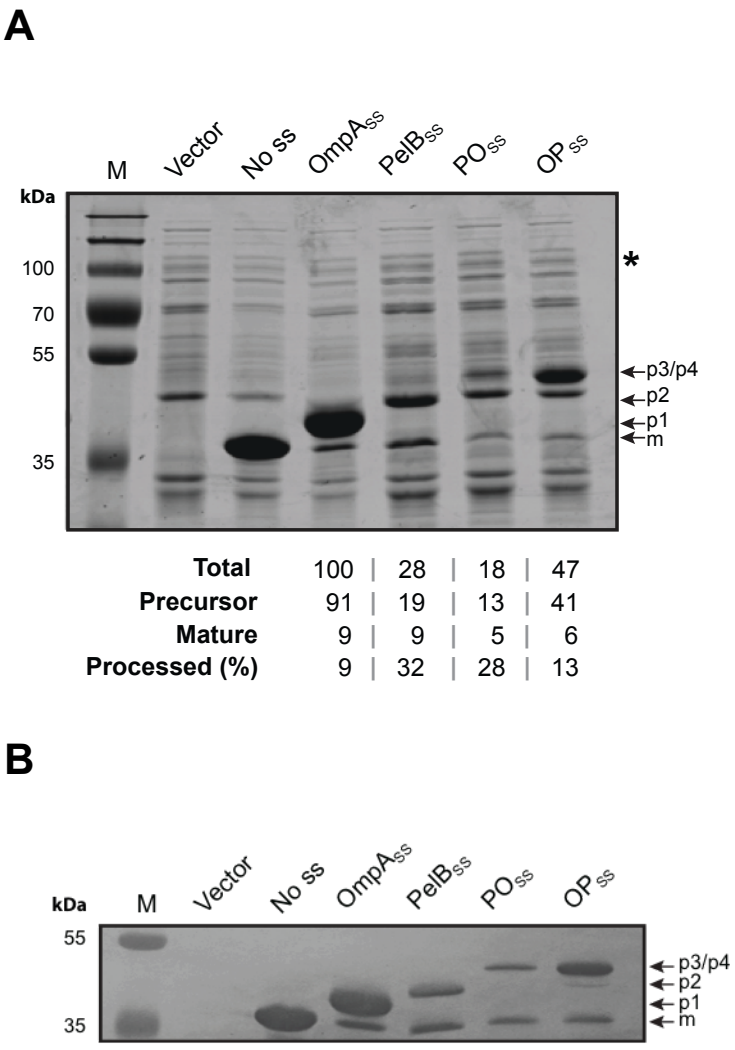

Figure 2.4 Influence of different signal peptides on MBP expression

A. HS2019 cells harboring pOmpAss-MBP, pPelBss-MBP, pPOss-MBP and pOPss-MBP were harvested 1.5h post-induction. Cells harboring the cloning vector pWZ100 were also ran on the gel to serve as negative control (vector). Arrows indicate the location of precursor versions of MBPs with *p1* corresponding to OmpAss-MBP, p2 to PelBss-MBP, p3 to POss-MBP and p4 to OPss-MBP. The migration position of mature MBP (*m*) is also.shown. The asterisk identifies the locations of the normalization band. Numbers below the gel correspond to the normalized intensity of precursor and mature species. Calculated processing efficiency are shown. Similar results were obtained in three separate experiments.

B. Immunoblotting of the same samples with anti-MBP antiserum.

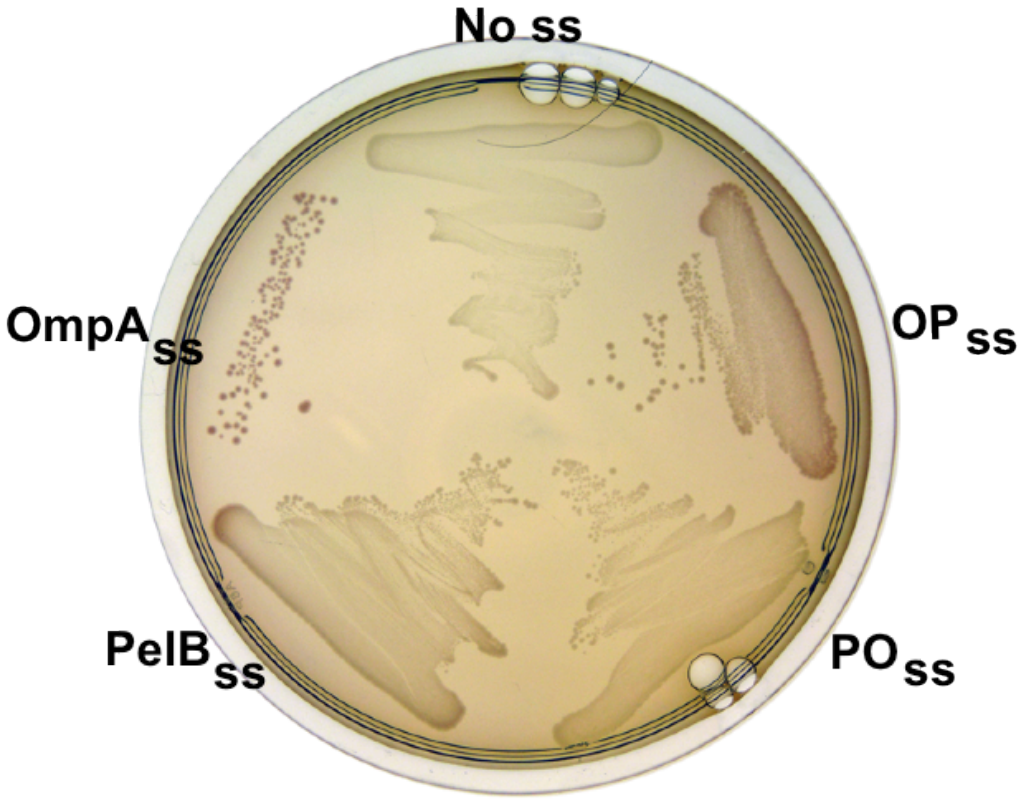

Figure 2.5 Influence of different signal peptides on MBP activity

HS2019 cells harboring pMBP, pOmpAss-mbp, pPelBss-MBP, pPOss-MBP and pOPss-MBP were streaked on maltose-MacConkey plates supplemented with 50 μg/mL kanamycin 1.5h post-induction. Plates were incubated at 37°C for 16h.

2.3.2 *Dual Signal Peptides are preferentially cleaved at their C-terminal SPase site*

The dual signal sequence constructs specify two potential cleavage sites for SPase I (Figure 2.1 B). In the case of OPss, we were indeed able to detect a small amount of immunoreactive (and presumably aggregated) product migrating at a position intermediate between those of mature MBP and uncleaved OPss-MBP (Figure 2.4 B). Interestingly, we failed to detect a similar internal cleavage product in the case of POss-MBP, perhaps due to lower expression, or to the fact that the OmpAss is more easily cleaved than the PelBss.(161-164). In both cases, however, the dominant precursors consisted of MBP with intact dual leader peptides (products p3 and p4 in Figure 2.4). Thus, although dual signal sequences are preferentially cleaved at the SPase I site located before the start of the mature protein, processing remains possible (albeit very inefficient) in at the internal site located at the junction of the signal sequences in the case of OPss construct.

2.4 CONCLUSIONS

In this chapter, we have shown that synthetic signal sequences created by fusing two archetypal Sec-dependent signal peptides to one another remain capable of supporting the secretion of MBP, a model periplasmic protein and that such dual signal peptides are primarily cleaved at the SPase I site proximal to the start of the mature protein. Although their use leads to a decrease in cell fitness and mature MBP production, OPss appears to give a slight increase in the amount of properly folded and bioactive MBP (Figure 2.5) while the use of POss results in the lowest levels of preprotein accumulation (Figure 2.4). Thus, dual signal peptides may have some advantages over traditional Sec-dependent leader sequences for secretory protein production.

Chapter 3 Influence of synthetic dual Signal Peptides, Trigger Factor and Signal Recognition Particle on Outer Membrane Protein biogenesis: Outer Membrane Protein A (OmpA) as a Case Study

3.1 INTRODUCTION

Based on insights from Chapter 2, we explored the use of dual signal peptides for the production on another type of secretory protein – outer membrane proteins (OMPs).

OMPs are β-barrel proteins that are located in the outer membrane of gram-negative bacteria, and make up 2-3% of their proteome (165). They carry a number of essential functions including maintenance of outer membrane integrity (e.g. OmpA), nutrient transport from the growth medium to the periplasm in substrate-specific (e.g. LamB, ScrY) or non-specific manner (e.g. OmpC, OmpF) (166), translocation across the outer membrane (e.g. BamA), and adhesion and virulence processes (e.g. autotransporter family) (165, 167, 168).

As discussed in Chapter 1, the molecular chaperone Trigger Factor (TF) participates in OMP biogenesis (10, 169, 170). TF engages newly synthesized preproteins, to prevent their premature folding by functioning as "holdase" and actively unfold misfolded nascent proteins through an "unfoldase" function (15), while Signal Recognition Particle also contributes to the biogenesis of some secretory proteins provided that their signal peptides are highly hydrophobic (16, 17, 19).

In this chapter, we study how single and dual signal peptides affect outer membrane protein biogenesis using OmpA as a model system (Figure 3.1). We also explored the role of Trigger Factor and SRP in the process in order to determine the rate limiting factor in the secretion of outer membrane proteins.

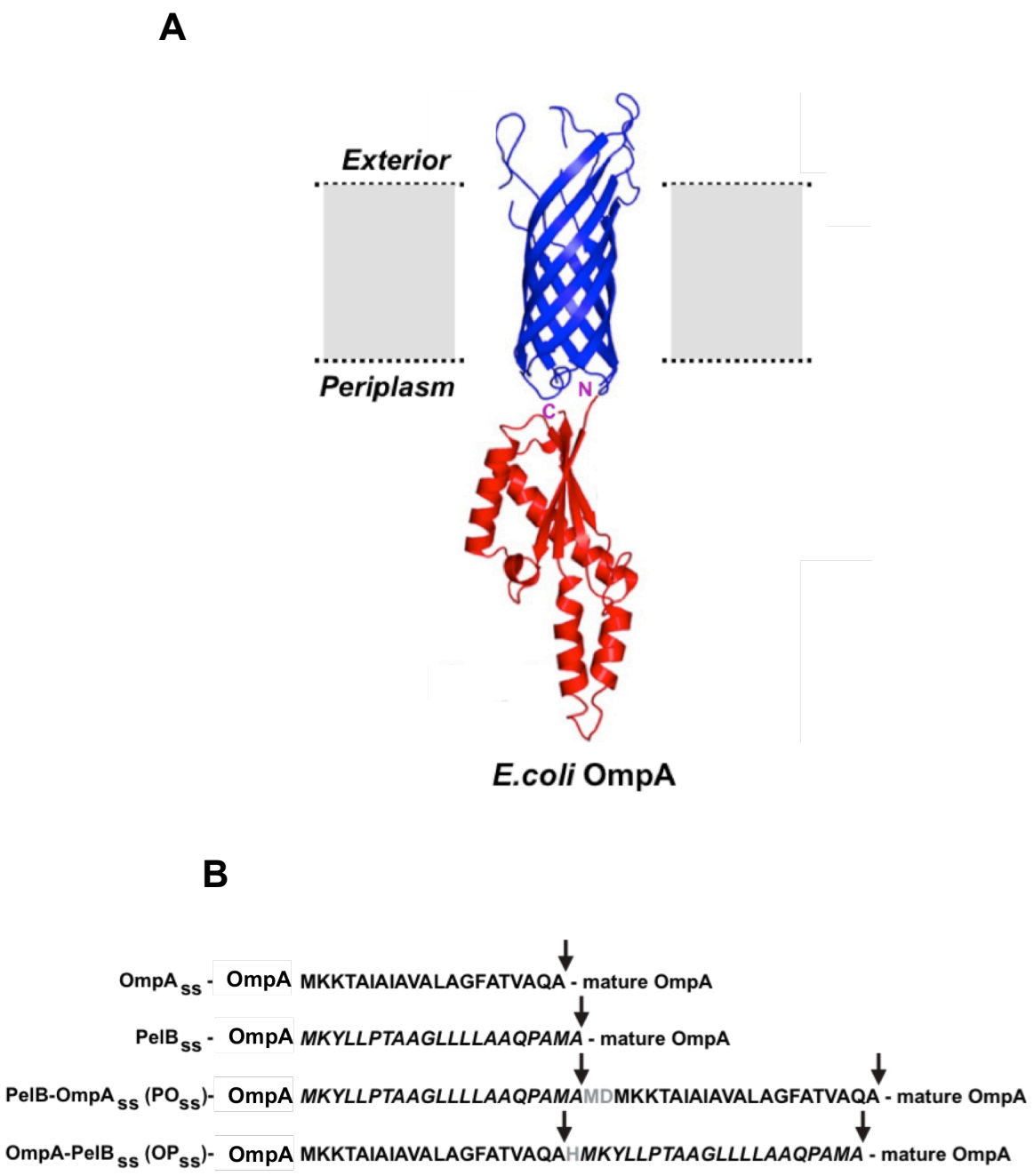

Figure 3.1 Structure of Outer Membrane Protein A (OmpA) and of single and dual signal sequences

A. OmpA structure and topology (picture adapted from (70)). N-terminal eight β-stranded barrel is colored in blue and C-terminal periplasmic domain in red.

B. Mature OmpA equipped with different signal peptides. Arrows indicate SPase I cleavage sites, letters in gray are extra amino acids inserted to preserve the reading frame.

3.2 MATERIALS AND METHODS

3.2.1 *Plasmid constructions*

Plasmid pWZ100 was described in Chapter 2. A DNA cassette encoding mature OmpA was amplified from the MC4100 genome using primer pair 5'-ACTCAGCTCATATGGCTCCGAAAGATAACAC-3' and 5'- CTACCACTCGAGA ACTTAAGCCTGCGG- 3' to introduce *Nde*I and *Xho*I site at 5' and 3' ends of the amplified fragment, respectively. The PCR product was digested with these enzymes and ligated in the same sites of pWZ100 to create pOmpA, a signal-sequence-less control. To build OmpAss-OmpA, mature OmpA with its native signal sequence was amplified using 5'-ACGAGGCCCATATGAAAAAGACAGCT ATG-3' and the reverse primer above. The resulting fragment was digested with *Nde*I and *Xho*I and inserted in the same sites on pWZ100 to yield pOmpAss-OmpA. Forward primer 5'-CTAGTACCATGGATGCTCCGAAAGATA-ACAC-3' and 5'-ACGAGGCCATGGATATGAAAAAGACAGC-3' paired with the same reverse primer above were used to amplify *Nco*I-*Xho*I flanked DNA fragments to ligate with digested pWZ100, which produced pPelBss-OmpA and pPOss-OmpA, respectively. To transpose OmpAss and PelBss, 5'-CGGACGCCCATA-TGAAAAAGACAGCTATCG-3' and 5'-TGATCTTTCATATGGGCCTGCGCTA-CGGTA-3' were used to clone OmpA signal peptide sequences out of pOmpAss-OmpA, *Nde*I digested fragment and pWZ100 were ligated together to produce pOPss-OmpA (construct with the correct orientation was selected and confirmed by DNA sequencing). In addition, a pWZ100 derived expression vector containing *Nde*I-*Nco*I flanked PO dual peptides was also built to facilitate inserting other model proteins. First, mutagenesis primers 5'-CAGCCGGCGATGGCTATGGATATGAAAAG-3' and 5'-

CTTTTTCATATC-CATAGCCATCGCCGGCTG-3' were employed to eliminate internal *Nco*I restriction sites at the C-terminus of PelB signal peptide, PO dual peptide fragments were then cloned out by 5'-CGGACGCCCATATGAAAAAG-ACAGCTATCG-3' and 5'-TATATTTCCATGGCCTGCGCTACGGTA-3' and ligated into *Nde*I-*Nco*I digested pWZ100 to yield the final product named as pPOss. All the OmpA constructs were transformed into BW25113 or KTD101 (Trigger Factor deletion isogenic strain of BW25113) for expression.

For Trigger Factor and overexpression studies, OmpA with different signal peptide fusions were co-transformed with either pMM102 (171) as a negative control or Plasmid pTFP, a pMM102 (171) derivative encoding the *tig* gene under native promoter control and producing a moderate amount of TF (Baneyx group unpublished data), and plasmid pSRP, a pMM102 derivative encoding the *ffh* and *ffs* genes under native promoter control and producing a moderate amount of SRP were used to study the effects of TF or SRP overproduction on OmpA biogenesis.

Strains and plasmids used in this chapter are listed in Table 3.1.

Table 3.1 Strains and plasmids used in Chapter 3

Name	Description	Source or reference
Strain		
Top10	F' *endA1 recA1 hsdR17* (r_K^-,m_K^+) λ^- *supE44 thi1 gyrA96 relA1* ϕ*80* Δ*lac* Δ*M15* Δ(*lacZYA-argF*)U169 *deoR*	Invitrogen
MC4100	F^- *araD* Δ(*argF-lac*)*U169 rpsL150 relA1 deoC1 ptsF25 flbB5301 rbsR*	(157)
BW25113	Δ(*araD-araB*)*567 ΔlacZ4787* (::*rrnB-3*) $lacI^p$*-4000*($lacI^Q$) λ^- *rph-1* Δ(*rhaD-rhaB*)*568 hsdR514*	(172)
KTD101	BW25113 Δ*tig100*	(171)
Plasmid		
pWZ100	pET-27(b)+ derivative in which the T7 promoter has been replaced with the P_{BAD} promoter and the *araC* gene.	Chapter 2
pOmpA	pWZ100 derivative encoding a signal-sequence-less version of OmpA under P_{BAD} promoter control	This study
pOmpAss-OmpA	pWZ100 derivative encoding a version of OmpA fitted with the OmpA signal sequence under P_{BAD} promoter control	This study
pPelBss-OmpA	pWZ100 derivative encoding a version of OmpA fitted with the PelB signal sequence under P_{BAD} promoter control	This study
pPOss-OmpA	pWZ100 derivative encoding a version of OmpA fitted with the synthetic PelB-OmpA signal sequence under P_{BAD} promoter control	This study
pOPss-OmpA	pWZ100 derivative encoding a version of OmpA fitted with the synthetic OmpA-PelB signal sequence under P_{BAD} promoter control	This study
pPOss	pWZ100 derivative encoding the synthetic PelB-OmpA dual signal sequence under P_{BAD} promoter control	This study
pMM102	pACYC184 derivative (Chl^R)	(171)
pTFP	pMM102 derivative encoding the *tig* (Trigger Factor) gene under native promoter control	Baneyx group unpublished data
pSRP	pMM102 derivative encoding the *ffs* and *ffh* genes under native promoter control	(171)

3.2.2 *Cell growth and protein expression*

Shake flasks (125mL) containing 25mL of LB media supplemented with 50 μg/mL kanamycin were inoculated and induced as described in Chapter 2. For sodium azide treatment experiments, 1.5mM NaN_3 was added to the cultures at the time of induction. Optical density was measured every 30 min to construct growth curves. At 1.5h post-induction, cells (1 mL) were collected and sedimented by centrifugation at 10,000*g* for 2 min. Pellets were washed with 20 mM Tris-HCl pH 7.5, resuspended in SDS-PAGE sample buffer and subjected to electrophoresis. In all cases, the volume of sample buffer added was normalized to the optical density at the time of harvest, so that each sample corresponded to the same amount of cells. Duplicate aliquots were loaded on duplicate 12.5% SDS gels, one of which was used for immunoblotting and the other stained with Coomassie blue. For Western blots, gels were incubated in transfer solution (25 mM Tris-HCl, pH 8.3, 0.2 M glycine, 3 mM SDS, 20% vol/vol methanol) and proteins were transferred to nitrocellulose overnight at 15 V and 4°C. Membranes were probed with rabbit anti-OmpA antibody (a generous gift of the Beckwith lab) at a 1:4000 dilution, incubated with goat-anti-rabbit IgG Alkaline Phosphatase (Biorad) at 1:3000 dilution, and immunoreactive species were detected by colorimetric staining with 5-bromo-4-chloro-3-indolyl phosphate and nitrotetrazodium blue. Band intensities were quantified using ImageJ (NIH).

3.2.3 *Viability Testing*

Viability testing experiments were carried out as described in section 2.2.4.

3.3 RESULTS AND DISCUSSION

3.3.1 *Influence of various signal peptides on OmpA secretion*

3.3.1.1 *Impact on growth and viability*

Cells producing variants of OmpA downstream of the native (OmpAss), PelBss, POss and OPss signal sequences were grown and induced as described in Materials and Methods. Compared to the signal sequence-less control, expression of all variants caused significant cellular toxicity (Figure 3.2 A). , Production of OmpA from the PelBss was most deleterious to cell growth, as evidenced by a sharp decrease in optical density 30-60min post-induction. Consistent with what was observed in Chapter 2, the use of the native OmpAss signal sequence led to low cell viability 1.5h post-induction. The growth of cells overexpressing OmpA from dual signal sequence variants became stunted 30-to-60 min post-induction. However, the viability of cells collected 1.5 h post-induction was 1 to 2 orders of magnitude higher than the single signal sequence variants (Figure 3.2 B).

Surprisingly, all cultures reached a comparable optical density (Figure 3.2 A) and exhibited similar viability after 24h of growth (Figure 3.3 A). The progressive recovery of cells producing OmpAss-OmpA or PelBss-OmpA 2h post-induction (Figure 3.2 A) suggested that this might be explained by the acquisition of a mutation that shut down OmpA production and allowed cells to recover. To test this hypothesis, we extracted plasmids from 24h cultures and reintroduced them into fresh BW25113 cells that were grown under kanamycin selective pressure to guarantee that plasmids were not lost. These cells were induced in mid-exponential phase and samples collected 1.5h post-induction fractionated by SDS-PAGE. Figure 3.3B shows

that at the exception of the signal sequence-less control, none of the plasmids encoding a secretory version of OmpA was capable of producing the protein.

We previously reported that the arabinose-inducible P_{BAD} promoter can spontaneously acquire mutations that lower the transcription of toxic inner membrane proteins in order to restore cell growth (173). To determine if a similar mechanism was at play, we sequenced the plasmid encoding PelBss-OmpA and found that a large portion of the DNA encoding the PelB signal peptide was deleted (depicted in Figure 3.3C) causing loss of reading frame and OmpA production in the context of an intact promoter region. Thus, the extreme stress of secretory OmpA overexpression leads to the rapid acquisition of signal peptide mutations that shut down the production of the offensive protein and restore cell growth. This mechanism is especially rapid with PelBss and OmpAss but is delayed with dual signal peptides delays, possibly because more efficient pre-OmpA production from single signal sequence leads to faster translocon jamming.

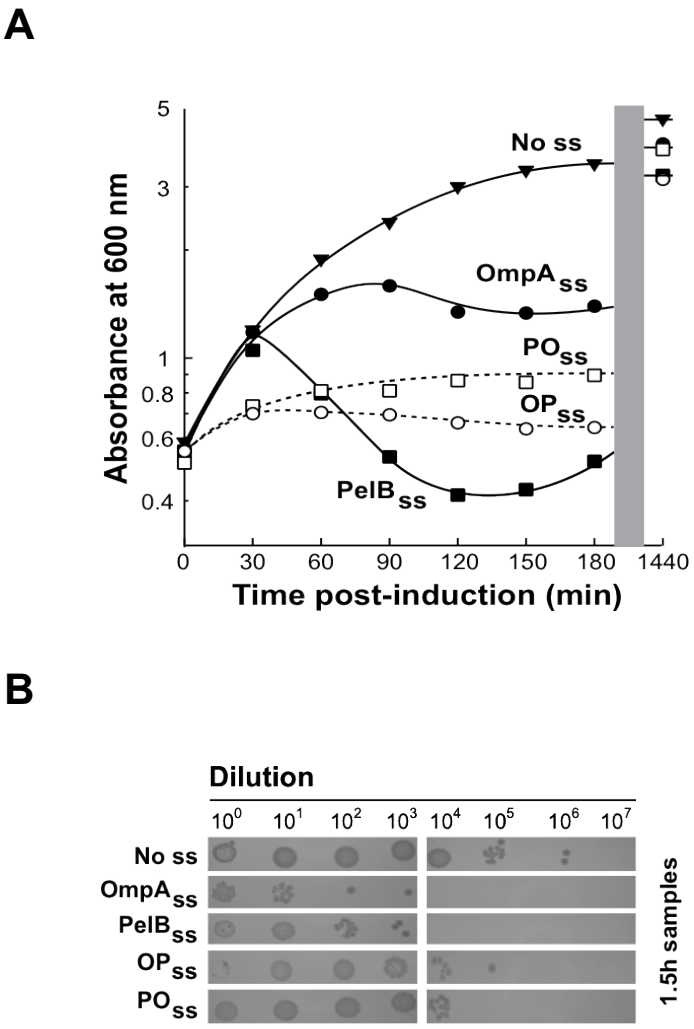

Figure 3.2 Influence of different signal peptides on the growth and viability of cells overexpressing OmpA

A. Growths of BW25113 Cells harboring OmpAs fused with different signal peptides at 37°C were monitored by optical density till 3h (180min) post induction. OD600 at 24h post-induction were also shown in the figure. Symbol representations are as follows:

Inverted triangles: NO ss; Closed circles: OmpAss; Closed square: PelBss;

Open square: POss; Open circles: OPss.

B. Viability testing was carried out on the cell samples harvested at 1.5h post-induction for each construct.

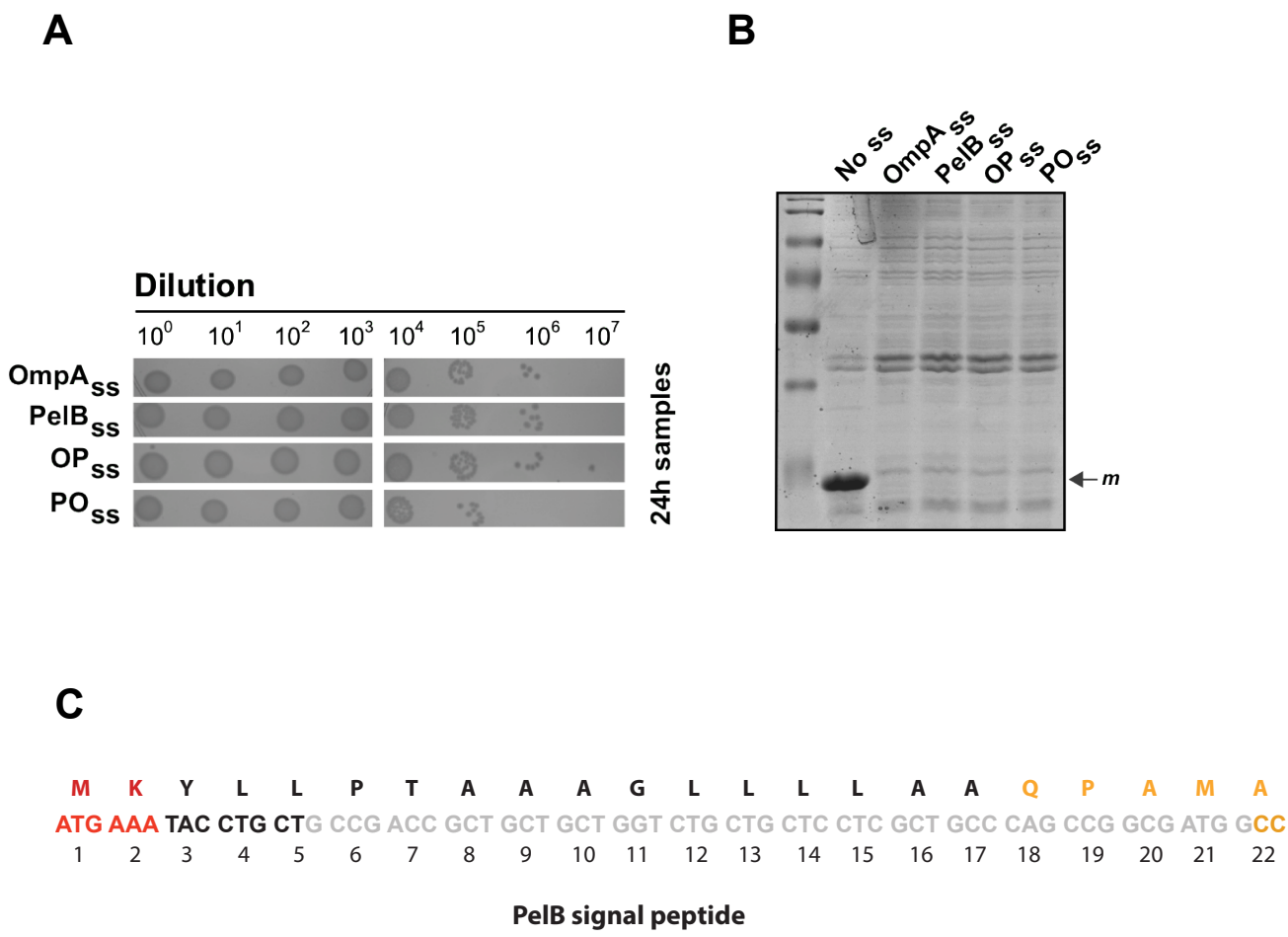

Figure 3.3 Plasmids harvested from 24h post-induction cultures are still viable but have lost the ability to produce OmpA

A. Influence of different signal peptides on viability of cells harvested at 24h post-induction.

B. Plasmids from 24h post-induction were extracted and transformed into BW25113, proteins were expressed at 37°C in the same fashion and 1.5h post-induction samples were shown on the gel where *m* indicated the location of mature OmpA protein.

C. PelBss-OmpA plasmid from 24h post-induction was sequenced and mutations were identified. Residues colored in red, black and yellow represent the n, h and c-region of the original PelB signal peptide, respectively. DNA sequences labeled in grey are the missing nucleotides recognized by sequencing.

3.3.1.2 *Dual Signal Peptide support OmpA biogenesis*

The N-terminal region of OmpA adopts a β-barrel conformation when it folds within the outer membrane (Figure 3.1A). Such structures are highly resistant to unfolding by detergent such as sodium dodecyl sulfate (SDS) at room temperature, leading to an abnormally fast migration pattern on SDS gels. However, boiling samples at 95°C for ~10min, destroys all secondary structure. Under these conditions, OmpA (and other OMPs) will migrate at a position corresponding to its actual molecular weight (Figure 3.4 A). This unique behavior – referred to as heat-modifiability – is often used as a surrogate measure of proper OmpA folding (76, 174-179). We took advantage of it to determine how much properly processed and folded versus unprocessed preproteins were produced with the various signal sequences.

Samples coming from all OmpA constructs at the same time point were also harvested and processed (Material and Methods) to check protein expression. Figure 3.4 B showed that when samples harvested 1.5h post-induction were fractionated by SDS-PAGE with or without heat treatment a major protein that migrated at ~28kDa in unboiled samples (arrow *f*) changed its position to 35kDa in boiled samples. This corresponds to species "*m*" in unboiled samples, the correctly processed but misfolded form of OmpA. The fact that *m* and *f* species could also be identified in cells producing OmpA from dual signal sequences confirm that these synthetic leaders are capable of supporting secretion of both periplasmic (Chapter 2) and outer membrane proteins.

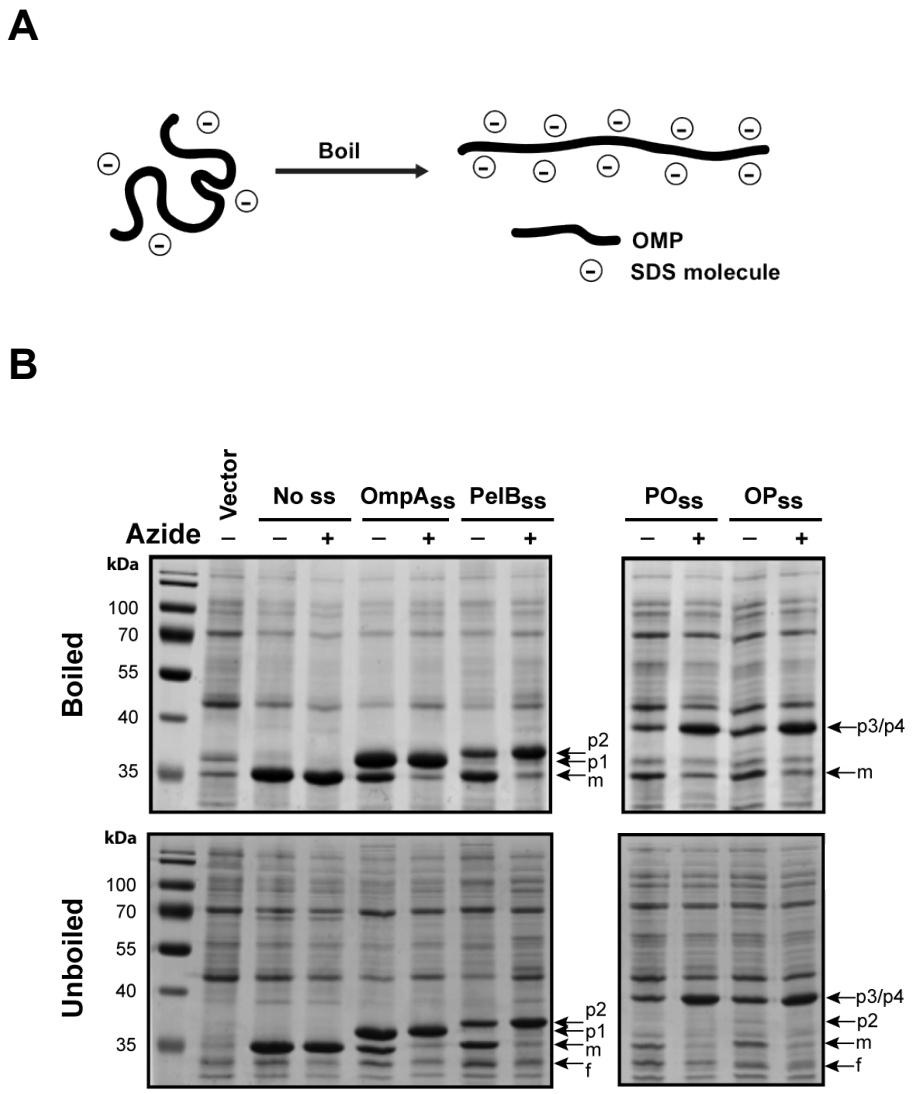

Figure 3.4 Heat modifiability and Sec-dependency of POss and OPss

A. Schematic illustration of the heat-modifiability of OMPs. Boiling destroys the b-barrel structure allowing SDS to bind to a random coil form of the protein.

B. BW25113 cells harboring pWZ100 (vector) or plasmids encoding signal sequence-less (NO ss), OmpAss, PelBss, OPss or POss versions of OmpA were grown to mid-exponential phase and induced with arabinose with (+) or without (-) concomitant sodium azide treatment. Samples collected 1.5h post-induction and corresponding to identical amounts of cells were resuspended in loading buffer and boiled for 15 min (top panel) or not (bottom panel) before being fractionated by SDS-PAGE. Arrows show the migration positions of precursor (p1-p4), mature and misfolded (m), and mature and correctly folded (f) OmpA (f).

3.3.1.3 *Export from dual signal sequences remains Sec-dependent*

Because it blocks the ATPase activity of SecA (180, 181), sodium azide ($NaN_{3)}$ is an effective inhibitor of Sec-dependent protein translocation (See section 1.2.1). To determine if the export of OmpA from dual signal sequences remained Sec-dependent, duplicate cultures were treated or not with 1.5 mM NaN_3 at the time of arabinose addition and 1.5h post-induction samples were fractionated by SDS-PAGE with or without boiling in loading buffer. As expected (181), azide completely blocked the export of OmpA from the native (OmpAss) and PelBss signal sequence and neither "m" or "f" mature species could be detected on the gels (Figure 3.4B). In addition, the dual signal sequence constructs appeared to exhibit a more stringent requirement on the SecA motor, considering that ~3 fold more p3 (POss-OmpA) or p4 OPss-OmpA) precursor accumulated in azide-treated cultures relative to untreated counterparts, while only slightly more p1 (OmpAss-OmpA) and ~2 fold more p2 (PelBss-OmpA) accumulated under the same conditions. We conclude that the dual signal sequences are fully dependent on the Sec system for export.

3.3.1.4 *Dual signal sequences reduce the accumulation of misfolded OmpA species while yielding similar amounts of folded protein*

We quantified the relative amounts of precursor, misfolded and correctly folded OmpA, by fractionating unboiled samples harvested 1.5h post-induction by SDS-PAGE and conducting normalized videodensitometric analysis of the resulting minigels. Figure 3.5 B showed that the identity of the signal peptide has no significant impact on the accumulation of properly processed and heat-modifiable OmpA (arrow f; white bars), which we take to be the functional form of the protein. However, the use of POss and OPss reduced the amount of misfolded mature protein (arrow m; black bars) by almost 50% and led to a significant decrease in the amount of aggregated precursor (arrows p1-p4; gray bars). In the most extreme case (OmpAss versus POss), the difference in precursor accumulation was more than 10 fold. Finally, as observed in the case of MBP (Chapter 2.3.2), trace amount of a precursor cleaved at the internal SPase I site could be detected when the OPss (but not POss) dual signal sequence was used to direct OmpA secretion (Figure 3.5 A). In short, dual signal sequences are as efficient at single leader peptides for the production of properly processed and folded OmpA but have the advantage of limiting the accumulation of misfolded precursor in the cytoplasm and mature protein in the periplasm.

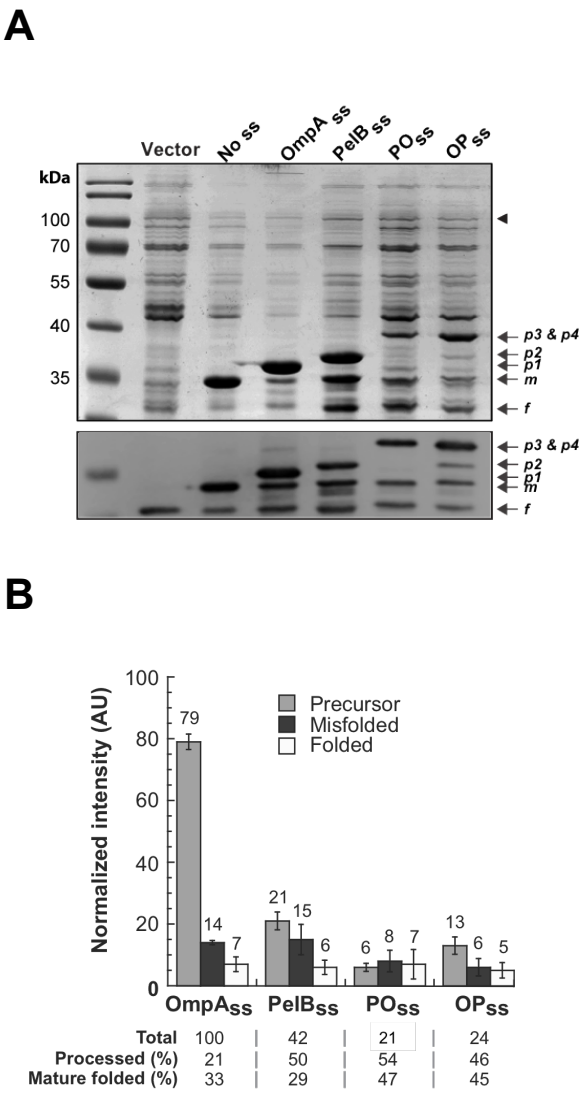

Figure 3.5 Influence of different signal peptides on OmpA expression

A. BW25113 cells harboring pWZ100 (vector) or plasmids encoding signal sequence-less (NO ss), OmpAss, PelBss, OPss or POss versions of OmpA were grown and induced as described in Methods and samples were collected 1.5h post-induction. Aliquots corresponding to identical amounts of cells were fractionated without boiling. Duplicate samples were transferred to nitrocellulose and the membrane was probed with anti-OmpA antiserum. Arrows in gel and blot indicate the migration position of precursor (p1-p4), mature and misfolded (m) and mature and correctly folded (f) OmpA. The arrowhead identifies the control band used for normalization purpose.

B. Protein yields were quantified according to the gel shown in (A) by ImageJ. For quantification purposes, half of the NO ss and OmpAss samples were loaded on separate gels. Error bars were obtained for independent quantification of samples harvested in three independent experiments.

3.3.2 *Influence of Trigger Factor (TF) and Signal Recognition Particle (SRP) on OmpA secretion*

3.3.2.1 *OmpA export via dual signal sequence exhibits a strong requirement on Trigger Factor*

The cytoplasmic molecular chaperone Trigger factor (TF) was originally isolated on the basis of its ability to form a stoichiometric complex with pro-OmpA (referred to as OmpAss-OmpA in this study) (182). To determine how OmpA variants equipped with dual signal sequence would interact with TF, the various plasmids were introduced in KTD101, a strain containing a deletion in the gene encoding TF (*tig*) but otherwise isogenic to BW25113 (171).

Growth and viability experiments revealed little difference in the growth and viability of Δ*tig* and *tig*$^+$ cells for all constructs (compare Figures 3.6 and 3.2), except for a slight improvement in the growth of PelBss and POss in the Δ*tig* background after induction of protein synthesis. On the other hand, there was increased accumulation of all precursor species and a concomitant decrease in the intensity of the m and f bands in *tig* null cells (Figure 3.7). We conclude that secretion of OmpA remains TF-dependent, irrespective of the identity of the signal sequence. In fact, the dual signal sequence constructs appeared exhibit a more stringent requirement on TF considering that ~3 fold more p3 and p4 accumulated in Δ*tig* cells compared to *tig*$^+$ cells, while only slightly more p1 and about twice as much p2 were found in Δ*tig* cells compared to *tig*$^+$ cells.

3.3.2.2 *TF overexpression does not improve OmpA secretion*

Lee and coworkers (170) have proposed that TF retards protein export by sequestering preproteins in the cytoplasm based on the observations that TF inactivation accelerates secretion while its overproduction markedly delays the process *in vivo.* The results of section 3.3.2.1, could therefore be explained by a scenario in which TF binds more efficiently to the more hydrophobic dual signal sequences. This could have the consequence of reducing the flux of p3 and p4 to the translocon and alleviating "jamming" effects. To test this idea, we increased the copy number of the *tig* gene by co-transforming plasmid pTF (Table 3.1) with the various OmpA expression plasmids.

Contrary to our expectations, raising the intracellular levels of TF had no obvious influence on cell growth, viability or OmpA expression levels, except for a small but reproducible decrease in culture turbidity (Figure 3.8 A). Additionally, precursor aggregation was slightly higher for all constructs 24h post-induction, likely due to be the pleiotropic effects of TF up-regulation. We conclude that the cellular supply of TF is not a limiting factor for OmpA secretion and that future attempts to enhance protein production from dual signal sequence variants might require fine-tuning or reprogramming of other cellular factors.

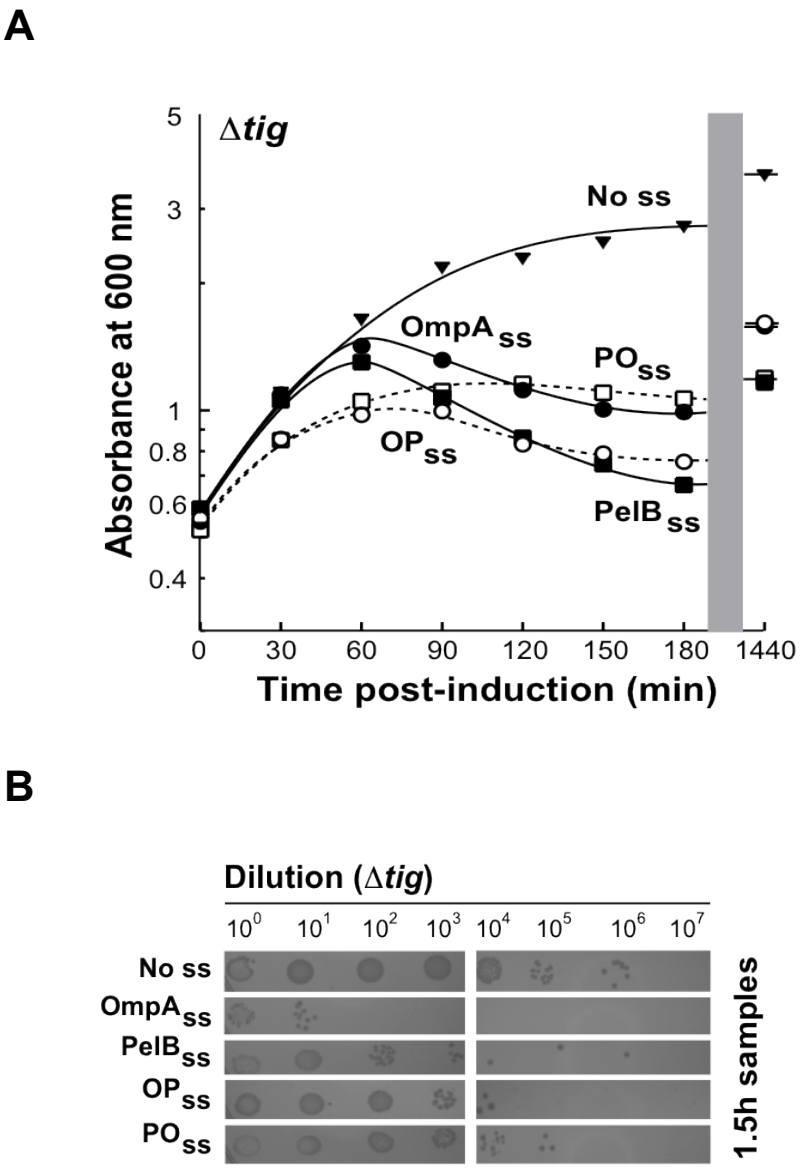

Figure 3.6 Influence of Trigger Factor inactivation on the growth and viability of cells overexpressing OmpA

A. Growths of KTD101 Cells harboring OmpAs fused with different signal peptides at 37°C were monitored by optical density till 3h (180min) post induction. OD600 at 24h post-induction were also shown in the figure. Symbol representations are as follows:

Inverted triangles: NO ss; Closed circles: OmpAss; Closed square: PelBss;

Open square: POss; Open circles: OPss.

B. Viability testing was carried out on the cell samples harvested at 1.5h post-induction for each construct.

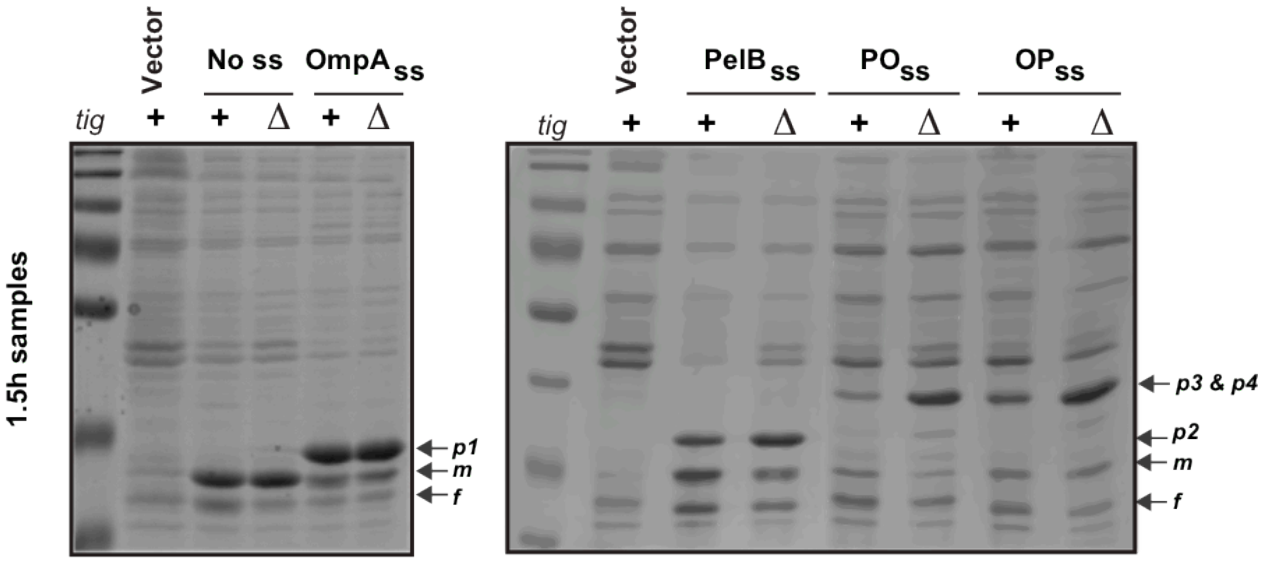

Figure 3.7 Influence of Trigger Factor inactivation on the accumulation of precursor and mature OmpA species

BW25113 (+) and KTD101 (Δ) cells harboring pWZ100 (vector) or plasmids encoding signal sequence-less (NO ss), OmpAss, PelBss, OPss or POss versions of OmpA were grown to mid-exponential phase and induced with arabinose. Samples collected 1.5h post-induction and corresponding to identical amounts of cells were resuspended in loading buffer before being fractionated by SDS-PAGE (without heat treatment). Arrows show the migration positions of precursor (p1-p4), mature and misfolded (m), and mature and correctly folded (f) OmpA (f).

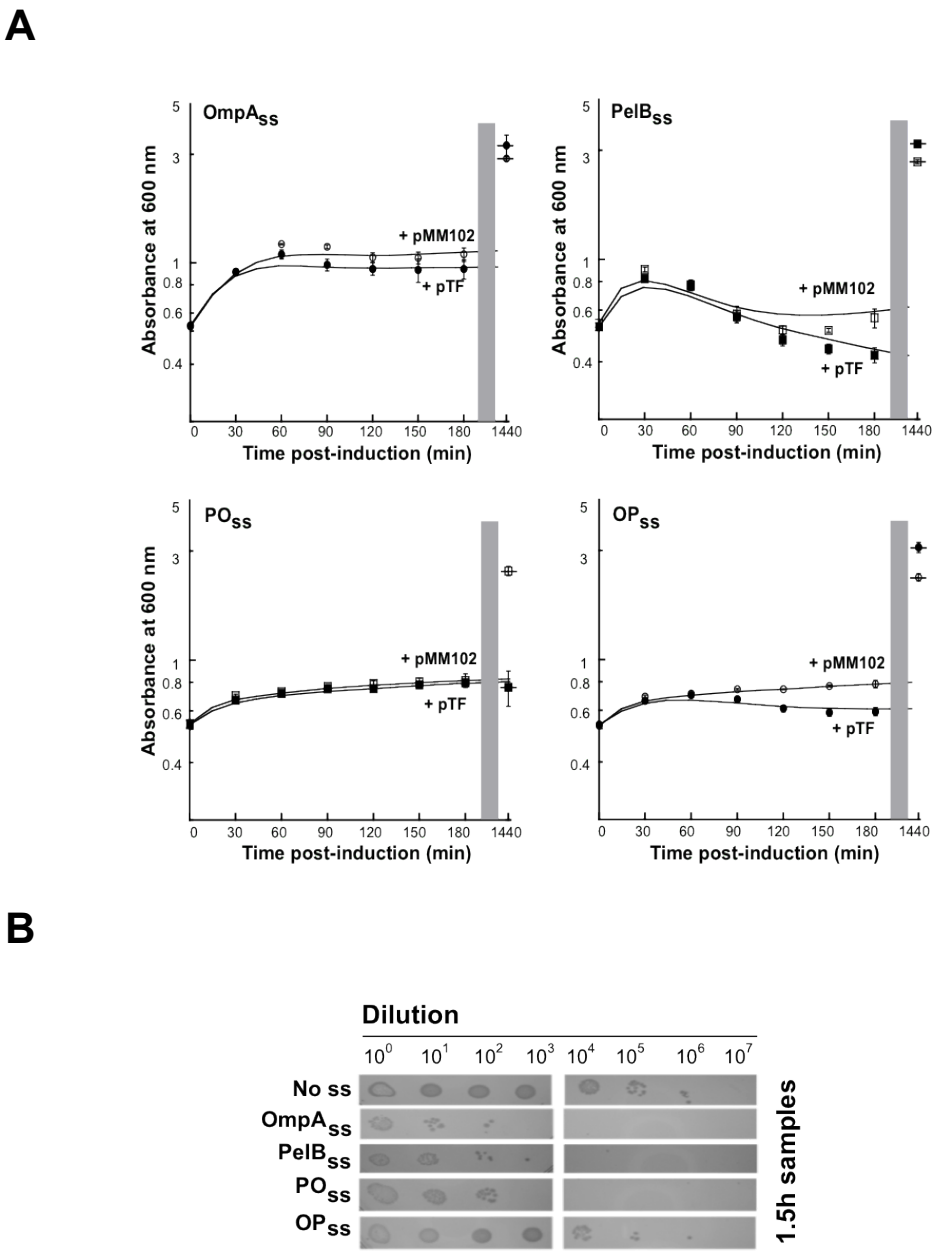

Figure 3.8 **Influence of Trigger Factor overexpression on the growth and viability of cells overexpressing OmpA**

A. BW25113 cells harboring pWZ100 (vector) or plasmids encoding pTFP along with OmpA were grown to mid-exponential phase and induced with arabinose. Growths were monitored by optical density till 3h (180min) post induction. OD600 at 24h post-induction were also shown in the figure. Open symbols: OmpA with pMM102 control plasmid. Closed symbols: OmpA with pTFP.

B. Viability testing was carried out on the TF-overexpression cell samples harvested at 1.5h post-induction.

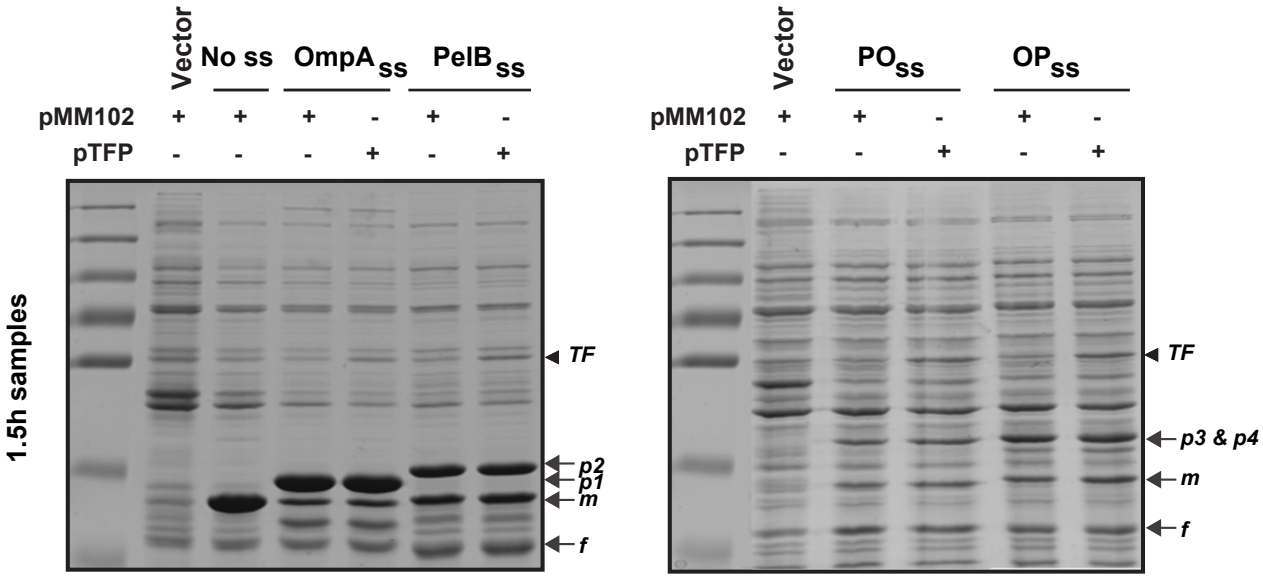

Figure 3.9 Influence of TF overexpression on OmpA expression (Unboiled)

BW25113 cells harboring pWZ100 (vector) or plasmids encoding TF along with OmpA were grown to mid-exponential phase and induced with arabinose. Samples collected 1.5h post-induction and corresponding to identical amounts of cells were resuspended in loading buffer before being fractionated by SDS-PAGE (without heat treatment). Arrows show the migration positions of precursor (p1-p4), mature and misfolded (m), and mature and correctly folded (f) OmpA (f). The migration position of TF is also indicated by arrow head.

3.3.2.3 *SRP-overexpression does not reroute secretion of dual signal sequence variants to the SRP-pathway*

Although the signal recognition particle (SRP) is primarily involved in facilitating the trafficking or α-helical membrane proteins to the plasma membrane (Chapter 1, section 1.2.2), it also supports the secretion of a subset of periplasmic proteins containing highly hydrophobic signal peptides (e.g. DsbA) (17, 183). Considering that dual signal peptides have higher hydrophobicity than their constituent leaders and that SRP co-expression can improve the secretory yields of heterologous proteins outfitted with SRP-dependent signal sequences (171, 184), we set out to determine if SRP overproduction would confer similar benefits to the dual signal peptide OmpA variants. To this end, we repeated the experiments of Figure 3.9 using a compatible plasmid that encodes the *ffh* and *ffs* genes under control of their native promoters and thus produces a complete SRP particle. However, there was no detectable difference in the levels of p3 and p4, or mature OmpA (m or f) between control and SRP-overexpressing cells (Figure 3.10). We conclude that tandem repeats of Sec-dependent signal are insufficient to reroute OmpA secretion to the SRP-dependent pathway, probably because the h regions of the OmpAss and PelBss are only of moderate hydrophobicity compared to the transmembrane domains of inner membrane proteins.

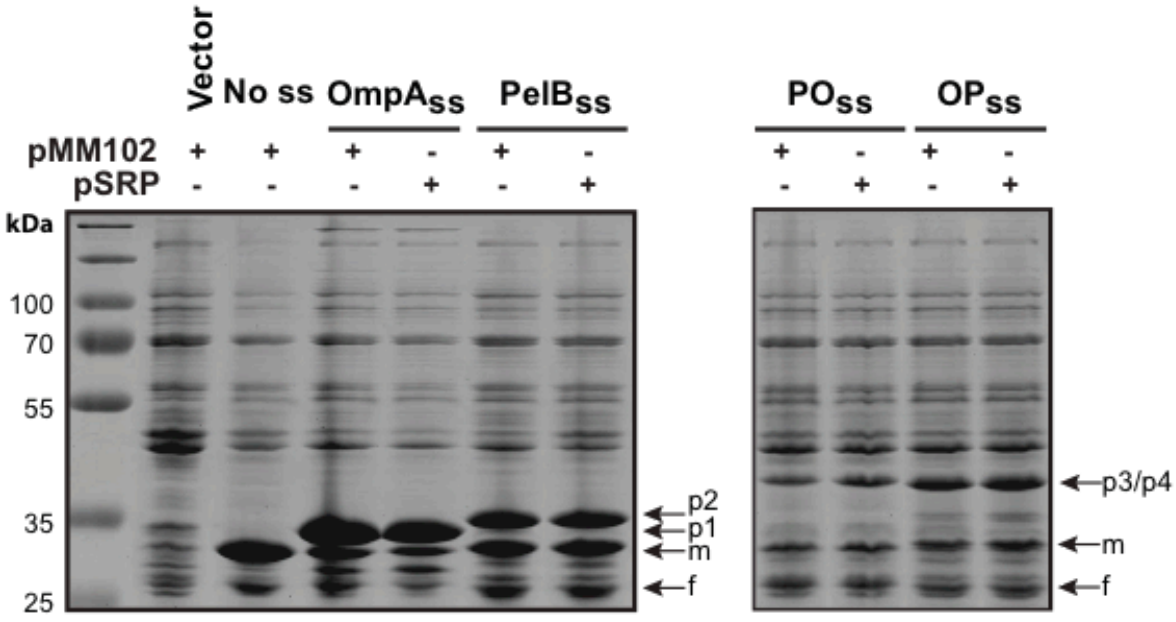

Figure 3.10 Influence of SRP overexpression on OmpA expression (Unboiled)

BW25113 cells harboring pWZ100 (vector) or plasmids encoding SRP along with OmpA were grown to mid-exponential phase and induced with arabinose. Samples collected 1.5h post-induction and corresponding to identical amounts of cells were resuspended in loading buffer before being fractionated by SDS-PAGE (without heat treatment). Arrows show the migration positions of precursor (p1-p4), mature and misfolded (m), and mature and correctly folded (f) OmpA.

3.4 CONCLUSIONS

In this chapter, we have shown that, in addition to soluble periplasmic proteins such as MBP, the POss and OPss dual signal sequences support the translocation of OMPs, a distinct class of secretory proteins. We confirmed that these synthetic peptides are preferentially cleaved at the SPase I site proximal to the mature protein and found that their use improves cell viability and decreases the accumulation of precursor and misfolded OmpA species without compromising the yield of properly folded material. Using sodium azide treatment, strains lacking TF, and SRP and TF overexpression, experiments, we further found that OmpA secretion from dual signal peptides is dependent on the presence of functional SecA and TF but that the cellular concentrations of the latter chaperone and that of SRP are not limiting for export. In short, dual signal sequences appear to function much like canonical signal sequences do although they have the advantage of reducing the accumulation of misfolded OMP species.

Chapter 4 Influence of various Signal Peptides on Outer Membrane Vesicle production

4.1 INTRODUCTION

Escherichia coli is well characterized and has been widely used for recombinant protein expression. Compared to cytoplasmic expression, secretory and extracellular recombinant protein production have the advantages of simplified downstream purification and processing, higher product stability due to reduced proteolytic activity, and in the case of toxic proteins, lower impact on cell physiology and viability (185, 186) (187).

Outer membrane vesicles (OMVs) are ubiquitously released from the outer membrane surface, contain properly oriented OMPs in their membranes and encapsulate periplasmic proteins within their lumen (see Chapter 1 for more information). These properties make them a promising alternative for extracellular protein expression, and especially useful for the production of engineered OMPs for vaccine, biotechnology and materials science applications. Pioneering studies by Kesty and Kuehn (151), Chen *et al.* (153) and Kim *et al.* (152) have demonstrated the feasibility of incorporating heterologous protein within OMVs by fusing them to partners known to be enriched in the vesicles.

Fluorescent Proteins have been widely used to study the organization and function of living systems and proven particularly useful as biomarkers for gene expression and as beacons for the localization of protein products (188). Among these is mCherry, a red fluorescent protein derivative with rapid maturation rate and moderate brightness, but with great photostability and causing lower autofluorescent cellular background when excited (189). Moreover, mCherry remains active when exported to the periplasm and its monomeric structure lends itself to the

construction of gene fusions, (190, 191). Here, we fused mCherry to OmpA, a protein known to be enriched in OMVs (112, 120, 151, 152) to investigate how various cellular factors would affect vesicle production.

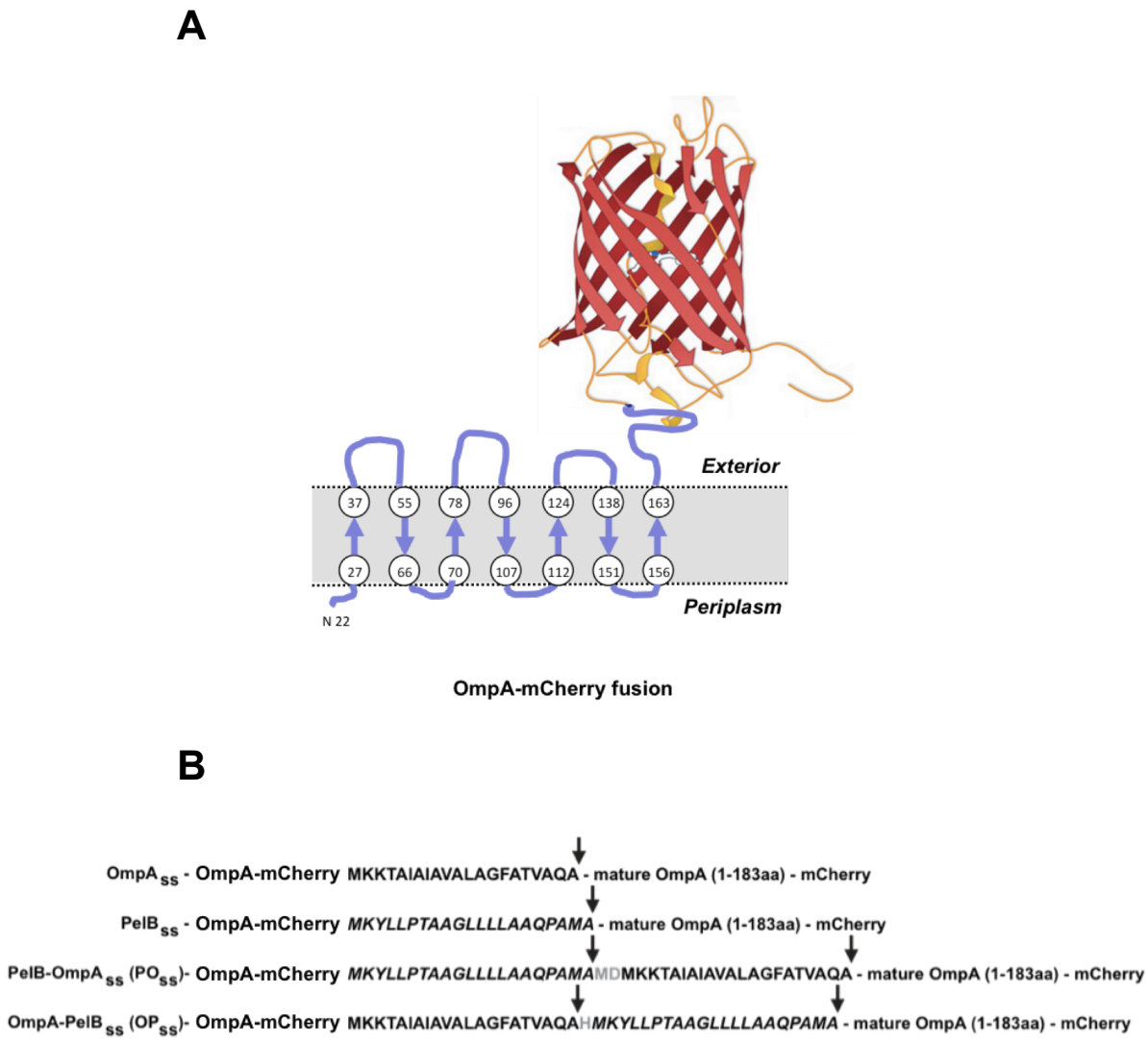

Figure 4.1 Schematic structure of the OmpA-mCherry construct

A. OmpA-mCherry fusion protein structure and topology. The last β-strand of the 8-stranded OmpA β-barrel along with the protein C-terminal periplasmic domain was replaced by mCherry, a fluorescent protein that also adopts a β-barrel when properly folded.

B. Structure of OmpA-mCherry equipped with different signal peptides. The arrows indicate SPase I cleavage site and letters in gray are extra amino acids inserted to preserve the reading frame.

4.2 MATERIALS AND METHODS

4.2.1 *Plasmid constructions*

Plasmid pGA3K3 (Courtesy of Dr. Eric Klavins) was used as a template to amplify mature mCherry with primers 5'-CGATATGCATGCTGATGGTTTCCA AGGGC-3' and 5'-CGCGTGCTCGAGTT-ACTTGTACAGTTCGTCCA-3' in order to introduce *Sph*I and *Xho*I site at the 5' and 3' ends of the amplified fragment, respectively. The PCR product was digested with these enzymes and ligated into the same sites of pOmpA, pOmpAss-OmpA, pPelBss-OmpA, pPOss-OmpA and pOPss-OmpA (Chapter 3). The resulting constructs encode OmpA-mCherry chimeras in which mCherry is fused to the first seven β-strands of OmpA (amino acids 1 to 183) with no signal sequence, or the OmpAss, PelBss, OPss and POss. The strains and plasmids used in this chapter are listed in Table 4.1.

4.2.2 *Quantification of extracellular $OmpA_{1-183}$-mCherry production*

Shake flasks (125ml) containing 25 mL of LB media supplemented with 50 μg/mL kanamycin were inoculated and induced as described in Chapter 3. At OD_{600} ~0.45, cultures were transferred from 37°C to water baths held at 25 or 30°C as indicated. Cultures were induced with arabinose (0.2% wt/vol) at $OD_{600} \approx 0.5$. Cells were harvested at the indicated times by sedimentation at 3,000*g* for 15 min and supernatants were filtered through 0.45 μm nitrocellulose membranes. Fluorescence was quantified at 610 nm using 1 mL samples following excitation at 587 nm using a Hitachi F-4500 fluorescent spectrophotometer with slit widths set at 5 nm.

Table 4.1 Strains and plasmids used in Chapter 4

Name	Description	Source or reference
Strain		
Top10	F' *endA1 recA1 hsdR17* (r_K^-,m_K^+) λ^- *supE44 thi1 gyrA96 relA1* ϕ*80* Δ*lac* Δ*M15*Δ(*lacZYA-argF*)U169 *deoR*	Invitrogen
BW25113	Δ(*araD-araB*)*567 ΔlacZ4787* (::*rrnB-3*) *lacI*^{p}*-4000*(*lacI*^{Q}) λ^- *rph-1* Δ(*rhaD-rhaB*)*568 hsdR514*	(172)
Plasmid		
pGA3K3-mCherry	Plasmid encoded an N-terminally His tagged version of mCherry under P_{lac} promoter control	Klavin's lab
pOmpA-mCherry	pOmpA derivative encoding a signal sequence-less version of the $OmpA_{1-183}$-mCherry fusion protein under P_{BAD} promoter control	This study
pOmpAss-OmpA-mCherry	pOmpAss-OmpA derivative encoding the $OmpA_{1-183}$-mCherry fusion protein downstream of the OmpAss and under P_{BAD} promoter control	This study
pPelBss-OmpA-mCherry	pPelBss-OmpA derivative encoding the $OmpA_{1-183}$-mCherry fusion protein downstream of the OmpAss and under P_{BAD} promoter control	This study
pPOss-OmpA-mCherry	pPOss-OmpA derivative encoding the $OmpA_{1-183}$-mCherry fusion protein downstream of the POss and under P_{BAD} promoter control	This study
pOPss-OmpA-mCherry	pOPss-OmpA derivative encoding the $OmpA_{1-183}$-mCherry fusion protein downstream of the OPss and under P_{BAD} promoter control	This study

4.2.3 *OMV purification*

OMVs were isolated from cell-free medium by modification of an established protocol (192). Briefly, shake flasks (1 L) containing 250 mL of LB medium supplemented with 50 μg/mL kanamycin were inoculated and induced as above. At OD_{600} ~0.45, cultures were transferred to 30°C, and induced with arabinose (0.2% wt/vol) at OD_{600} ≈ 0.5. Cells were harvested 6h post-induction and centrifuged at 3000*g* for 15min at 4°C. The supernatant was collected and filtered through a 0.45μm nitrocellulose filter into a 1 L beaker. Ammonium sulfate (129 g) was added and the solution was stirred at room temperature at moderate speed until all solid was dissolved. OMV precipitation was allowed to proceed at 4°C overnight before centrifugation for 20 min at 10,000*g*. The pellet was carefully resuspended in 10 mL of 50 mM HEPES pH 7.5, dialyzed overnight against 3.5 L of the same buffer, pooled and concentrated to ~250 μL using a 10,000 molecular weight cut-off Amicon Ultra centrifugation units.

4.2.4 *Characterization techniques*

Dynamic light scattering size measurements were performed on a Zetasizer Nano ZS (Malvern Instruments). OMVs (5 μL) were diluted 200-fold with ultra pure sterile water, and filtered into a clean, dust-free 1.5 mL cuvette using a 0.25 μm syringe filter. Triplicate measurements were carried out for each sample.

For AFM visualization, OMVs (10 μL) were diluted 3-fold with ultra pure sterile water, and 15 μL of solution was deposited on a freshly cleaved mica surface. After 15 min incubation at room temperature, the chip was rinsed twice with and dried with filtered air. AFM images were collected in tapping mode on a Bruker Dimension Icon using a Tetra 15 cantilever (K-tek).

4.3 RESULTS AND DISCUSSION

4.3.1 *The PelBss directs the most $OmpA_{1-183}$-mCherry to the extracellular medium*

To expose mCherry to the outside of vesicles, we replaced the last β-strand and large periplasmic domain of OmpA by the fluorescent protein (Figure 4.1). A series of P_{BAD} expression plasmids encoding $OmpA_{1-183}$-mCherry preceded by no signal sequence, OmpAss, PelBss, POss or OPss were constructed as described in Materials and Methods. To determine how signal sequence identity and growth conditions would affect OMV production, we measured mCherry fluorescence in the extracellular medium.

For initial experiments, cultures were grown in LB at 37°C, cell-free samples were harvested 1.5h post-induction and sample fluorescence was measured at 610 nm. Figure 4.2 A shows that the identity of the signal sequence had a significant impact on the levels of $OmpA_{1-183}$-mCherry fluorescence present in the extracellular fluid. The native OmpAss was the worst performer, yielding only a marginal improvement in fluorescence over a signal sequence-less control. Use of the dual signal peptides (POss and OPss) led to an about twofold increase in fluorescence, but the best results were achieved with the PelBss with an about 9-fold increase in fluorescence relative to OmpAss.

In an effort to increase yields, we repeated these experiments at different temperatures and harvest times. Figure 4.2 B shows that little fluorescence was present in the medium of 1.5h post-induction cells if growth took place at 25°C but that extracellular fluorescence increased with time for at least 16 h post-induction when expression was conducted at 30°C (data not shown). As a compromise between expression levels and experimental convenience, we repeated

signal sequence experiments using cells cultivated at 30°C and 6h post-induction samples. Consistent with the results of Figure 4.2, the PelBss was the most efficient at driving the production of fluorescent $OmpA_{1-183}$-mCherry in the extracellular fluid (Figure 4.3 A). However, OmpAss was second best under these conditions, while the dual signal peptides were much poorer performers. Thus, dual signal sequences may prove the most useful when cells experience extreme stress.

4.3.2 *OMV characterization*

We used dynamic light scattering (DLS) and atomic force microscopy (AFM) to confirm that the fluorescent material present in the extracellular fluid was under the form of OMVs. Because nonpathogenic *E. coli* produces low amounts of vesicles, we modified an ammonium sulfate precipitation protocol (192) to concentrate extracellular material from cells producing $OmpA_{1-183}$-mCherry equipped with the PelBss or lacking a signal sequence as a control. The 1000-fold concentrated material was 13-times more fluorescent when a signal sequence was used, revealing efficient excretion of $OmpA_{1-183}$-mCherry from PelBss (Figure 4.3 B).

DLS analysis confirmed that both strains secreted particles ranging in size from about 20 to 300 nm and with average diameter of 90 nm into the extracellular medium (Figure 4.4 B). These values are in good agreement with the typical size of OMVs (20-250 nm). Further analysis by AFM (Figure 4.5) confirmed the presence of OMVs in both NOss and PelBss fusions with a size range in agreement with DLS data. Larger vesicles visualized by AFM had a diameter of about 100 nm but were less than 10 nm tall (Figure 4.5 A height graph). This has been consistent with other OMVs imaged by AFM (113, 127) and has been attributed to hydrophilic interactions between OMVs and the mica substrate. (193). Smaller vesicles with their diameter ranging from

~20nm to sub-100nm were also detected by AFM. In addition, AFM PelBss fusion appeared to create more vesicles that fall within the size range of typical OMVs than the NOss control, indicating its ability to up-regulating the OMV production process.

Taking together, our data indicate that whereas production of mostly non-fluorescent OMVs occurs as expected in cells lacking a signal sequence to target $OmpA_{1-183}$-mCherry to the outer membrane, the presence of PelBss leads to the production of fluorescent OMVs due to the incorporation of $OmpA_{1-183}$-mCherry in their membrane. These OMVs have diameters that fall in the expected size range but appear to exhibit higher polydispersity and be enriched in smaller vesicles.

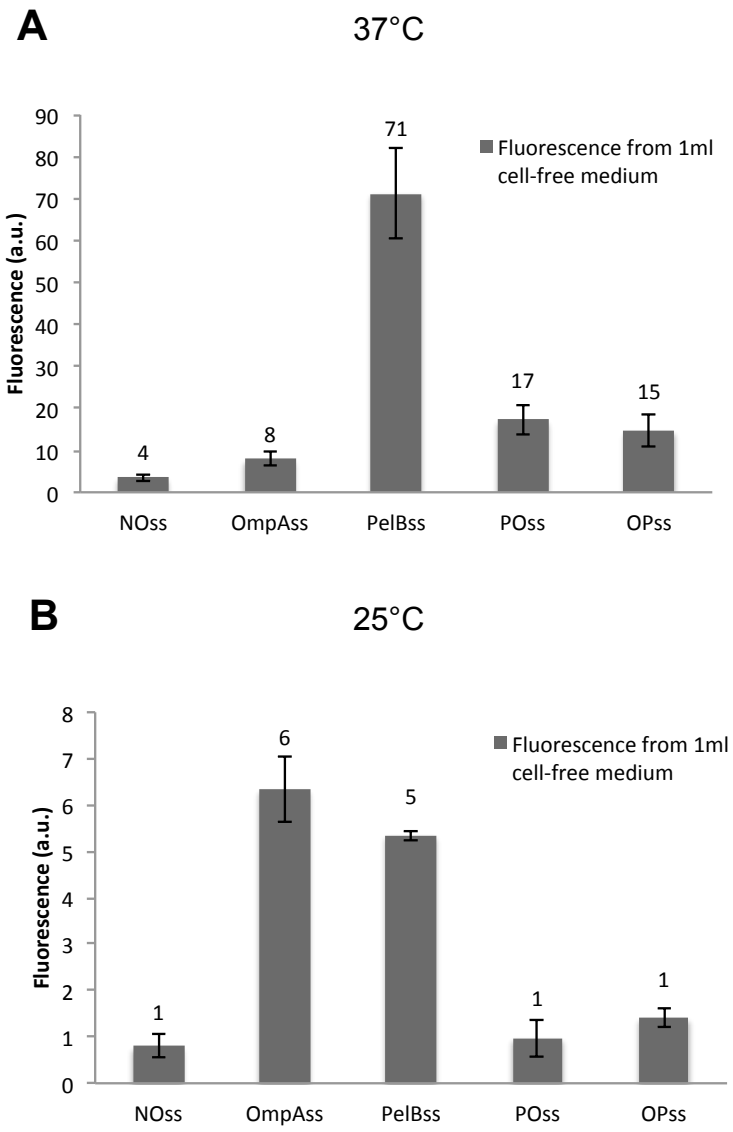

Figure 4.2 mCherry fluorescence in the extracellular medium under different growth condition

A. Extracellular fluorescence measurements after 1.5h of post-induction growth at 37°C. Cell-free medium (1 mL) collected from 25 mL cells harboring OmpA1-183-mCherry construct fitted with the indicated signal peptides were excited at 587 nm and fluorescence emission was quantified at 610nm. Error bars correspond to triplicate independent experiments.

B. As above except that the protein expression was conducted at 25°C.

A

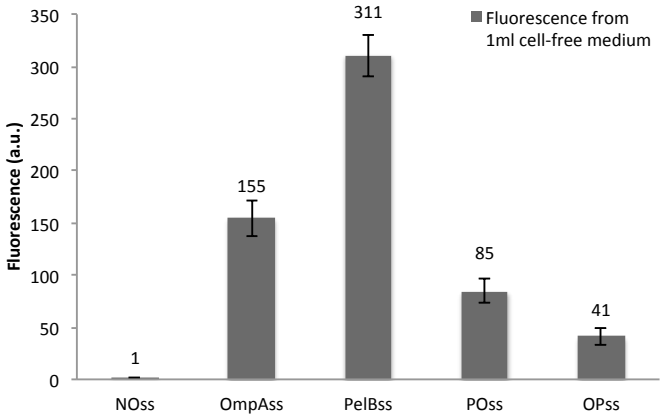

B

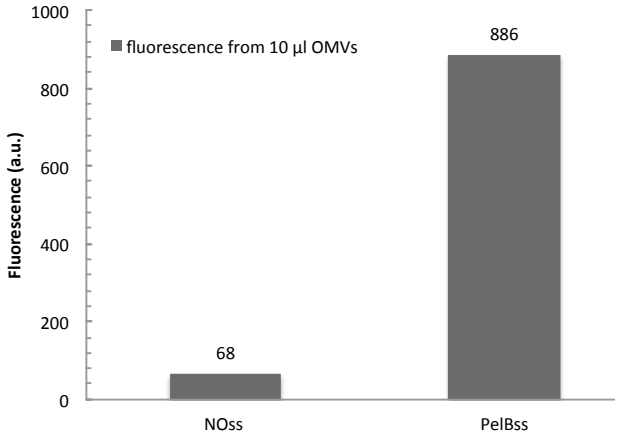

Figure 4.3 Fluorescence from extracellular medium and purified OMVs at 30°C 6h post-induction

A. Extracellular fluorescence measurement at optimized condition (30°C 6h post-induction), cell-free medium (1 mL) collected from 25 cells harboring OmpA1-183-mCherry construct fitted with the indicated signal peptides were excited at 587 nm and fluorescence emission was quantified at 610nm. Error bars correspond to triplicate independent experiments.

B. OMVs from PelBss and NOss control were purified as described in the text, 10 µL out of the total 250 µL purified OMVs from each sample was subject to fluorescent measurement under the same condition.

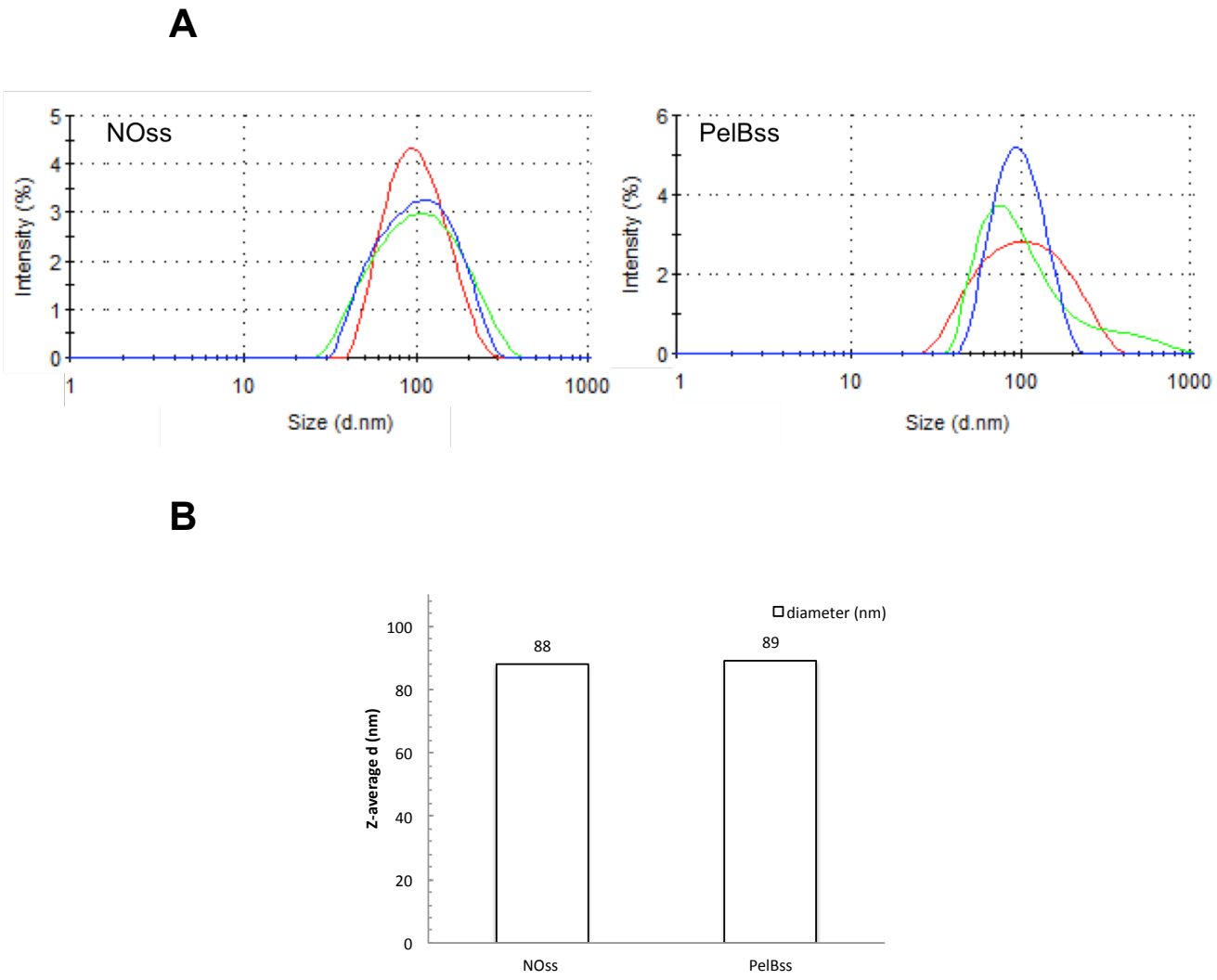

Figure 4.4 DLS analysis of OMVs collected from cells producing $OmpA_{1-183}$-mCherry without a signal sequence (NOss) or with the PelBss.

A. OMVs from each sample were diluted in sterile deionized water and hydrodynamic diameters were measured by DLS. Three measurements were performed on three different samples and curves were overlaid.

B. Z-average hydrodynamic diameters were derived from intensity graph using the instrument's software.

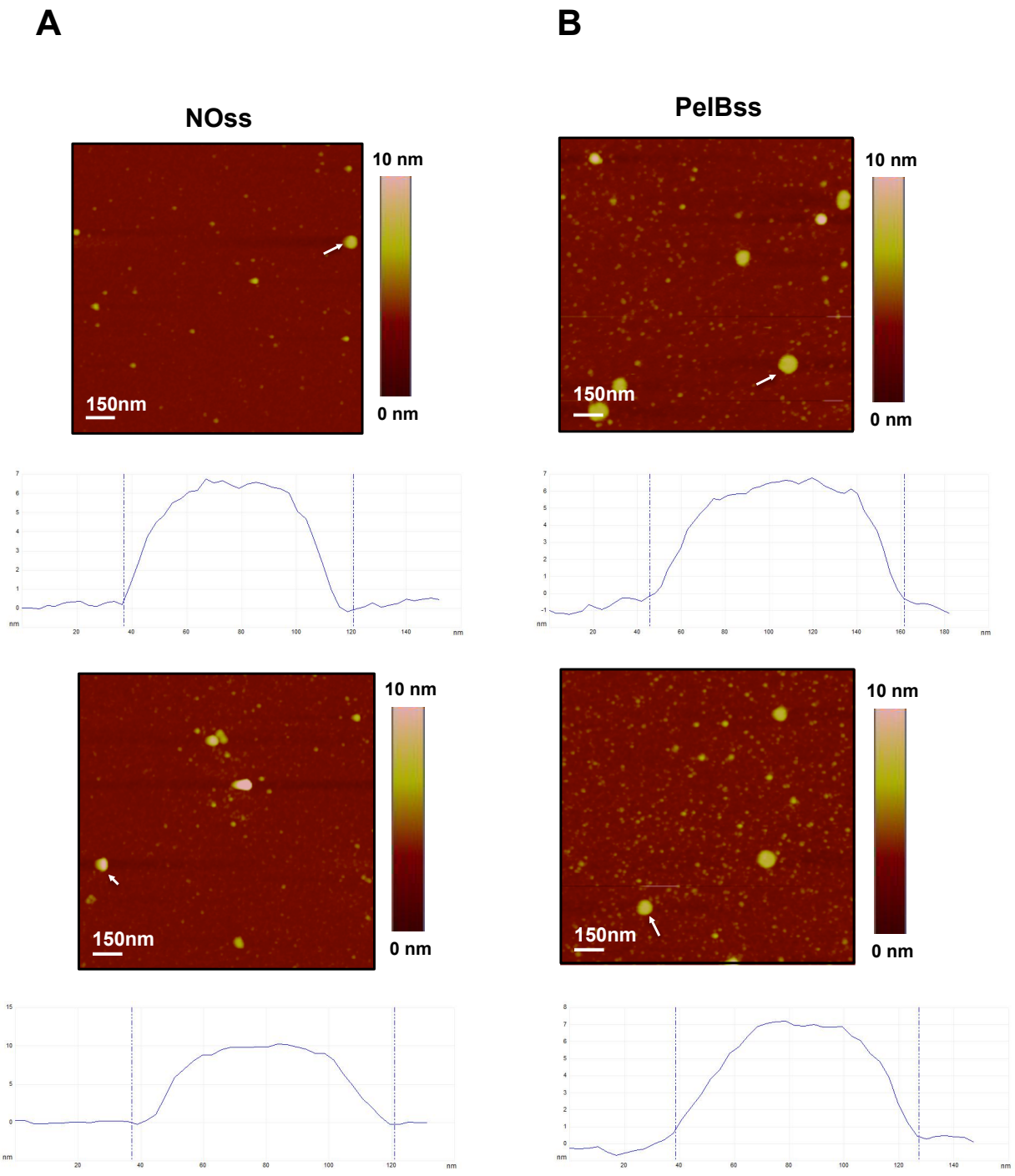

Figure 4.5 AFM images of OMVs collected from cells producing $OmpA_{1-183}$-mCherry without a signal sequence (NOss) or with the PelBss.

OMVs were prepared and imaged as described in the Materials and Methods. Two representative fields are shown for each sample. A. NOss control. B. PelBss. Line scans were performed on the vesicle identified by an arrow.

4.4 CONCLUSIONS

In this chapter, we used $OmpA_{1-183}$-mCherry as an efficient reporter of the production of OMVs that incorporate engineered proteins within the their membranes and optimized signal sequence identity, temperature and harvest time to produce significant amount of fluorescent vesicles that retain fluorescence and exhibit the expected size range of 20-300 nm with a mean diameter of approximately 100 nm. Unfortunately, although they remain functional for secretion and the ultimate delivery of $OmpA_{1-183}$-mCherry to OMVs, our dual signal peptides do not outperform the PelBss for OMV production.

Chapter 5 Influence of Periplasmic Chaperones and Bam components on Outer Membrane Vesicle production

5.1 INTRODUCTION

In Chapter 4, we demonstrated that among all signal peptides tested, PelBss gave the highest yields of $OmpA_{1-183}$-mCherry incorporation into OMVs (~1.2 mg/L, See Appendix for details). However, in addition to signal sequences, a number of folding modulators and the Bam machinery play crucial roles in OMP biogenesis (Chapter 1). How these systems influence OMV formation has not been explored to date.

Here, we set out to determine if overproduction of periplasmic chaperones or components of the Bam translocon would increase the yield of extracellular OMV production. We used PelBss-$OmpA_{1-183}$-mCherry as a reporter, along with combinations of the periplasmic chaperone Skp and SurA and of the BamA, BamB and BamD components of the Bam machinery. The influence of BamC and BamE, two non-essential components of the Bam system (93) (194) was not tested in this chapter.

5.2 MATERIALS AND METHODS

5.2.1 *Plasmid constructions*

The plasmid vector used for encoding the periplasmic chaperones and Bam components was pMM102, a chloramphenicol-resistant pACYC184 derivative (171) with chloramphenicol resistance. It has a p15A origin of replication, which will be compatible with the ColE1-ori plasmid encoding PelBss-OmpA-mCherry as described in Chapter 4.

A DNA fragment specifying *skp* and its native promoter was amplified from *E. coli* MC4100 genomic DNA on a *Hind*III-*Bam*HI fragment using primers 5'-GCAGCTAAGCTTTGATTACGAATGTGC-3' and 5'- TTTATTGGATCCCCTAA-ATGCTCACGG - 3'. The PCR product was digested with these enzymes and ligated into the same sites of pMM102, a chloramphenicol-resistant pACYC184 derivative (171). The *surA* gene along with its native promoter was also cloned into pMM102 except that primers 5'-AGTCAGAAGCTTGACCAGTAACTCCAGC-3' and 5'- ACCTTCTCTAGACAGACA-ACCATCGCAC - 3' were used to amplify an *Hind*III-*EcoR*I fragment that was ligated in the same sites of pMM102. The same *Hind*III-*EcoR*I fragment was ligated to *Hind*III-*EcoR*I digested pSkp to create pSkpSurA.

To build a series of pMM102 derivatives encoding components of the Bam machinery, the *bamA* and *bamB* genes with amplified along with their native promoters from MC4100 DNA using primer pairs 5'-GTAAACGCCGGCATGGTAAAGCGATTGG-3' and 5'-GCTCGCGGATCCTCATCG-CTACACTACC-3' for *bamA* and 5'- CTGCACGA-TATCATCAGGTTGATTCTGC-3' and 5'-GCCGACAGAAGCTTTTAACGTGTAATA-

GAGT-3' for *bamB*. Amplified fragments were digested with *NgoM*IV-*BamH*I (*bamA*) or *EcoR*V-*Hind*III (*bamB*) and ligated into the same sites of pMM102, yielding pBamA and pBamB.. Since the cloning of *bamD* involved digestion with *Bcl*I, a restriction enzyme whose activity is blocked by *dam* methylation, pMM102 was introduced into and purified from the *dam* strain CC160, digested with *Bcl*I and *NgoM*IV and ligated with a *Bcl*I-*NgoM*IV fragment encoding *bamD* under native promoter control that had been PCR-amplified from MC4100 DNA using primers 5'-TAATGATGATCAGCATTCAGTACCGTGCC-3' and 5'-GATTATGCCGGCTTCAGGTTTCTGTTATG - 3'. This plasmid was named pBamD. To build a plasmid encoding all three components of the Bam system we first created a pBamD derivative called pBamD^{M}, in which an internal *BamH*I site located upstream of the *bamD* promoter was eliminated by site-directed mutagenesis witrh primer pair 5'-CGCTGGT-CGAGGATCTATTCTTTTATTCGC-3' and 5'- GCGAATAAAAGAATAGAT-CCTCGACCAGCG-3'. Plasmids pBamD^{M} was next digested with *Bcl*I and *NgoM*IV and the fragment encoding *bamD* was ligated into the same sites of pBamB to create pBamBD, That plasmid was subjected to *NgoM*IV-*BamH*I digestion and ligated to a *NgoM*IV-*BamH*I fragment encoding the *bamA* gene and obtained from pBamA. The final plasmid was named pBamABD. The strains and plasmids used in this chapter are listed in Table 5.1.

Table 5.1 Strains and plasmids used in Chapter 5

Name	Description	Source or reference
Strain		
Top10	F' *endA1 recA1 hsdR17* (r_K^-,m_K^+) λ^- *supE44 thi1 gyrA96 relA1* ϕ*80* Δ*lac* Δ*M15*Δ(*lacZYA-argF*)U169 *deoR*	Invitrogen
BW25113	Δ(*araD-araB*)*567 ΔlacZ4787* (::*rrnB-3*) *lacI*^{p}*-4000*(*lacI*^{Q}) λ^- *rph-1* Δ(*rhaD-rhaB*)*568 hsdR514*	(172)
CC160	F$^-$ *thr leu thi lacY galK galT ara fhuA tsx dam dcm supE44*	(195)
Plasmid		
pPelBss-OmpA1-183-mCherry	pPelBss-OmpA derivative encoding the $OmpA_{1-183}$-mCherry fusion protein downstream of the OmpAss and under P_{BAD} promoter control	Chapter 4
pMM102	pACYC184 derivative expression system (Chl^R)	(171)
pSkp	pMM102 derivative encoding *skp* under native promoter control	This study
pSurA	pMM102 derivative encoding *surA* under native promoter control	This study
pSkpSurA	pMM102 derivative encoding both *skp* and *surA* under native promoter control	This study
pBamA	pMM102 derivative encoding *bamA* under native promoter control	This study
pBamB	pMM102 derivative encoding *bamB* under native promoter control	This study
pBamD	pMM102 derivative encoding *bamD* under native promoter control	This study
pBamD^M	pBamD derivative containing a C to T mutation to eliminate the *Bam*HI site located upstream of the *bamD* promoter region	This study
pBamABD	pMM102 derivative encoding the *bamD*, *bamA* and *bamB* genes under control of their native promoters	This study

5.2.2 *Cell growth and OMV characterization*

E. coli BW25113 harboring pPelBss-OmpA$_{1-183}$-mCherry along with the pMM102 vector or plasmids enclosing chaperones or components of the Bam system was grown in 125 mL shake flasks containing 25 mL of LB supplemented with 50 μg/mL kanamycin and 34 μg/mL chloramphenicol. At OD_{600} ~0.45, cultures were transferred from 37°C to 30°C, and induced with 0.2% (wt/vol) arabinose at $OD_{600} \approx 0.5$. OmpA$_{1-183}$-mCherry was allowed to accumulate at 30°C for 6h. Cells were sedimented at 3000*g* for 15min and the cell-free supernatant was filtered through a 0.45 μm nitrocellulose membrane. Fluorescence emission at 610 nm was quantified on a Hitachi F-4500 fluorescent spectrophotometer with excitation at 587 nm and slit widths set at 5 nm. OMV purification was carried out as described in Chapter 4 except that the medium contained 34 μg/mL chloramphenicol. OMVs were characterized as described in Chapter 4.

5.3 RESULTS AND DISCUSSION

5.3.1 *Influence of Skp, SurA and BamABD on OMV production*

A series of plasmids encoding the *skp*, *surA*, *bamA*, *bamB* and *bamD* genes under transcriptional control of their native promoters, as well as derivatives of these plasmids encoding *skp* and *surA* and *bamABD* were constructed as described in Materials and Methods. The plasmids or the pMM102 control vector were introduced with pPelBss-$OmpA_{1-183}$-mCherry in BW25113 cells and triplicate cultures were grown and induced as described in Chapter 4. Cell free supernatants were collected after 6h of post-induction growth at 30°C and the fluorescence present in 1 mL samples were quantified to determine the levels of OMV synthesis.

Figure 5.1 shows that co-expression of most gene products led to moderate (20-60%) improvements in the yields of extracellular fluorescent material. One surprising exception was Skp, a chaperone that has been shown to interact with OmpA *in vivo* (70) and that we would have therefore expected to improve $OmpA_{1-183}$-mCherry biogenesis, and consequently the yields of OMVs incorporating the reporter. For comparison, co-expression of SurA which counts OmpA among its substrates (77) led to an about 30% increase in medium fluorescence relative to the control ($p = 0.1$). While co-expression of Skp and SurA appeared to synergistically improve yields, a Student t-test revealed a p value of ≈ 0.2 when comparing the influence of Skp and SurA to that of SurA alone. It is therefore likely that the periplasmic chaperone Skp only plays a minor role in the extracellular secretion of $OmpA_{1-183}$-mCherry. In agreement with this conclusion, SurA is believed to be the primary chaperone in charge of escorting OMPs across the periplasm (79).

All component of the Bam system tested improved the yields of extracellular fluorescence. However, BamA and BamB co-expression led to the highest gains (58 % and 45 % respectively) while BamD was less efficient (20% increase compared to the control). This was unexpected because although the depletion of BamB hampers the assembly of OMPs, BamA and D are the only essential components in the Bam machinery (194) (196). More surprisingly, concomitant co-expression of all three members of the Bam system did not improve yields compared to BamA alone, suggesting that the main component of the Bam machinery is rate-limiting for OMP biogenesis.

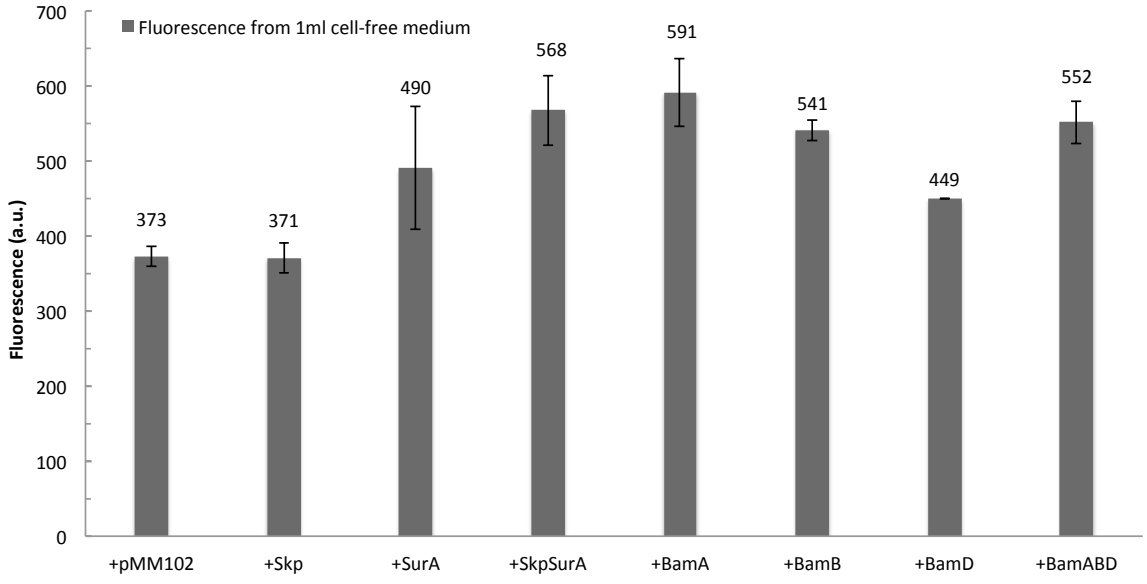

Figure 5.1 Influence of periplasmic chaperones and Bam components overexpression on the production of extracellular $OmpA_{1-183}$-mCherry

Fluorescence measurements were conducted on 1mL of cell-free medium collected after 6h of post-induction at 30°C. Cells harbored pPelBss-OmpA-mCherry along with compatible plasmids specifying the indicated proteins or the control vector pMM102.

5.3.2 *OMV characterization*

As in Chapter 4, we sought to establish a direct correlation between extracellular fluorescence and the presence of OMVs. To this end we purified and concentrated OMVs from the supernatant of cells harboring pPelBss-OmpA$_{1-183}$-mCherry and either pMM102 as a control or pSkpSurA. Figure 5.2 shows that ammonium sulfate treatment efficiently concentrated the fluorescent material and that the medium of pSkpSurA cotransformants was about 70% more fluorescent that of control cells. This is comparable to the 50% improvement observed in Figure 5.1 and confirms that SurA co-expression (and possibly that of Skp) enhance OMV production.

Dynamic light scattering analysis (Figure 5.3) confirmed the presence of particles that were relatively homogeneous (a single peak identified from the intensity graph but it had a broad size distribution). The mean hydrodynamic diameter of particles secreted by control cells (d≈116nm) was slightly larger than that measured without pMM102 (Figure 4.4 B; d≈90nm). More interestingly, the particles excreted by pSkpSurA cotransformant were are almost twice as large (d≈213nm) as the control. Although AFM analysis will be needed to confirm this finding, these results suggest that it may be possible to control OMV size by manipulating the concentration of periplasmic chaperones.

In addition, based on the correlation established in Chapter 4, we estimate that cells coexpressing pSkpSurA yields about 4 mg of OMV-incorporated OmpA$_{1-183}$-mCherry per liter of culture compared to 2.4 mg/L for the control (For details please see Appendix).

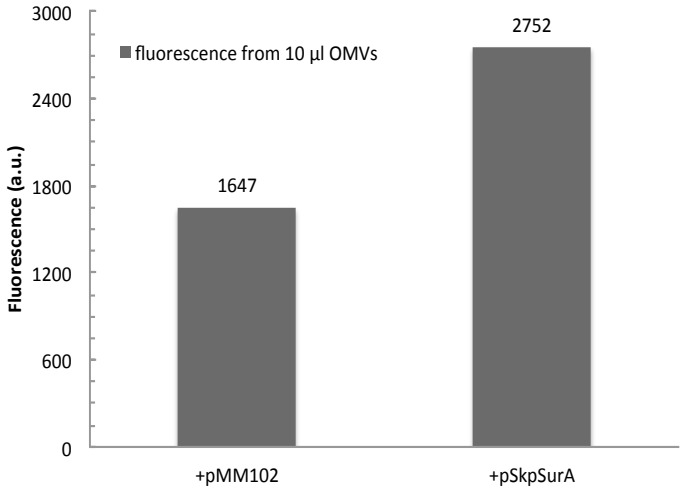

Figure 5.2 Fluorescence of OMVs concentrated from the medium of the indicated cells after 6h of post-induction growth at 30°C

OMVs from PelBss co-expressed with pMM102 control or pSkpSurA were purified as described in the text, 10 µL out of the total 250 µL purified OMVs from each sample was subject to fluorescent measurement under the same condition (excite at 587nm and emission was recorded at 610nm).

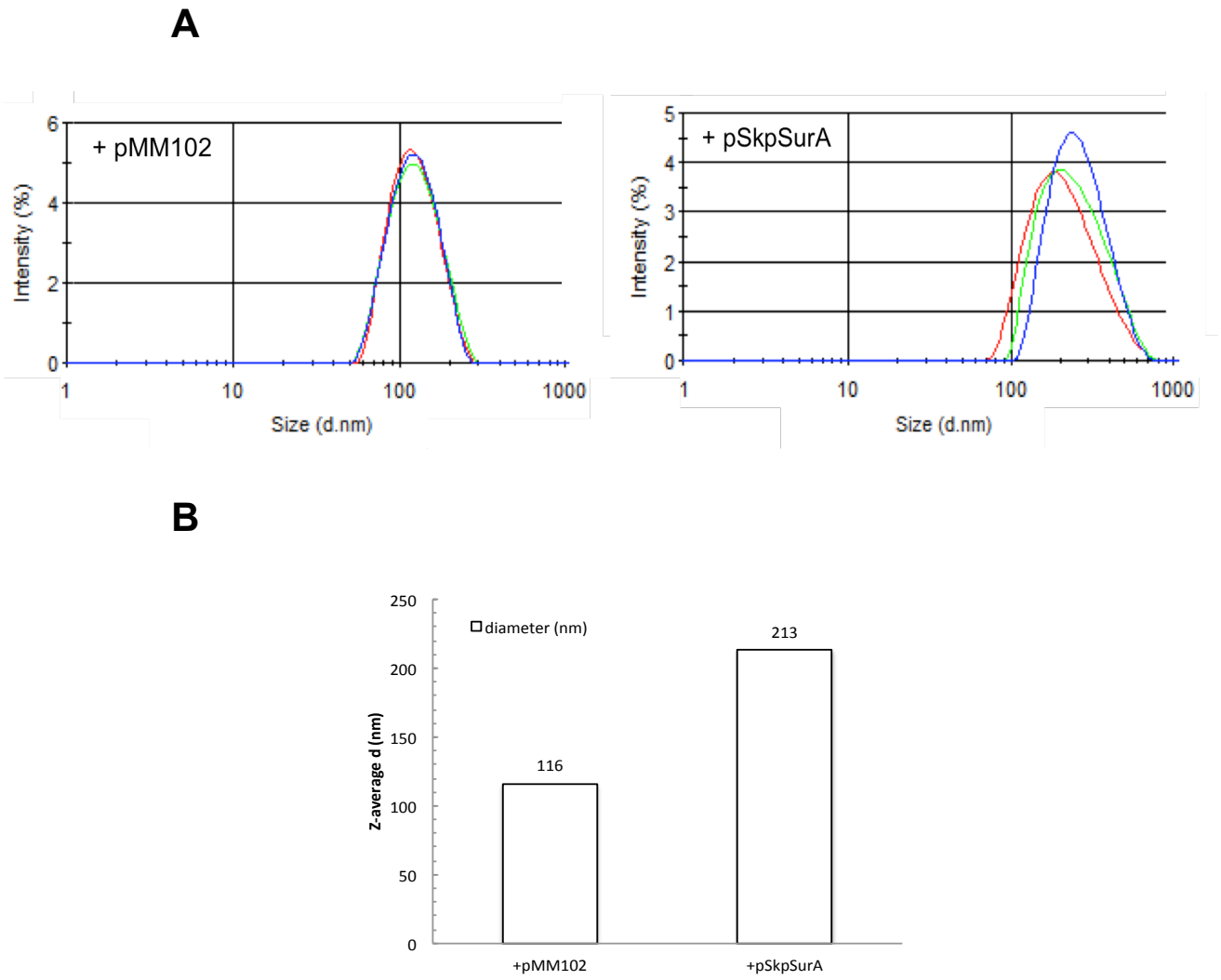

Figure 5.3 DLS size analysis of OMVs from PelBss-OmpA-mCherry with control plasmid and pSkpSurA

A. OMVs from each sample were diluted in sterile deionized water and their hydrodynamic diameters were measured using dynamic light scattering technique. Three repeats were performed on three different samples and curves were overlaid.

B. Z-average hydrodynamic diameters were derived from intensity graphs using the instrument's software.

5.4 CONCLUSIONS

In this chapter, we explored the possibility of increasing the yield of OMVs by coexpressing periplasmic chaperones or components of the Bam machinery. Our results indicate that SurA and BamA co-expression exert the most positive effect on OMV biogenesis, and that a nearly twofold increase in extracellular $OmpA_{1-183}$-mCherry production (about 4 mg/L culture) can be achieved upon Skp-SurA co-expression. From an engineering perspective, it will be interesting to determine if simultaneous co-expression of SurA and BamA synergistically increase yields. This is not unlikely since SurA has been shown to collaborate with BamA in OMP biogenesis (76, 104). Our DLS data also revealed a nearly twofold increase in the hydrodynamic diameter of OMVs produced by cells that overexpress Skp and SurA. Although confirmatory experiments will be required, these results raise the exciting possibility that it may be possible to control OMV diameter by chaperone engineering.

Chapter 6 Functionalized OMVs: using of a Silica Binding Tag in facilitating OMV Purification and beyond

6.1 INTRODUCTION

Outer membrane vesicles (OMVs) have been identified as a novel yet ubiquitous secretion mechanism (111). However, isolating OMVs from the extracellular fluid is not a trivial task due to their low abundance. Purification strategies developed to date require large amounts of effort and/or access to high-end instrumentation (192, 197). These methods include ultrafiltration, ultracentrifugation and precipitation. The first two approaches, can involve hours of processing time on sophisticated instruments (e.g., at least 3h of ultracentrifugation at 300,000*g*) and while ammonium sulfate precipitation exerts lower demands on equipment (see Chapters 4 and 5), the subsequent dialysis steps can add days to the processing time. Here, we explored the possibility of making use of a silica binding tag discovered by our group (198) to develop a rapid and cost-effective OMV purification process.

Car9, a dodecapeptide of amino acid sequence DSARGFKKPGKR was first identified for its ability to bind to carbonaceous substrates (199) and later found to exhibit micromolar affinity for silica (198). Proteins modified with a C-terminal Car9 tag efficiently bind to silica gel and can be eluted from the matrix with L-lysine or L-arginine (198). It was also shown that Car9-tagged proteins can be purified from crude cell lysates in less than 15 min using a disposable column packed with silica (198). This is significant decrease in the time required for any protein purification. In addition, the affinity tag can also be excised by the OmpT protease if removal is needed.

To explore the potential of Car9 tagging for affinity purification of OMVs, we modified $OmpA_{1-183}$-mCherry by connecting a Car9 tag to its C-terminal via a GGGS linker. We show here that when secretion of the fusion protein is directed by a PelBss signal sequence, it becomes possible to purify OMV from the extracellular fluid by affinity chromatography on silica. The potential of this modified OMVs for materials science applications is also discussed.

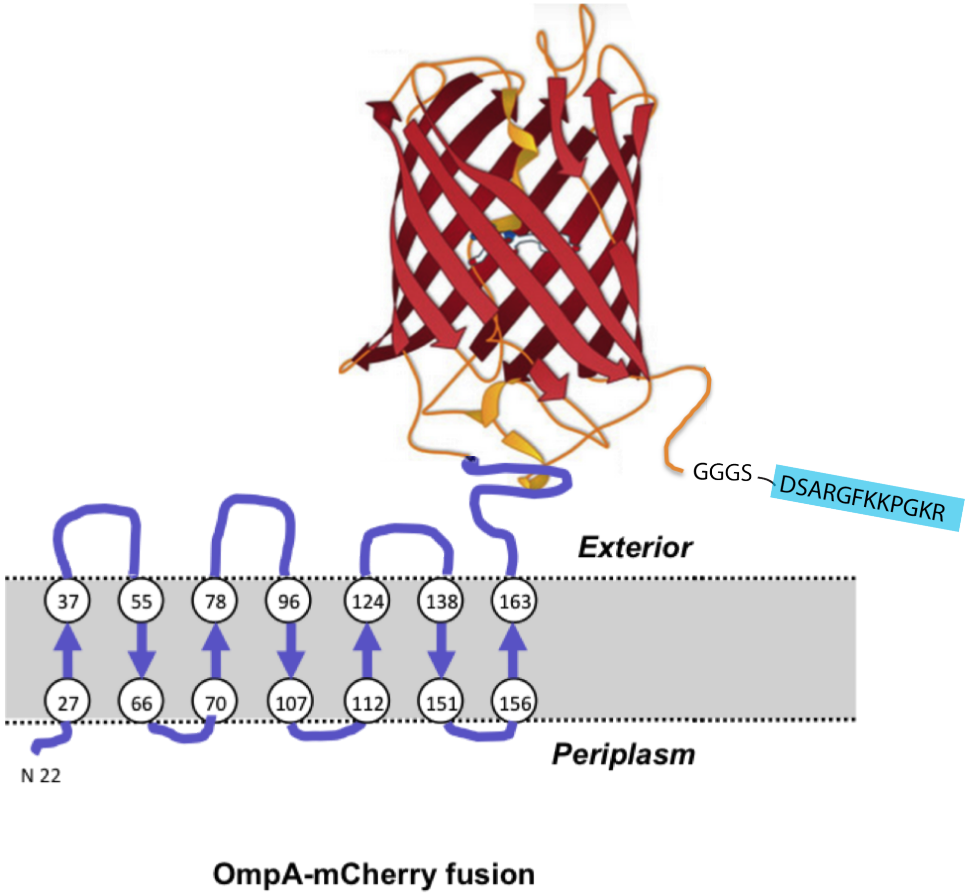

Figure 6.1 Schematic structure of the OmpA-mCherry-Car9 fusion protein

The mature and membrane-embedded OmpA-mCherry-Car9 fusion protein is schematically depicted above. The last β-strand of the 8 β-stranded barrel and the C-terminal periplasmic domain of OmpA is replaced by full length mCherry protein which is followed by a flexible GGGS linker and the Car9 tag (light blue). The structure of mCherry is adapted from PDB 2H5Q (200).

6.2 MATERIALS AND METHODS

6.2.1 *Plasmid constructions*

To fuse the Car9 tag to the C-terminus of PelBss-OmpA-mCherry, we used the phosphorylated oligonucleotides 5'- GTACAAGGGAGGCGGTAGCGACAGTGCTCGCG-GGTTTAAAAAGCCTGGGAAGCGGTAATAAC -3' and 5'- TCGAGTTATTA-CCGCTTCCCAGGCTTTTTAAACCCGCGAGCACTGTCGCTACCGCCTCCCTT - 3' which encode terminal *BsrG*I and *Xho*I restriction sites as well as the GGGSDSARGFKKPGKR sequence. Oligonucleotides were annealed and ligated to *BsrG*I-*Xho*I digested pPelBss-OmpA-mCherry. The resulting plasmid pPelBss-OmpA-mCherry-GGGS-Car9 was verified by DNA sequencing and introduced, along with the untagged pPelBss-OmpA-mCherry control, in the Δ*ompT* strain SF100 for subsequent expression. A summary of the strains and plasmids used in this Chapter is provided in Table 6.1.

Table 6.1 Strains and plasmids used in Chapter 6

Name	Description	Source or reference
Strain		
Top10	F' *endA1 recA1 hsdR17* (r_K^-,m_K^+) λ^- *supE44 thi1 gyrA96 relA1* ϕ*80* Δ*lac* Δ*M15*Δ(*lacZYA-argF*)U169 *deoR*	Invitrogen
SF100	F' Δ*lacX74 galE galK thi rps*L(*strA*) Δ*phoA* Δ*ompT*	(201)
Plasmid		
pPelBss-OmpA-mCherry	pWZ100 derivative encoding residues 1-183 of mature OmpA followed by mCherry downstream of the PelB signal sequence and under transcriptional control of the P_{BAD} promoter.	This study
pPelBss-OmpA-mCherry-GGGS-Car9	pPelBss-OmpA-mCherry derivative modified with a C-terminal Car9 affinity tag connected by a GGGS linker	This study

6.2.2 *OMV-silica interactions*

Seed cultures of SF100 cells harboring pPelBss-OmpA-mCherry or pPelBss-OmpA-mCherry-GGGS-Car9 were used to inoculate 25mL of LB medium supplemented with 50 µg/mL kanamycin. Protein expression was induced at 30°C as previously described, and cell-free supernatants were harvested 6h post-induction and filtered through 0.45 µm nitrocellulose membranes. The protocol for silica binding was adapted from reference (198). Silica gel (60-220 µm particles with 6 nm pore size) purchased from Sigma-Aldrich was washed with 20 mM Tris-HCl, pH 7.5 to remove impurities and 200 mg of settled powder was transferred to pre-weighted 1.5 mL Eppendorf tubes. Extracellular medium (500 µL) was added and the mixture was incubated for 1h at room temperature. Supernatants were aspired with a pipette (only 400 µL was removed to avoid disturbing the silica gel) and fluorescence was quantified at 610nm on a Hitachi F-4500 fluorescent spectrophotometer with excitation at 587nm and slit width set at 5 nm. Approximately 10 µL of beads from each sample was transferred to microscope slides and imaged by phase-contrast microscopy on a Nikon Eclipse TE2000-U equipped with a CCD camera (Photometrics Coolsnap ES). Images were captured at 4X magnification and with the same exposure levels. Fluorescence images were acquired using an excitation/emission filter set for mCherry.

6.2.3 *Affinity purification of OMVs*

To determine if OMVs incorporating OmpA-mCherry-Car9 could be purified by affinity chromatography on silica, extracellular medium from a 50 mL was prepared as above. Washed silica gel (3g) was loaded in the barrel of a 60 mL syringe that had been plugged with glass wool

and connected to a second 60 mL syringe through a plastic two-way check valve. A perforated plastic disc was placed on top of the silica bed to keep the stationary phase settled. About 50 mL of fresh cell-free medium was dispensed on top of the bed and the fluid was aspired at a flow rate of ≈ 30 mL/min. The flow through recovered from the bottom syringe was aspired twice more through the silica bed to ensure complete binding. One mL of the final flow-through (~50 mL) was used for fluorescence measurements. The column was washed with 50 mL of 20 mM Tris-HCl pH7.5 and bound OMVs were eluted with two applications of 50 mL of 1 M L-lysine 20 mM Tris-HCl pH 8.5. Fractions (1 mL) from each elution step were used for fluorescence quantification.

6.3 RESULTS AND DISCUSSION

6.3.1 *Characterization of OMV-silica interactions*

A derivative of $OmpA_{1-183}$-mCherry outfitted with a C-terminal Car9 tag as schematically depicted in Figure 6.1 was built as described in Materials and Methods. In this construct, transcription is controlled by the P_{BAD} promoter and secretion is driven by the PelBss. OMVs incorporating $OmpA_{1-183}$-mCherry-Car9 or the $OmpA_{1-183}$-mCherry control protein in their membrane were isolated from SF100 (Δ*ompT*) cells after 6h of post-induction growth at 30°C. As an initial test of silica binding, 1 mL of extracellular medium was harvested and mCherry fluorescence was measured before and after 1h of incubation with washed silica gel to determine how much adsorption had taken place.

For reasons that remain unclear, about 30% more mCherry fluorescence was present in the supernatant of cells producing the Car9-tagged version of $OmpA_{1-183}$-mCherry (Figure 6.2 B) Batch incubation of this fluid with silica gel led to a reproducible 60% decrease in fluorescence. However, when the medium harvested from cells producing the untagged version of the protein was incubated with silica, we measured an about 40% decrease in fluorescence (Figure 6.2 B). This suggests that there is extensive nonspecific binding under these experimental conditions. On the other hand, fluorescence microscopy imaging of silica contacted with extracellular fluid from both preparations revealed that the particles incubated with medium from $OmpA_{1-183}$-mCherry-Car9 expressing cells had a much higher degree of fluorescence (Figure 6.3).

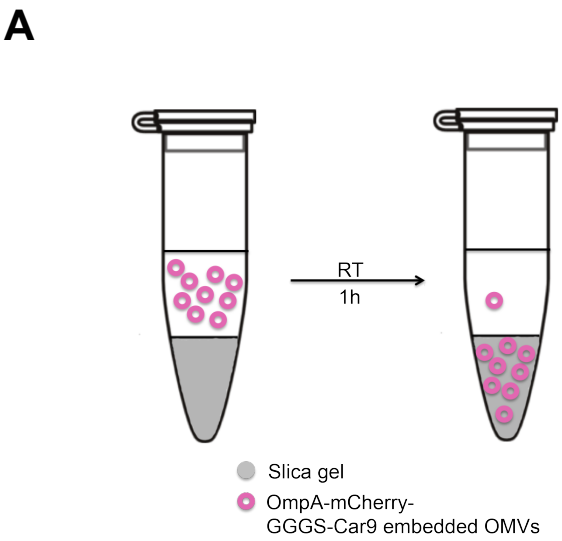

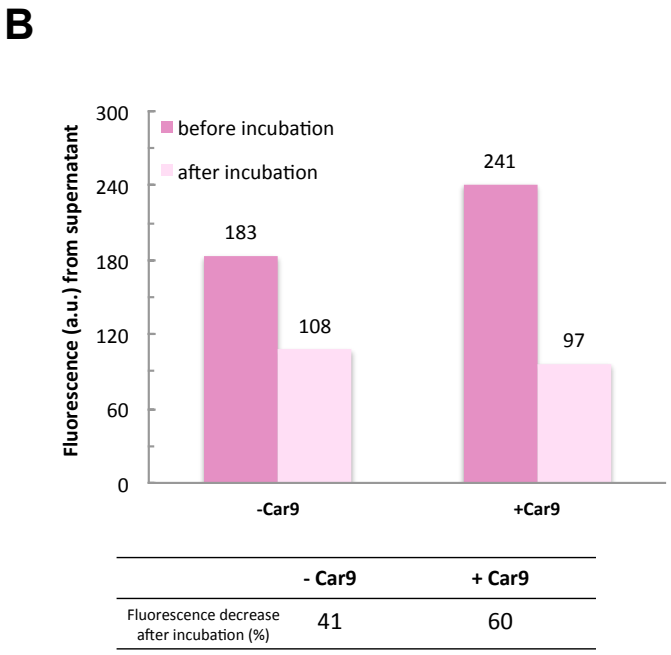

	- Car9	+ Car9
Fluorescence decrease after incubation (%)	41	60

Figure 6.2 Fluorescence depletion experiments in the presence of silica

A. Cartoon representation of the batch binding experiment. Extracellular medium harvested from cells producing an untagged or Car9-tagged version of OmpA1-183-mCherry were incubated with silica gel for 1h at room temperature. The fluorescence decrease in the supernatant is associated with Car9-mediated as well as nonspecific binding to silica.

B. The fluorescence decrease in the supernatant is associated with Car9-mediated as well as nonspecific binding to silica.

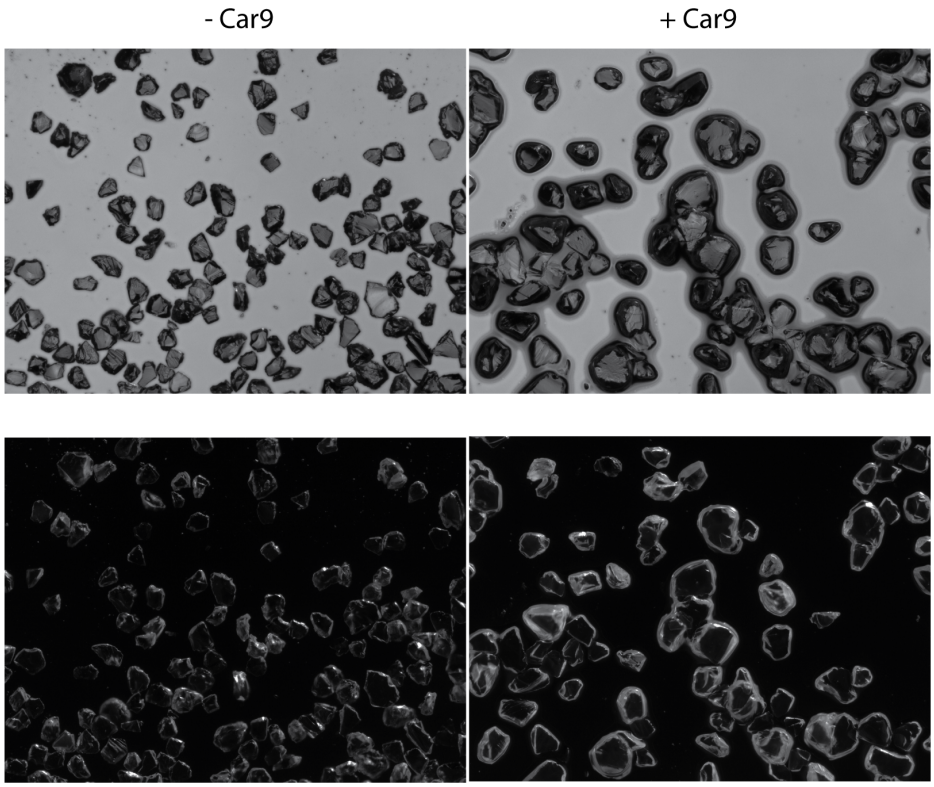

Figure 6.3 Fluorescence microscopy reveals preferential binding of $OmpA_{1-183}$-mCherry-Car9 to silica

Ten µl of silica beads from each sample were imaged as described in the text. The upper panels show phase contrast images while lower panel show fluorescent images.

6.3.2 *Affinity purification of OMVs*

To determine if binding specificity would be improved in chromatography mode, and to explore the possibility of OMV affinity purification, we assembled the device of Figure 6.4 A. Extracellular medium from the two constructs (50 mL) was loaded into the top syringe, aspirated through the silica bed, and the flow was re-applied to the gel to maximize binding. Consistent with the results of Figure 6.2 B, we observed a 35% and 67% decrease in the fluorescence of extracellular fluid collected from cells expressing untagged or tagged versions of $OmpA_{1-183}$-mCherry, respectively. We conclude that Car9-mediated affinity binding does occur (although in a non-quantitative manner) but that there are still significant levels of non-specific binding.

Elution of bound material was performed with 1 M L-Lysine in a pH=8.5 buffer which improved recovery. Figure 6.4 C shows that nearly 90% of the bound $OmpA_{1-183}$-mCherry-Car9 could be recovered (compared to 60% recovery from the starting OMV-containing medium), as to the tag-less control, on the contrary, although 65% of all Silica-bound materials was eluted out by lysine, there's only a ~20% recovery rate overall, representing the non-specific binding between silica gel and a variety of molecules that are present in the cell-free extracellular medium.

A

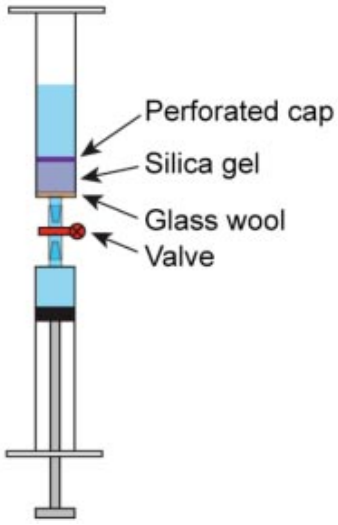

B

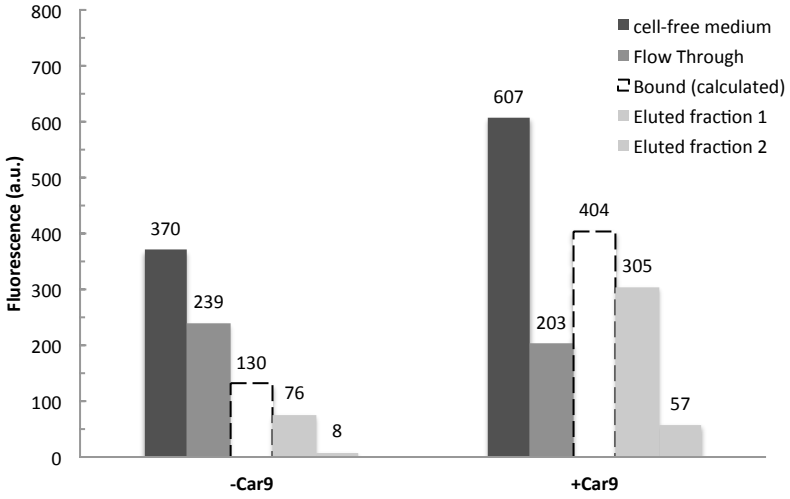

C

PelBss-OmpA-mCherry	- Car9	+ Car9
Bound / cell-free medium (%)	35	67
Eluted (fraction 1 and 2 combined) / Bound (%)	65	90
Eluted (fraction 1 and 2 combined) / cell-free medium (%)	23	60

Figure 6.4 Characterization of Car9-aided silica binding in flow mode

A. Cartoon representation of the affinity purification setup (from reference (198). The device was assembled as described in section 6.2.3. Extracellular medium was aspirated through the silica-packed top syringe, after washing the column with 50 mL Tris-HCl buffer (pH 7.5), bound materials was eluted out with 1M L-lysine buffer. Each fraction (flow through, elute 1 and 2) was collected for fluorescent measurement.

B. Fluorescence from each fraction was quantified. Bound material was calculated by subtracting flow through from load fluorescence. Binding and elution efficiencies are tabulated in (C).

6.4 CONCLUSIONS AND FUTURE WORK

In this chapter, we explored the possibility of functionalizing OMVs by adding a C-terminal silica binding tag to the $OmpA_{1-183}$-mCherry protein in order to facilitate rapid and cost-effective purification of vesicles that had incorporated the fusion protein. Our preliminary data indicate that although Car9 increases the binding of extracellular fluorescent material to silica gel, there is significant nonspecific adsorption of OMVs containing an untagged $OmpA_{1-183}$-mCherry. A possible culprit may be the mCherry domain itself since this fluorescent reporter appears to have some affinity for silica (Baneyx group unpublished data). In addition, the lipidic components of OMVs might also contribute to this process (202). Further investigations will be needed to pinpoint the source of non-specific interactions.

Chapter 7 CONCLUSIONS

Secretory proteins make up approximately 30% of all polypeptides synthesized in bacteria and are involved in a variety of essential biochemical processes. In gram-negative bacteria, periplasmic and outer membrane proteins (OMPs) are marked for export by a cleavable N-terminal signal peptide (SP) about 20 residues in length, and their translocation across the inner membrane is mainly accomplished via the Sec-dependent pathway.

In nature, extended signal sequences have proven particularly effective at targeting serine protease autotransporters of *E.coli* and *Shigella* to the outer membrane. Inspired by this unusual phenomenon, our first goal was to determine if extended signal peptides built from traditional ones would benefit secretory protein overproduction, particularly that of soluble periplasmic and outer membrane proteins. To this end, we fused the signal sequences of *E. carotovora* PelB and *E. coli* OmpA to one another to produce synthetic PelB-OmpA (POss) and OmpA-PelB (OPss) leader peptides.

In Chapter 2, we demonstrated that such dual signal peptides support the translocation of maltose binding protein to the periplasm and that, although they contain two signal peptidase I (SPase I) cleavage sites, they are preferentially processed at the location that is vicinal to the mature protein. Although the use of dual signal sequences led to a decrease in cell fitness and mature MBP production, OPss-mediated export conferred a slight improvement in the amount of properly folded and bioactive MBP, while POss-mediated export resulted in the lowest levels of preprotein accumulation.

We further investigated the potential usefulness of dual signal peptides using OmpA overproduction from the P_{BAD} promoter as a model system (Chapter 3). We found that export

remained SecA-dependent, and that OmpA variants equipped with dual leaders exhibited a stronger requirement for the chaperone Trigger Factor. From a practical standpoint, there was reduced accumulation of misfolded precursor and mature species and a delay in the acquisition of plasmid mutations that restore cell growth by shutting down OmpA synthesis.

Thus dual signal peptides have limitations but also distinct advantages over traditional Sec-dependent leader sequences for the production of both periplasmic and outer membrane proteins.

Next, we turned our attention to the extracellular secretion (or excretion) of outer membrane vesicles (OMVs). These particles are ubiquitously released upon pinching of the outer membrane surface and therefore contain properly oriented outer membrane proteins (OMPs) in their walls and periplasmic fluid and proteins within their lumen. They hold great potential for the production of engineered vaccine, and in biotechnology and materials science applications. Several pioneering studies have recently demonstrated the feasibility of incorporating heterologous protein within OMVs by fusing them to partners known to be enriched in the vesicles.

In Chapter 4, we built and used a fluorescent $OmpA_{1\text{-}183}$-mCherry fusion protein as a reporter of OMVs production. We confirmed that fluorescent OMVs with average diameter of 100 nm were produced and optimized signal sequence identity, temperature and harvest time to maximize production. Although dual signal peptides remain functional for secretion and ultimate delivery of $OmpA_{1\text{-}183}$-mCherry to OMVs, they did not outperform the PelBss.

Chapter 5 further explored the possibility of increasing OMV yield of by co-expression of periplasmic molecular chaperones and components of the Bam machinery. We found that SurA and BamA co-expression exerted the most positive effect on OMV biogenesis, and that a

nearly twofold increase in extracellular $OmpA_{1-183}$-mCherry production (approximately 4 mg/L culture) could be achieved upon Skp/SurA co-expression. In addition, we discovered that co-expression of these two chaperones increased vesicle size. Although additional work will be required, these results raise the exciting possibility that OMV size can be tuned via chaperone engineering.

In chapter 6, we functionalized outer membrane vesicles by adding a silica binding tag to the C-terminus of $OmpA_{1-183}$-mCherry with the aim of achieving rapid and cost-effective purification of OMVs. Preliminary results confirmed silica binding but also revealed complications due to nonspecific protein adsorption. Further investigations will be needed to pinpoint the reasons for non-specific binding and optimize the purification process. These results, however, laid the groundwork for future studies exploring the potential of OMVs in bionanotechnology.

Native secretory proteins, and especially outer membrane proteins (OMPs) of medical or technological interest, are often produced at levels that are insufficient for structural analysis or for use in vaccine or bionanotechnology applications. To make matters worse, OMP overexpression often does not improve yields and typically induce severe toxicity in host cells. In this work, we showed that a novel signal peptide consisting of fused Sec-dependent leader sequences supports the translocation of both periplasmic proteins and OMPs across the inner membrane. Although the benefits of such synthetic dual signal peptides will have to be evaluated on a case-by-case basis, they proved effective at delaying host toxicity and at reducing the accumulation of precursor and misfolded forms of OmpA without compromising the yield of properly folded product. These novel leader peptides may also be useful to protein engineers

who aim at improving the production yield of difficult-to-express proteins in the E. coli periplasm.

Excretion of OMPs into the growth medium under the form of outer membrane vesicles (OMVs) could be a useful alternative for the production of recombinant OMPs. Just like in the case of excreted soluble proteins, production of OMPs within OMVs should simplify protein purification and possibly mitigate toxicity effects. In this work, we showed not only that this approach was viable, but that it could be combined with chaperone pathway engineering – the coexpression of the target secretory protein with periplasmic chaperone and/or components of the β-barrel assembly machinery (Bam) – to improve yields by nearly twofold. These results confirmed that the periplasmic protein SurA serves as a the primary molecular chaperone in charge of escorting OMPs to their final destination and the main component of the Bam machinery BamA is a rate-limiting factors in recombinant OMP biogenesis. Although future work will be necessary to verify this finding, we also presented preliminary evidence that chaperone coexpression may influence the size of OMVs that pinch out from the cell membrane. Facile production of functionalized OMVs produced by genetic engineering of constituent OMPs should also open the door to new applications in the bionanotechnology arena.

APPENDIX

OUTER MEMBRANE VESICLE YIELD QUANTIFICATION

To quantify the amount of $OmpA_{1\text{-}183}$-mCherry present in OMVs, we used purified mCherry to correlate protein concentration with fluorescence intensity. To this end, serial dilutions of purified mCherry protein were fractionated by SDS-PAGE and the intensity of each band was quantified using ImageJ. As expected in the dynamic range, there was a linear correlation between amount of protein loaded and band intensity. The fluorescence of each sample was also determined to establish a correlation between mCherry mass and fluorescence (Figure 8.1):

$$y = 136.07x - 85.158\ (R^2 = 0.99701)$$

where: $x =$ Mass of purified mCherry protein (μg); y = Fluorescence units

Thus, for a fluorescent signal y = 500, $x = \frac{(500+85.158)}{136.07} = 4.3\ \mu g$ or 0.16 nmol considering the molecular mass of mCherry is 27kDa. Assuming that fusion to $OmpA_{1\text{-}183}$ does not affect mCherry fluorescence and considering that $OmpA_{1\text{-}183}$ -mCherry has a molecular mass of ~45kDa, the same 500 units of fluorescence correspond to 7.2 μg of fusion protein.

Data from Figure 4.3 B shows that 10 μL of OMVs incorporating $OmpA_{1\text{-}183}$-mCherry produce about 800 units of fluorescence. Therefore, a total of $\frac{250\ \mu l}{10\ \mu l} \times 800 = 20{,}000\ fluorescent\ units$ emitted from 250 μL OMVs, which are concentrated from a 250 mL culture. Applying the correlation above, we can calculate that $\frac{20{,}000}{500} \times 7.2 =$

$288\ \mu g$ of $OmpA_{1\text{-}183}$-mCherry is retrieved from a 250 mL culture, a yield of $288 \times \frac{1000\ mL}{250\ mL} = 1152\ \mu g$ or approximately 1.2 mg/L.

For the OMVs coming from PelBss-$OmpA_{1\text{-}183}$-mCherry coexpressed with either pMM102 control plasmid or pSkpSurA, their yields were calculated based on the same principle, and the results were tabulated in Table 8.1 as below.

A

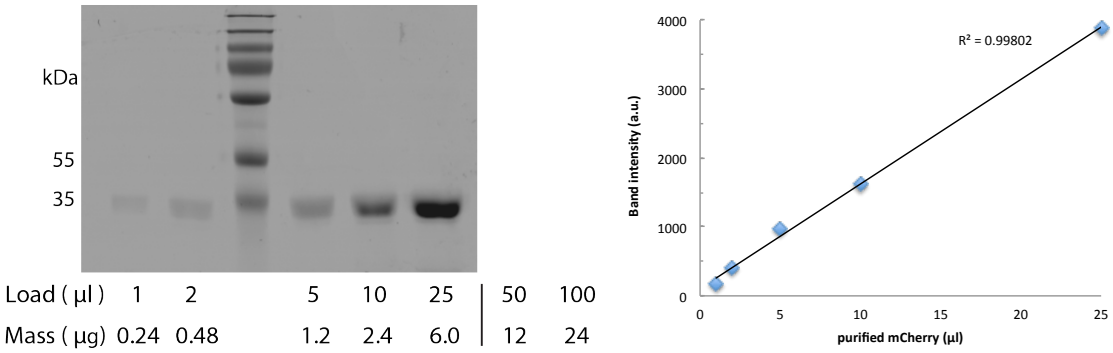

B

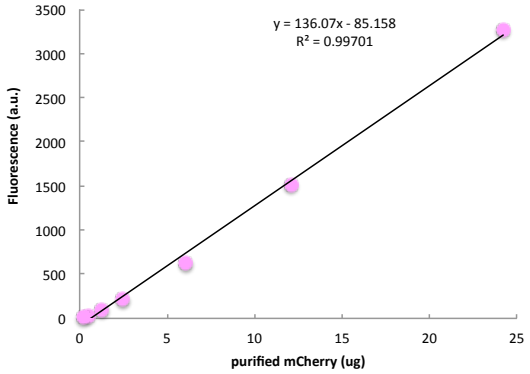

protein mass (µg)	Fluorescence (a.u.)
0.24	15
0.48	34
1.2	91
2.4	222
6.0	627
12	1511
24	3263

Figure 0.1 Correlation of fluorescence intensity with mCherry mass

A. Serial dilutions of purified mCherry were loaded onto an SDS-PAGE gel and the intensities of the protein bands quantified using ImageJ. Loaded volume and protein mass were calculated and are tabulated under the gel.

B. Duplicates of each dilution was subjected to fluorescent measurement and a linear correlation between protein mass and fluorescence was derived using Excel.

Table 0.1 OMV yield quantification for PelBss-OmpA$_{1-183}$-mCherry with control plasmid or pSkpSurA

PelBss-OmpA-mCherry	+pMM102	+pSkpSurA
Fluorescence (a.u.) from 10 µl of OMVs	1647	2752
protein mass (µg) from 10 µl of OMVs	24	40
protein mass (µg) from 250 µl of OMV	592	988
protein mass (µg) from 1000 µl of OMV	2366	3954
protein mass (mg) from equivalent of 1L culture	2.4	4.0

BIBLIOGRAPHY

1. Dautin N, Bernstein HD. Protein secretion in gram-negative bacteria via the autotransporter pathway. Annu Rev Microbiol. 2007;61:89-112.
2. Auclair SM, Bhanu MK, Kendall DA. Signal peptidase I: cleaving the way to mature proteins. Protein Sci. 2012;21(1):13-25.
3. Desvaux M, Cooper LM, Filenko NA, Scott-Tucker A, Turner SM, Cole JA, et al. The unusual extended signal peptide region of the type V secretion system is phylogenetically restricted. FEMS Microbiol Lett. 2006;264(1):22-30.
4. Chagnot C, Zorgani MA, Astruc T, Desvaux M. Proteinaceous determinants of surface colonization in bacteria: bacterial adhesion and biofilm formation from a protein secretion perspective. Front Microbiol. 2013;4:303.
5. Walther DM, Rapaport D, Tommassen J. Biogenesis of beta-barrel membrane proteins in bacteria and eukaryotes: evolutionary conservation and divergence. Cell Mol Life Sci. 2009;66(17):2789-804.
6. Tommassen J. Assembly of outer-membrane proteins in bacteria and mitochondria. Microbiology. 2010;156(Pt 9):2587-96.
7. Knowles TJ, Scott-Tucker A, Overduin M, Henderson IR. Membrane protein architects: the role of the BAM complex in outer membrane protein assembly. Nat Rev Microbiol. 2009;7(3):206-14.
8. Tokuda H. Biogenesis of outer membranes in Gram-negative bacteria. Biosci Biotechnol Biochem. 2009;73(3):465-73.
9. Bos MP, Robert V, Tommassen J. Biogenesis of the gram-negative bacterial outer membrane. Annu Rev Microbiol. 2007;61:191-214.
10. Oh E, Becker AH, Sandikci A, Huber D, Chaba R, Gloge F, et al. Selective ribosome profiling reveals the cotranslational chaperone action of trigger factor in vivo. Cell. 2011;147(6):1295-308.
11. Sala A, Bordes P, Genevaux P. Multitasking SecB chaperones in bacteria. Front Microbiol. 2014;5:666.

12. Driessen AJ, Nouwen N. Protein translocation across the bacterial cytoplasmic membrane. Annu Rev Biochem. 2008;77:643-67.

13. Mori H, Ito K. The Sec protein-translocation pathway. Trends Microbiol. 2001;9(10):494-500.

14. Ferbitz L, Maier T, Patzelt H, Bukau B, Deuerling E, Ban N. Trigger factor in complex with the ribosome forms a molecular cradle for nascent proteins. Nature. 2004;431(7008):590-6.

15. Hebert DN, Chandrasekhar KD, Gierasch LM. You got to know when to hold (or unfold) 'em…. Mol Cell. 2012;48(1):3-4.

16. Bowers CW, Lau F, Silhavy TJ. Secretion of LamB-LacZ by the signal recognition particle pathway of Escherichia coli. J Bacteriol. 2003;185(19):5697-705.

17. Schierle CF, Berkmen M, Huber D, Kumamoto C, Boyd D, Beckwith J. The DsbA signal sequence directs efficient, cotranslational export of passenger proteins to the Escherichia coli periplasm via the signal recognition particle pathway. J Bacteriol. 2003;185(19):5706-13.

18. Martoglio B, Dobberstein B. Signal sequences: more than just greasy peptides. Trends Cell Biol. 1998;8(10):410-5.

19. Luirink J, Sinning I. SRP-mediated protein targeting: structure and function revisited. Biochim Biophys Acta. 2004;1694(1-3):17-35.

20. Akopian D, Shen K, Zhang X, Shan SO. Signal recognition particle: an essential protein-targeting machine. Annu Rev Biochem. 2013;82:693-721.

21. Lee PA, Tullman-Ercek D, Georgiou G. The bacterial twin-arginine translocation pathway. Annu Rev Microbiol. 2006;60:373-95.

22. Palmer T, Sargent F, Berks BC. Export of complex cofactor-containing proteins by the bacterial Tat pathway. Trends Microbiol. 2005;13(4):175-80.

23. Rodrigue A, Chanal A, Beck K, Müller M, Wu LF. Co-translocation of a periplasmic enzyme complex by a hitchhiker mechanism through the bacterial tat pathway. J Biol Chem. 1999;274(19):13223-8.

24. Dubini A, Sargent F. Assembly of Tat-dependent [NiFe] hydrogenases: identification of precursor-binding accessory proteins. FEBS Lett. 2003;549(1-3):141-6.

25. Palmer T, Berks BC. The twin-arginine translocation (Tat) protein export pathway. Nat Rev Microbiol. 2012;10(7):483-96.

26. Hoffmann A, Bukau B, Kramer G. Structure and function of the molecular chaperone Trigger Factor. Biochim Biophys Acta. 2010;1803(6):650-61.

27. Lakshmipathy SK, Tomic S, Kaiser CM, Chang HC, Genevaux P, Georgopoulos C, et al. Identification of nascent chain interaction sites on trigger factor. J Biol Chem. 2007;282(16):12186-93.

28. Hoffmann A, Becker AH, Zachmann-Brand B, Deuerling E, Bukau B, Kramer G. Concerted action of the ribosome and the associated chaperone trigger factor confines nascent polypeptide folding. Mol Cell. 2012;48(1):63-74.

29. Beckwith J. The Sec-dependent pathway. Res Microbiol. 2013;164(6):497-504.

30. Huber D, Boyd D, Xia Y, Olma MH, Gerstein M, Beckwith J. Use of thioredoxin as a reporter to identify a subset of Escherichia coli signal sequences that promote signal recognition particle-dependent translocation. J Bacteriol. 2005;187(9):2983-91.

31. Kudva R, Denks K, Kuhn P, Vogt A, Müller M, Koch HG. Protein translocation across the inner membrane of Gram-negative bacteria: the Sec and Tat dependent protein transport pathways. Res Microbiol. 2013;164(6):505-34.

32. Hartl FU, Lecker S, Schiebel E, Hendrick JP, Wickner W. The binding cascade of SecB to SecA to SecY/E mediates preprotein targeting to the E. coli plasma membrane. Cell. 1990;63(2):269-79.

33. Castanié-Cornet MP, Bruel N, Genevaux P. Chaperone networking facilitates protein targeting to the bacterial cytoplasmic membrane. Biochim Biophys Acta. 2014;1843(8):1442-56.

34. Gouridis G, Karamanou S, Sardis MF, Schärer MA, Capitani G, Economou A. Quaternary dynamics of the SecA motor drive translocase catalysis. Mol Cell. 2013;52(5):655-66.

35. Chatzi KE, Sardis MF, Economou A, Karamanou S. SecA-mediated targeting and translocation of secretory proteins. Biochim Biophys Acta. 2014;1843(8):1466-74.

36. Gouridis G, Karamanou S, Gelis I, Kalodimos CG, Economou A. Signal peptides are allosteric activators of the protein translocase. Nature. 2009;462(7271):363-7.

37. Huber D, Rajagopalan N, Preissler S, Rocco MA, Merz F, Kramer G, et al. SecA interacts with ribosomes in order to facilitate posttranslational translocation in bacteria. Mol Cell. 2011;41(3):343-53.

38. Lycklama A Nijeholt JA, Driessen AJ. The bacterial Sec-translocase: structure and mechanism. Philos Trans R Soc Lond B Biol Sci. 2012;367(1592):1016-28.

39. Zimmer J, Nam Y, Rapoport TA. Structure of a complex of the ATPase SecA and the protein-translocation channel. Nature. 2008;455(7215):936-43.

40. Frauenfeld J, Gumbart J, Sluis EO, Funes S, Gartmann M, Beatrix B, et al. Cryo-EM structure of the ribosome-SecYE complex in the membrane environment. Nat Struct Mol Biol. 2011;18(5):614-21.

41. Ménétret JF, Schaletzky J, Clemons WM, Osborne AR, Skånland SS, Denison C, et al. Ribosome binding of a single copy of the SecY complex: implications for protein translocation. Mol Cell. 2007;28(6):1083-92.

42. Miller A, Wang L, Kendall DA. Synthetic signal peptides specifically recognize SecA and stimulate ATPase activity in the absence of preprotein. J Biol Chem. 1998;273(19):11409-12.

43. Wang L, Miller A, Kendall DA. Signal peptide determinants of SecA binding and stimulation of ATPase activity. J Biol Chem. 2000;275(14):10154-9.

44. Akita M, Sasaki S, Matsuyama S, Mizushima S. SecA interacts with secretory proteins by recognizing the positive charge at the amino terminus of the signal peptide in Escherichia coli. J Biol Chem. 1990;265(14):8164-9.

45. Nishiyama K, Tokuda H. Preparation of a highly translocation-competent proOmpA/SecB complex. Protein Sci. 2010;19(12):2402-8.

46. Kulothungan SR, Das M, Johnson M, Ganesh C, Varadarajan R. Effect of crowding agents, signal peptide, and chaperone SecB on the folding and aggregation of E. coli maltose binding protein. Langmuir. 2009;25(12):6637-48.

47. Lilly AA, Crane JM, Randall LL. Export chaperone SecB uses one surface of interaction for diverse unfolded polypeptide ligands. Protein Sci. 2009;18(9):1860-8.

48. Randall LL, Hardy SJ. High selectivity with low specificity: how SecB has solved the paradox of chaperone binding. Trends Biochem Sci. 1995;20(2):65-9.

49. Izard JW, Kendall DA. Signal peptides: exquisitely designed transport promoters. Mol Microbiol. 1994;13(5):765-73.

50. Lecker SH, Driessen AJ, Wickner W. ProOmpA contains secondary and tertiary structure prior to translocation and is shielded from aggregation by association with SecB protein. EMBO J. 1990;9(7):2309-14.

51. Von Heijine, Gunnar. Topical review: The signal peptide. JMembrane Biol. 1990(115):7.

52. Wang P, Shim E, Cravatt B, Jacobsen R, Schoeniger J, Kim AC, et al. Escherichia coli signal peptide peptidase A is a serine-lysine protease with a lysine recruited to the nonconserved amino-terminal domain in the S49 protease family. Biochemistry. 2008;47(24):6361-9.

53. Nam SE, Paetzel M. Structure of Signal Peptide Peptidase A with C-Termini Bound in the Active Sites: Insights into Specificity, Self-Processing, and Regulation. Biochemistry. 2013.

54. Belin D, Bost S, Vassalli JD, Strub K. A two-step recognition of signal sequences determines the translocation efficiency of proteins. EMBO J. 1996;15(3):468-78.

55. Kurys G, Tagaya Y, Bamford R, Hanover JA, Waldmann TA. The long signal peptide isoform and its alternative processing direct the intracellular trafficking of interleukin-15. J Biol Chem. 2000;275(39):30653-9.

56. Li Y, Bergeron JJ, Luo L, Ou WJ, Thomas DY, Kang CY. Effects of inefficient cleavage of the signal sequence of HIV-1 gp 120 on its association with calnexin, folding, and intracellular transport. Proc Natl Acad Sci U S A. 1996;93(18):9606-11.

57. Chevalier N, Moser M, Koch HG, Schimz KL, Willery E, Locht C, et al. Membrane targeting of a bacterial virulence factor harbouring an extended signal peptide. J Mol Microbiol Biotechnol. 2004;8(1):7-18.

58. Szabady RL, Peterson JH, Skillman KM, Bernstein HD. An unusual signal peptide facilitates late steps in the biogenesis of a bacterial autotransporter. Proc Natl Acad Sci U S A. 2005;102(1):221-6.

59. Henderson IR, Navarro-Garcia F, Desvaux M, Fernandez RC, Ala'Aldeen D. Type V protein secretion pathway: the autotransporter story. Microbiol Mol Biol Rev. 2004;68(4):692-744.

60. Henderson IR, Navarro-Garcia F, Nataro JP. The great escape: structure and function of the autotransporter proteins. Trends Microbiol. 1998;6(9):370-8.

61. Peterson JH, Szabady RL, Bernstein HD. An unusual signal peptide extension inhibits the binding of bacterial presecretory proteins to the signal recognition particle, trigger factor, and the SecYEG complex. J Biol Chem. 2006;281(14):9038-48.

62. Sijbrandi R, Urbanus ML, ten Hagen-Jongman CM, Bernstein HD, Oudega B, Otto BR, et al. Signal recognition particle (SRP)-mediated targeting and Sec-dependent translocation of an extracellular Escherichia coli protein. J Biol Chem. 2003;278(7):4654-9.

63. Leyton D, de Luna M, Sevastsyanovich Y, Jensen K, Browning D, Tucker A, et al. The unusual extended signal peptide region is not required for secretion and function of an Escherichia coli autotransporter. FEMS Microbiol Lett. 2010(311):7.

64. Chen R, Henning U. A periplasmic protein (Skp) of Escherichia coli selectively binds a class of outer membrane proteins. Mol Microbiol. 1996;19(6):1287-94.

65. Walton TA, Sousa MC. Crystal structure of Skp, a prefoldin-like chaperone that protects soluble and membrane proteins from aggregation. Mol Cell. 2004;15(3):367-74.

66. Hagan CL, Silhavy TJ, Kahne D. β-Barrel membrane protein assembly by the Bam complex. Annu Rev Biochem. 2011;80:189-210.

67. Bulieris PV, Behrens S, Holst O, Kleinschmidt JH. Folding and insertion of the outer membrane protein OmpA is assisted by the chaperone Skp and by lipopolysaccharide. J Biol Chem. 2003;278(11):9092-9.

68. Qu J, Mayer C, Behrens S, Holst O, Kleinschmidt JH. The trimeric periplasmic chaperone Skp of Escherichia coli forms 1:1 complexes with outer membrane proteins via hydrophobic and electrostatic interactions. J Mol Biol. 2007;374(1):91-105.

69. Qu J, Behrens-Kneip S, Holst O, Kleinschmidt JH. Binding regions of outer membrane protein A in complexes with the periplasmic chaperone Skp. A site-directed fluorescence study. Biochemistry. 2009;48(22):4926-36.

70. Walton TA, Sandoval CM, Fowler CA, Pardi A, Sousa MC. The cavity-chaperone Skp protects its substrate from aggregation but allows independent folding of substrate domains. Proc Natl Acad Sci U S A. 2009;106(6):1772-7.

71. Schäfer U, Beck K, Müller M. Skp, a molecular chaperone of gram-negative bacteria, is required for the formation of soluble periplasmic intermediates of outer membrane proteins. J Biol Chem. 1999;274(35):24567-74.

72. Tormo A, Almirón M, Kolter R. surA, an Escherichia coli gene essential for survival in stationary phase. J Bacteriol. 1990;172(8):4339-47.

73. Behrens-Kneip S. The role of SurA factor in outer membrane protein transport and virulence. Int J Med Microbiol. 2010;300(7):421-8.

74. Bitto E, McKay DB. The periplasmic molecular chaperone protein SurA binds a peptide motif that is characteristic of integral outer membrane proteins. J Biol Chem. 2003;278(49):49316-22.

75. Hennecke G, Nolte J, Volkmer-Engert R, Schneider-Mergener J, Behrens S. The periplasmic chaperone SurA exploits two features characteristic of integral outer membrane proteins for selective substrate recognition. J Biol Chem. 2005;280(25):23540-8.

76. Sklar JG, Wu T, Kahne D, Silhavy TJ. Defining the roles of the periplasmic chaperones SurA, Skp, and DegP in Escherichia coli. Genes Dev. 2007;21(19):2473-84.

77. Lazar SW, Kolter R. SurA assists the folding of Escherichia coli outer membrane proteins. J Bacteriol. 1996;178(6):1770-3.

78. Rouvière PE, Gross CA. SurA, a periplasmic protein with peptidyl-prolyl isomerase activity, participates in the assembly of outer membrane porins. Genes Dev. 1996;10(24):3170-82.

79. Vertommen D, Ruiz N, Leverrier P, Silhavy TJ, Collet JF. Characterization of the role of the Escherichia coli periplasmic chaperone SurA using differential proteomics. Proteomics. 2009;9(9):2432-43.

80. Solov'eva TF, Novikova OD, Portnyagina OY. Biogenesis of β-barrel integral proteins of bacterial outer membrane. Biochemistry (Mosc). 2012;77(11):1221-36.

81. Ricci DP, Silhavy TJ. The Bam machine: a molecular cooper. Biochim Biophys Acta. 2012;1818(4):1067-84.

82. Hansen G, Hilgenfeld R. Architecture and regulation of HtrA-family proteins involved in protein quality control and stress response. Cell Mol Life Sci. 2013;70(5):761-75.

83. Goemans C, Denoncin K, Collet JF. Folding mechanisms of periplasmic proteins. Biochim Biophys Acta. 2014;1843(8):1517-28.

84. Krojer T, Sawa J, Schäfer E, Saibil HR, Ehrmann M, Clausen T. Structural basis for the regulated protease and chaperone function of DegP. Nature. 2008;453(7197):885-90.

85. Sawa J, Heuck A, Ehrmann M, Clausen T. Molecular transformers in the cell: lessons learned from the DegP protease-chaperone. Curr Opin Struct Biol. 2010;20(2):253-8.

86. Subrini O, Betton JM. Assemblies of DegP underlie its dual chaperone and protease function. FEMS Microbiol Lett. 2009;296(2):143-8.

87. Antonoaea R, Fürst M, Nishiyama K, Müller M. The periplasmic chaperone PpiD interacts with secretory proteins exiting from the SecYEG translocon. Biochemistry. 2008;47(20):5649-56.

88. Arié JP, Sassoon N, Betton JM. Chaperone function of FkpA, a heat shock prolyl isomerase, in the periplasm of Escherichia coli. Mol Microbiol. 2001;39(1):199-210.

89. Saul FA, Arié JP, Vulliez-le Normand B, Kahn R, Betton JM, Bentley GA. Structural and functional studies of FkpA from Escherichia coli, a cis/trans peptidyl-prolyl isomerase with chaperone activity. J Mol Biol. 2004;335(2):595-608.

90. Matern Y, Barion B, Behrens-Kneip S. PpiD is a player in the network of periplasmic chaperones in Escherichia coli. BMC Microbiol. 2010;10:251.

91. Sachelaru I, Petriman NA, Kudva R, Koch HG. Dynamic interaction of the sec translocon with the chaperone PpiD. J Biol Chem. 2014;289(31):21706-15.

92. Ni D, Wang Y, Yang X, Zhou H, Hou X, Cao B, et al. Structural and functional analysis of the β-barrel domain of BamA from Escherichia coli. FASEB J. 2014;28(6):2677-85.

93. Rigel NW, Silhavy TJ. Making a beta-barrel: assembly of outer membrane proteins in Gram-negative bacteria. Curr Opin Microbiol. 2012;15(2):189-93.

94. Kim S, Malinverni JC, Sliz P, Silhavy TJ, Harrison SC, Kahne D. Structure and function of an essential component of the outer membrane protein assembly machine. Science. 2007;317(5840):961-4.

95. Gatzeva-Topalova PZ, Warner LR, Pardi A, Sousa MC. Structure and flexibility of the complete periplasmic domain of BamA: the protein insertion machine of the outer membrane. Structure. 2010;18(11):1492-501.

96. Gatzeva-Topalova PZ, Walton TA, Sousa MC. Crystal structure of YaeT: conformational flexibility and substrate recognition. Structure. 2008;16(12):1873-81.

97. Heuck A, Schleiffer A, Clausen T. Augmenting β-augmentation: structural basis of how BamB binds BamA and may support folding of outer membrane proteins. J Mol Biol. 2011;406(5):659-66.

98. Ricci DP, Hagan CL, Kahne D, Silhavy TJ. Activation of the Escherichia coli β-barrel assembly machine (Bam) is required for essential components to interact properly with substrate. Proc Natl Acad Sci U S A. 2012;109(9):3487-91.

99. Rigel NW, Ricci DP, Silhavy TJ. Conformation-specific labeling of BamA and suppressor analysis suggest a cyclic mechanism for β-barrel assembly in Escherichia coli. Proc Natl Acad Sci U S A. 2013;110(13):5151-6.

100. Ureta AR, Endres RG, Wingreen NS, Silhavy TJ. Kinetic analysis of the assembly of the outer membrane protein LamB in Escherichia coli mutants each lacking a secretion or targeting factor in a different cellular compartment. J Bacteriol. 2007;189(2):446-54.

101. Ieva R, Tian P, Peterson JH, Bernstein HD. Sequential and spatially restricted interactions of assembly factors with an autotransporter beta domain. Proc Natl Acad Sci U S A. 2011;108(31):E383-91.

102. Wu S, Ge X, Lv Z, Zhi Z, Chang Z, Zhao XS. Interaction between bacterial outer membrane proteins and periplasmic quality control factors: a kinetic partitioning mechanism. Biochem J. 2011;438(3):505-11.

103. Harms N, Koningstein G, Dontje W, Muller M, Oudega B, Luirink J, et al. The early interaction of the outer membrane protein phoe with the periplasmic chaperone Skp occurs at the cytoplasmic membrane. J Biol Chem. 2001;276(22):18804-11.

104. Bennion D, Charlson ES, Coon E, Misra R. Dissection of β-barrel outer membrane protein assembly pathways through characterizing BamA POTRA 1 mutants of Escherichia coli. Mol Microbiol. 2010;77(5):1153-71.

105. Kim KH, Paetzel M. Crystal structure of Escherichia coli BamB, a lipoprotein component of the β-barrel assembly machinery complex. J Mol Biol. 2011;406(5):667-78.

106. Warner LR, Varga K, Lange OF, Baker SL, Baker D, Sousa MC, et al. Structure of the BamC two-domain protein obtained by Rosetta with a limited NMR data set. J Mol Biol. 2011;411(1):83-95.

107. Albrecht R, Zeth K. Structural basis of outer membrane protein biogenesis in bacteria. J Biol Chem. 2011;286(31):27792-803.

108. Knowles TJ, Browning DF, Jeeves M, Maderbocus R, Rajesh S, Sridhar P, et al. Structure and function of BamE within the outer membrane and the β-barrel assembly machine. EMBO Rep. 2011;12(2):123-8.

109. Chatterjee SN, Das J. Electron microscopic observations on the excretion of cell-wall material by Vibrio cholerae. J Gen Microbiol. 1967;49(1):1-11.

110. Beveridge TJ. Structures of gram-negative cell walls and their derived membrane vesicles. J Bacteriol. 1999;181(16):4725-33.

111. Kulp A, Kuehn MJ. Biological functions and biogenesis of secreted bacterial outer membrane vesicles. Annu Rev Microbiol. 2010;64:163-84.

112. Bonnington KE, Kuehn MJ. Protein selection and export via outer membrane vesicles. Biochim Biophys Acta. 2014;1843(8):1612-9.

113. Schwechheimer C, Sullivan CJ, Kuehn MJ. Envelope control of outer membrane vesicle production in Gram-negative bacteria. Biochemistry. 2013;52(18):3031-40.

114. Baker JL, Chen L, Rosenthal JA, Putnam D, DeLisa MP. Microbial biosynthesis of designer outer membrane vesicles. Curr Opin Biotechnol. 2014;29:76-84.

115. Chatterjee SN, Chaudhuri K. Outer membrane vesicles of bacteria. 1 ed: Springer-Verlag Berlin Heidelberg; 2012.

116. Braun V. Covalent lipoprotein from the outer membrane of Escherichia coli. Biochim Biophys Acta. 1975;415(3):335-77.

117. Macdonald IA, Kuehn MJ. Stress-induced outer membrane vesicle production by Pseudomonas aeruginosa. J Bacteriol. 2013;195(13):2971-81.

118. McBroom AJ, Kuehn MJ. Release of outer membrane vesicles by Gram-negative bacteria is a novel envelope stress response. Mol Microbiol. 2007;63(2):545-58.

119. McBroom AJ, Johnson AP, Vemulapalli S, Kuehn MJ. Outer membrane vesicle production by Escherichia coli is independent of membrane instability. J Bacteriol. 2006;188(15):5385-92.

120. Lee EY, Choi DS, Kim KP, Gho YS. Proteomics in gram-negative bacterial outer membrane vesicles. Mass Spectrom Rev. 2008;27(6):535-55.

121. Lee EY, Bang JY, Park GW, Choi DS, Kang JS, Kim HJ, et al. Global proteomic profiling of native outer membrane vesicles derived from Escherichia coli. Proteomics. 2007;7(17):3143-53.

122. Manning AJ, Kuehn MJ. Functional advantages conferred by extracellular prokaryotic membrane vesicles. J Mol Microbiol Biotechnol. 2013;23(1-2):131-41.

123. Mashburn-Warren L, McLean RJ, Whiteley M. Gram-negative outer membrane vesicles: beyond the cell surface. Geobiology. 2008;6(3):214-9.

124. Ellis TN, Kuehn MJ. Virulence and immunomodulatory roles of bacterial outer membrane vesicles. Microbiol Mol Biol Rev. 2010;74(1):81-94.
125. Renelli M, Matias V, Lo RY, Beveridge TJ. DNA-containing membrane vesicles of Pseudomonas aeruginosa PAO1 and their genetic transformation potential. Microbiology. 2004;150(Pt 7):2161-9.
126. Dorward DW, Garon CF. DNA Is Packaged within Membrane-Derived Vesicles of Gram-Negative but Not Gram-Positive Bacteria. Appl Environ Microbiol. 1990;56(6):1960-2.
127. Chatterjee D, Chaudhuri K. Association of cholera toxin with Vibrio cholerae outer membrane vesicles which are internalized by human intestinal epithelial cells. FEBS Lett. 2011;585(9):1357-62.
128. Kadurugamuwa JL, Beveridge TJ. Natural release of virulence factors in membrane vesicles by Pseudomonas aeruginosa and the effect of aminoglycoside antibiotics on their release. J Antimicrob Chemother. 1997;40(5):615-21.
129. van der Ley P, van den Dobbelsteen G. Next-generation outer membrane vesicle vaccines against Neisseria meningitidis based on nontoxic LPS mutants. Hum Vaccin. 2011;7(8):886-90.
130. Li Z, Clarke AJ, Beveridge TJ. A major autolysin of Pseudomonas aeruginosa: subcellular distribution, potential role in cell growth and division and secretion in surface membrane vesicles. J Bacteriol. 1996;178(9):2479-88.
131. Li Z, Clarke AJ, Beveridge TJ. Gram-negative bacteria produce membrane vesicles which are capable of killing other bacteria. J Bacteriol. 1998;180(20):5478-83.
132. Horstman AL, Kuehn MJ. Enterotoxigenic Escherichia coli secretes active heat-labile enterotoxin via outer membrane vesicles. J Biol Chem. 2000;275(17):12489-96.
133. Wai SN, Lindmark B, Söderblom T, Takade A, Westermark M, Oscarsson J, et al. Vesicle-mediated export and assembly of pore-forming oligomers of the enterobacterial ClyA cytotoxin. Cell. 2003;115(1):25-35.
134. Kato S, Kowashi Y, Demuth DR. Outer membrane-like vesicles secreted by Actinobacillus actinomycetemcomitans are enriched in leukotoxin. Microb Pathog. 2002;32(1):1-13.
135. Tashiro Y, Sakai R, Toyofuku M, Sawada I, Nakajima-Kambe T, Uchiyama H, et al. Outer membrane machinery and alginate synthesis regulators control membrane vesicle production in Pseudomonas aeruginosa. J Bacteriol. 2009;191(24):7509-19.

136. Kadurugamuwa JL, Clarke AJ, Beveridge TJ. Surface action of gentamicin on Pseudomonas aeruginosa. J Bacteriol. 1993;175(18):5798-805.

137. Manning AJ, Kuehn MJ. Contribution of bacterial outer membrane vesicles to innate bacterial defense. BMC Microbiol. 2011;11:258.

138. Mashburn LM, Whiteley M. Membrane vesicles traffic signals and facilitate group activities in a prokaryote. Nature. 2005;437(7057):422-5.

139. Schooling SR, Hubley A, Beveridge TJ. Interactions of DNA with biofilm-derived membrane vesicles. J Bacteriol. 2009;191(13):4097-102.

140. Yonezawa H, Osaki T, Kurata S, Fukuda M, Kawakami H, Ochiai K, et al. Outer membrane vesicles of Helicobacter pylori TK1402 are involved in biofilm formation. BMC Microbiol. 2009;9:197.

141. Yonezawa H, Osaki T, Woo T, Kurata S, Zaman C, Hojo F, et al. Analysis of outer membrane vesicle protein involved in biofilm formation of Helicobacter pylori. Anaerobe. 2011;17(6):388-90.

142. Matlakowska R, Skłodowska A, Nejbert K. Bioweathering of Kupferschiefer black shale (Fore-Sudetic Monocline, SW Poland) by indigenous bacteria: implication for dissolution and precipitation of minerals in deep underground mine. FEMS Microbiol Ecol. 2012;81(1):99-110.

143. Vipond C, Wheeler JX, Jones C, Feavers IM, Suker J. Characterization of the protein content of a meningococcal outer membrane vesicle vaccine by polyacrylamide gel electrophoresis and mass spectrometry. Hum Vaccin. 2005;1(2):80-4.

144. Collins BS. Gram-negative outer membrane vesicles in vaccine development. Discov Med. 2011;12(62):7-15.

145. Rosenthal JA, Chen L, Baker JL, Putnam D, DeLisa MP. Pathogen-like particles: biomimetic vaccine carriers engineered at the nanoscale. Curr Opin Biotechnol. 2014;28:51-8.

146. Kelly DF, Rappuoli R. Reverse vaccinology and vaccines for serogroup B Neisseria meningitidis. Adv Exp Med Biol. 2005;568:217-23.

147. Perrett KP, Pollard AJ. Towards an improved serogroup B Neisseria meningitidis vaccine. Expert Opin Biol Ther. 2005;5(12):1611-25.

148. Sadarangani M, Pollard AJ. Serogroup B meningococcal vaccines-an unfinished story. Lancet Infect Dis. 2010;10(2):112-24.

149. Su EL, Snape MD. A combination recombinant protein and outer membrane vesicle vaccine against serogroup B meningococcal disease. Expert Rev Vaccines. 2011;10(5):575-88.
150. Mitka M. New vaccine should ease meningitis fears. JAMA. 2005;293(12):1433-4.
151. Kesty NC, Kuehn MJ. Incorporation of heterologous outer membrane and periplasmic proteins into Escherichia coli outer membrane vesicles. J Biol Chem. 2004;279(3):2069-76.
152. Kim JY, Doody AM, Chen DJ, Cremona GH, Shuler ML, Putnam D, et al. Engineered bacterial outer membrane vesicles with enhanced functionality. J Mol Biol. 2008;380(1):51-66.
153. Chen DJ, Osterrieder N, Metzger SM, Buckles E, Doody AM, DeLisa MP, et al. Delivery of foreign antigens by engineered outer membrane vesicle vaccines. Proc Natl Acad Sci U S A. 2010;107(7):3099-104.
154. Gao W, Fang RH, Thamphiwatana S, Luk BT, Li J, Angsantikul P, et al. Modulating Antibacterial Immunity via Bacterial Membrane-Coated Nanoparticles. Nano Lett. 2015;15(2):1403-9.
155. Park M, Sun Q, Liu F, DeLisa MP, Chen W. Positional assembly of enzymes on bacterial outer membrane vesicles for cascade reactions. PLoS One. 2014;9(5):e97103.
156. Boyd D, Traxler B, Beckwith J. Analysis of the topology of a membrane protein by using a minimum number of alkaline phosphatase fusions. J Bacteriol. 1993;175(2):553-6.
157. Lippincott J, Traxler B. MalFGK complex assembly and transport and regulatory characteristics of MalK insertion mutants. J Bacteriol. 1997;179(4):1337-43.
158. Nelson BD, Traxler B. Exploring the role of integral membrane proteins in ATP-binding cassette transporters: analysis of a collection of MalG insertion mutants. J Bacteriol. 1998;180(9):2507-14.
159. Nannenga BL, Baneyx F. Reprogramming chaperone pathways to improve membrane protein expression in Escherichia coli. Protein Sci. 2011;20(8):1411-20.
160. Sedlak RH, Hnilova M, Grosh C, Fong H, Baneyx F, Schwartz D, et al. Engineered Escherichia coli silver-binding periplasmic protein that promotes silver tolerance. Appl Environ Microbiol. 2012;78(7):2289-96.
161. Chen H, Kim J, Kendall DA. Competition between functional signal peptides demonstrates variation in affinity for the secretion pathway. J Bacteriol. 1996;178(23):6658-64.
162. Chen H, Kendall DA. Artificial transmembrane segments. Requirements for stop transfer and polypeptide orientation. J Biol Chem. 1995;270(23):14115-22.

163. Ghrayeb J, Kimura H, Takahara M, Hsiung H, Masui Y, Inouye M. Secretion cloning vectors in Escherichia coli. EMBO J. 1984;3(10):2437-42.

164. Puertas JM, Betton JM. Engineering an efficient secretion of leech carboxypeptidase inhibitor in Escherichia coli. Microb Cell Fact. 2009;8:57.

165. Wimley WC. The versatile beta-barrel membrane protein. Curr Opin Struct Biol. 2003;13(4):404-11.

166. Schirmer T. General and specific porins from bacterial outer membranes. J Struct Biol. 1998;121(2):101-9.

167. Mogensen JE, Otzen DE. Interactions between folding factors and bacterial outer membrane proteins. Mol Microbiol. 2005;57(2):326-46.

168. Galdiero S, Galdiero M, Pedone C. beta-Barrel membrane bacterial proteins: structure, function, assembly and interaction with lipids. Curr Protein Pept Sci. 2007;8(1):63-82.

169. Guthrie B, Wickner W. Trigger factor depletion or overproduction causes defective cell division but does not block protein export. J Bacteriol. 1990;172(10):5555-62.

170. Lee HC, Bernstein HD. Trigger factor retards protein export in Escherichia coli. J Biol Chem. 2002;277(45):43527-35.

171. Puertas J-M, Nannenga BL, Dornfeld KT, Betton J-M, Baneyx F. Enhancing the secretory yields of leech carboxypeptidase inhibitor in Escherichia coli: Influence of trigger factor and signal recognition particle. Protein Expression and Purification. 2010.

172. Datsenko KA, Wanner BL. One-step inactivation of chromosomal genes in Escherichia coli K-12 using PCR products. Proc Natl Acad Sci U S A. 2000;97(12):6640-5.

173. Nannenga BL, Baneyx F. Enhanced expression of membrane proteins in E. coli with a P(BAD) promoter mutant: synergies with chaperone pathway engineering strategies. Microb Cell Fact. 2011;10:105.

174. Burgess NK, Dao TP, Stanley AM, Fleming KG. Beta-barrel proteins that reside in the Escherichia coli outer membrane in vivo demonstrate varied folding behavior in vitro. J Biol Chem. 2008;283(39):26748-58.

175. Reusch RN. Insights into the structure and assembly of Escherichia coli outer membrane protein A. FEBS J. 2012;279(6):894-909.

176. Rath A, Glibowicka M, Nadeau VG, Chen G, Deber CM. Detergent binding explains anomalous SDS-PAGE migration of membrane proteins. Proc Natl Acad Sci U S A. 2009;106(6):1760-5.

177. Dornmair K, Kiefer H, Jähnig F. Refolding of an integral membrane protein. OmpA of Escherichia coli. J Biol Chem. 1990;265(31):18907-11.

178. Otzen DE, Andersen KK. Folding of outer membrane proteins. Arch Biochem Biophys. 2013;531(1-2):34-43.

179. Beher MG, Schnaitman CA, Pugsley AP. Major heat-modifiable outer membrane protein in gram-negative bacteria: comparison with the ompA protein of Escherichia coli. J Bacteriol. 1980;143(2):906-13.

180. Chun SY, Randall LL. In vivo studies of the role of SecA during protein export in Escherichia coli. J Bacteriol. 1994;176(14):4197-203.

181. Oliver DB, Cabelli RJ, Dolan KM, Jarosik GP. Azide-resistant mutants of Escherichia coli alter the SecA protein, an azide-sensitive component of the protein export machinery. Proc Natl Acad Sci U S A. 1990;87(21):8227-31.

182. Crooke E, Guthrie B, Lecker S, Lill R, Wickner W. ProOmpA is stabilized for membrane translocation by either purified E. coli trigger factor or canine signal recognition particle. Cell. 1988;54(7):1003-11.

183. Zhou Y, Ueda T, Müller M. Signal recognition particle and SecA cooperate during export of secretory proteins with highly hydrophobic signal sequences. PLoS One. 2014;9(4):e92994.

184. Yosef I, Bochkareva ES, Bibi E. Escherichia coli SRP, its protein subunit Ffh, and the Ffh M domain are able to selectively limit membrane protein expression when overexpressed. MBio. 2010;1(2).

185. Choi JH, Lee SY. Secretory and extracellular production of recombinant proteins using Escherichia coli. Appl Microbiol Biotechnol. 2004;64(5):625-35.

186. Yoon SH, Kim SK, Kim JF. Secretory production of recombinant proteins in Escherichia coli. Recent Pat Biotechnol. 2010;4(1):23-9.

187. Ni Y, Chen R. Extracellular recombinant protein production from Escherichia coli. Biotechnol Lett. 2009;31(11):1661-70.

188. Chudakov DM, Matz MV, Lukyanov S, Lukyanov KA. Fluorescent proteins and their applications in imaging living cells and tissues. Physiol Rev. 2010;90(3):1103-63.

189. Wang Y, Shyy JY, Chien S. Fluorescence proteins, live-cell imaging, and mechanobiology: seeing is believing. Annu Rev Biomed Eng. 2008;10:1-38.

190. Shaner NC, Campbell RE, Steinbach PA, Giepmans BN, Palmer AE, Tsien RY. Improved monomeric red, orange and yellow fluorescent proteins derived from Discosoma sp. red fluorescent protein. Nat Biotechnol. 2004;22(12):1567-72.

191. Fink D, Wohrer S, Pfeffer M, Tombe T, Ong CJ, Sorensen PH. Ubiquitous expression of the monomeric red fluorescent protein mCherry in transgenic mice. Genesis. 2010;48(12):723-9.

192. Chutkan H, MacDonald I, Manning A, Kuehn MJ. Quantitative and qualitative preparations of bacterial outer membrane vesicles. In: Delcour AH, editor. Bacterial cell surfaces: methods and protocols. 966: Springer 2013.

193. Ruozi B, Tosi G, Leo E, Vandelli MA. Application of atomic force microscopy to characterize liposomes as drug and gene carriers. Talanta. 2007;73(1):12-22.

194. Misra R, Stikeleather R, Gabriele R. In Vivo Roles of BamA, BamB and BamD in the Biogenesis of BamA, a Core Protein of the β-Barrel Assembly Machine of Escherichia coli. J Mol Biol. 2015;427(5):1061-74.

195. Strauch EM, Georgiou G. A bacterial two-hybrid system based on the twin-arginine transporter pathway of E. coli. Protein Sci. 2007;16(5):1001-8.

196. Wu T, Malinverni J, Ruiz N, Kim S, Silhavy TJ, Kahne D. Identification of a multicomponent complex required for outer membrane biogenesis in Escherichia coli. Cell. 2005;121(2):235-45.

197. Klimentová J, Stulík J. Methods of isolation and purification of outer membrane vesicles from gram-negative bacteria. Microbiol Res. 2015;170:1-9.

198. Coyle BL, Baneyx F. A cleavable silica-binding affinity tag for rapid and inexpensive protein purification. Biotechnol Bioeng. 2014;111(10):2019-26.

199. Coyle BL, Rolandi M, Baneyx F. Carbon-binding designer proteins that discriminate between sp2- and sp3-hybridized carbon surfaces. Langmuir. 2013;29(15):4839-46.

200. Shu X, Shaner NC, Yarbrough CA, Tsien RY, Remington SJ. Novel chromophores and buried charges control color in mFruits. Biochemistry. 2006;45(32):9639-47.

201. Baneyx F, Georgiou G. In Vivo Degradation of Secreted Fusion Proteins by the Escherichia coliOuter Membrane Protease OmpT. Journal of Bacteriology. 1990;172(1).

202. Strobl FG, Seitz F, Westerhausen C, Reller A, Torrano AA, Bräuchle C, et al. Intake of silica nanoparticles by giant lipid vesicles: influence of particle size and thermodynamic membrane state. Beilstein J Nanotechnol. 2014;5:2468-78.